EARTH-FISSURE MOVEMENTS ASSOCIATED WITH FLUCTUATIONS IN GROUND-WATER LEVELS NEAR THE PICACHO MOUNTAINS, SOUTH-CENTRAL ARIZONA, 1980-84

U.S. GEOLOGICAL SURVEY
Open-File Report 90 – 561

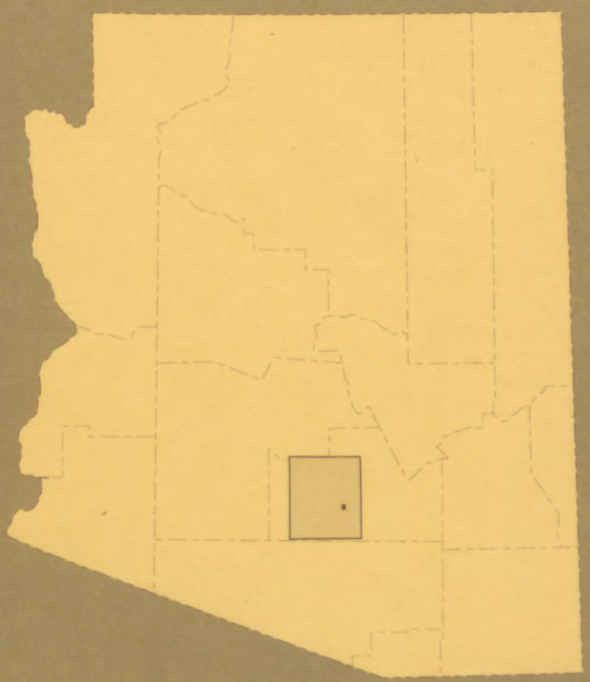

EARTH-FISSURE MOVEMENTS ASSOCIATED WITH FLUCTUATIONS IN GROUND-WATER LEVELS NEAR THE PICACHO MOUNTAINS, SOUTH-CENTRAL ARIZONA, 1980-84

By M.C. CARPENTER

U.S. GEOLOGICAL SURVEY
Open-File Report 90 – 561

Tucson, Arizona
August 1991

U.S. DEPARTMENT OF THE INTERIOR
MANUEL LUJAN, Jr., Secretary

U.S. GEOLOGICAL SURVEY
Dallas L. Peck, Director

For additional information
write to:

District Chief
U.S. Geological Survey
375 South Euclid Avenue
Tucson, Arizona 85719

Copies of this report can be
purchased from:

U.S. Geological Survey
Books and Open-File Reports Section
Federal Center, Box 25425
Denver, Colorado 80225

CONTENTS

ILLUSTRATIONS

ILLUSTRATIONS

Page

Page

TABLES

CONVERSION FACTORS AND VERTICAL DATUM

Multiply	By	To obtain
micrometer (μm)	0.00003937	inch (in.)
millimeter (mm)	0.03937	inch (in.)
meter (m)	3.281	foot (ft)
kilometer (km)	0.6214	mile (mi)
hectare (ha)	2.471	acre
cubic meter (m^3)	0.0008107	acre-foot (acre-ft)
liter per second (L/s)	15.85	gallon per minute (gal/min)
kilometer per second (km/s)	3,281	foot per second (ft/s)
kilogram (kg)	2.205	pound mass (lbm)
newton (N)	0.2248	pound force (lbf)
kilopascal (kPa)	0.1450	pound per square inch (lb/in^2)
degree Celsius (°C)	°F=(9/5°C)+32	degree Fahrenheit (°F)

Normal strain (dimensionless) is obtained by dividing measured change in length between two points by the distance between the points. One microstrain is $1x10^{-6}$ strain.

Sea level: In this report, "sea level" refers to the National Geodetic Vertical Datum of 1929 (NGVD of 1929)—a geodetic datum derived from a general adjustment of the first-order level nets of both the United States and Canada, formerly called "*Sea Level Datum of 1929*."

EARTH-FISSURE MOVEMENTS ASSOCIATED WITH FLUCTUATIONS IN GROUND-WATER LEVELS NEAR THE PICACHO MOUNTAINS, SOUTH-CENTRAL ARIZONA, 1980-84

By

M.C. Carpenter

ABSTRACT

The Picacho earth fissure transects subsiding alluvial sediments near the east periphery of the Picacho basin in south-central Arizona. The basin has undergone land subsidence of as much as 3.8 meters since the 1930's owing to compaction of the aquifer system in response to ground-water-level declines that have exceeded 100 meters. The fissure, which extends generally north-south for 15 kilometers, exhibits horizontal tensile failure and as much as 0.6 meter of normal dip-slip movement at the land surface. The west side of the fissure is downthrown. The fissure was observed as early as 1927 and is the longest earth fissure in Arizona.

Vertical and horizontal displacements were monitored along a line normal to the fissure. The survey line extends from a bedrock outcrop in the Picacho Mountains on the east, past an observation well near the fissure, to a point 1,422 meters to the west. From May 1980 to May 1984, the downthrown west side of the fissure subsided 167 ±1.8 millimeters and moved 18 ±1.5 millimeters westward into the basin. Concurrently, the relatively upthrown east side subsided 147 ±1.8 millimeters and moved 14 ±1.5 millimeters westward. Dislocation modeling of deformation along the survey line near the fissure indicates that dip-slip movement has occurred along a vertical fault surface that extends from the land surface to a depth of about 300 meters. Slip was 9 millimeters from May to December 1980 and also 9 millimeters from March to November 1981.

Continuous measurements were made of horizontal movement across the fissure using a buried invar-wire horizontal extensometer, while water-level fluctuations were continuously monitored in four piezometers nested in two observation wells. The range of horizontal movement was 4.620 millimeters, and the range of water-level fluctuation in the nearest piezometer in the deep alluvium was 9.05 meters. The maximum annual opening of the fissure during the study period was 3.740 millimeters from March to October 1981, while the water level declined 7.59 meters. The fissure closed 1.033 millimeters from October 1981 to March 1982, while the water level recovered 6.94 meters. Opening and closing of the fissure were smooth and were correlated with water-level decline and recovery, respectively, recorded in the nearby piezometers. Pearson correlation coefficients between the water-level fluctuations in the deeper piezometers and horizontal movement ranged from 0.913 to 0.925. The correlogram with water-level decline as ordinate and horizontal strain as abscissa exhibits hysteresis loops for annual cycles of water-level fluctuation as well as near-vertical excursions for shorter cycles of pumping and recovery.

Vertical and horizontal displacements also were monitored along a second survey line 1 kilometer north of and nearly parallel to the first survey line. The north line extends from bedrock on the east across three fissures to a point 582 meters to the west but does not cross the Picacho earth fissure. From May 1980 to May 1984, the fissure farthest from the mountain front along this line exhibited 20 ±1 millimeters of opening and 33.3 ±1.1 millimeters of vertical offset; the west side of the fissure was downthrown. During the same period, the zone between this fissure and the mountain front exhibited compression.

The hypothesis of generalized differential compaction is supported at the study site for several reasons. First, the vertical offset across fissures and the fit of deformation to a dislocation model are consistent with an elastic model of differential vertical movement deep in the alluvium. Second, correlation is high between horizontal movement across the Picacho earth fissure and water-level fluctuations in the deeper local piezometers. Third, correlation is high between horizontal movement across the fissure and compaction farther west in the basin. The hypothesis of rotation of a rigid plate is not supported because fissures sometimes opened by movements toward the mountain front, fissures opened between existing fissures and the mountain front, and predominant movement of the Picacho earth fissure was vertical offset. The hypothesis of horizontal seepage stresses is not supported because of the low correlation between fissure movement and horizontal head gradients.

INTRODUCTION

Earth fissures are long, linear tensile cracks at the land surface, with or without vertical offset. In the arid Southwest, earth fissures have caused damage to manmade structures and pose additional future hazards. Structures damaged by fissures include highways, railroads, sewers, canals, buildings, and flood-control dikes. Potential damage from earth fissures forced a major rerouting of the Central Arizona Project aqueduct. Erosionally enlarged fissure gullies present a hazard to hikers, vehicles, grazing livestock, and wildlife. Aquifer contamination may occur through rupture of pipelines, surreptitious dumping of hazardous waste into fissures, and capture of surface flow containing agricultural chemicals. Fissures can be conduits for direct recharge of contaminants to deep aquifers. Surficial radon gas emanations can be increased by stresses induced by fissure movement, and fissures can be conduits for radon gas that is released as a result of nearby pumping stresses (Fleischer, 1981; Harvey, 1981). Vertical offset presents the greatest potential for earth-fissure damage to structures such as large buildings, pipelines, and airport runways.

The U.S. Geological Survey operated a recording horizontal extensometer across the Picacho earth fissure near the Picacho Mountains in south-central Arizona (fig. 1) from November 14, 1980, to December 13, 1984. In addition, from May 31, 1980, to May 15, 1984, seven sets of precise horizontal-distance and leveling surveys were made along a line that crosses the fissure at nearly a right angle.

Purpose and Scope

The purposes of this study were to test the hypothesis that the opening, closing, and vertical offset of a major earth fissure can be correlated with water-level fluctuations in nearby piezometers and to use dislocation modeling of land-surface deformation near an earth fissure to characterize the mechanism and geometry of fissure evolution. The study concentrated on characterizing and interpreting the horizontal and vertical movement of the Picacho earth fissure from May 1980 to December 1984.

This report presents the hypotheses of earth-fissure development, a description of the measurement techniques and instrumentation used in this study, and descriptive results. The correlation between horizontal movement of the fissure and water-level fluctuations in nearby piezometers and the results of dislocation modeling analysis are described. Analysis of the hydrologic data includes determination of seasonal and long-term interrelations among continuously monitored horizontal strain across the Picacho earth fissure, water-level fluctuations in nearby piezometers, and repeated surveys of displacements of stations near the fissure. This study provides the first continuous long-term measurements of earth-fissure movements.

Previous Investigations

Leonard (1929) first reported a fissure about 5 km southeast of Picacho, Arizona, on September 12, 1927, after a severe rainstorm. Leonard also reported that unusual cracks had occurred on September 11, 1927, at the El Tiro Mine near Silver Bell, Arizona, about 13 km south of the study area. After considering several hypotheses for the formation of the fissure, Leonard tentatively concluded that an earthquake, which occurred on September 11, 1927, 270 km from Tucson, Arizona, either caused the fissure or triggered release of accumulated strain at the site. Mountains that form the skyline in a photograph taken by Leonard do not line up at any point along the present 15-kilometer-long Picacho earth fissure. The mountains form the proper skyline at an inactive fissure several hundred meters to the northwest (Holzer and others, 1979). This photographic evidence indicates that the fissure that Leonard observed in 1927 was not the present-day Picacho earth fissure.

Photographic documentation indicates that the Picacho earth fissure existed as early as 1927. Archived photographs dated November 13, 1927 (University of Arizona Tree Ring Laboratory photographs GEOL 27-1 and GEOL 27-2), show Professor A.E. Douglas at the edge of an earth fissure. The mountain skyline to the south lines up at a point along the present-day Picacho earth fissure. This fissure was also attributed to the earthquake on September 11, 1927. Some sections of the Picacho earth fissure are identifiable as lines of denser vegetation on aerial photographs taken in 1936 (U.S. Soil Conservation Service, 1936).

Beginning in the early 1950's, several observers reported the occurrence of earth fissures. Feth (1951) attributed earth fissures west of the Picacho Mountains to induced differential compaction of poorly consolidated alluvium over the edge of a buried pediment. He noted the

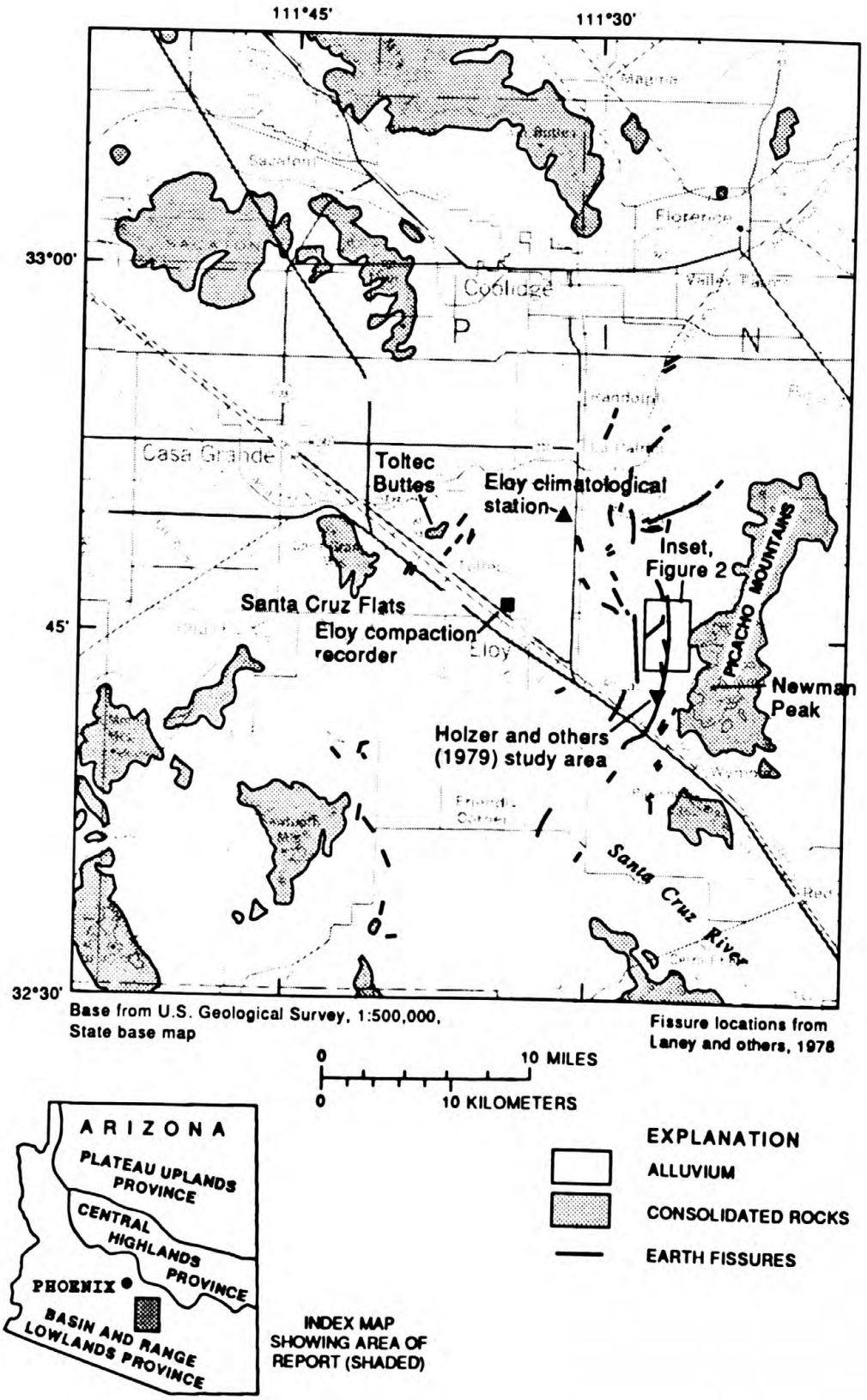

Figure 1.--Location of study area, climatological station, selected earth fissures, and Eloy compaction recorder.

opening of fissures during and after storms and the ability of fissures to accept large quantities of runoff to great depth. Fletcher and others (1954) attributed earth fissures to piping erosion. Heindl and Feth (1955) rejected the piping hypothesis because earth fissures drain internally. Pashley (1961) suggested that hydrocompaction was a possible mechanism for earth fissuring near Casa Grande, Arizona. He documented a flow of water of about 20 L/s from a breached irrigation ditch into a fissure for 18 hours before the fissure filled.

Robinson and Peterson (1962) noted the increased frequency of observation of fissures beginning about 1949. They reported that fissures occurred in several areas in central, south-central, and southeastern Arizona and included fissures in areas with no ground-water pumping north of Phoenix and in south-central Arizona. North of Phoenix, some fissures are in semiconsolidated sedimentary rock rather than alluvium. Robinson and Peterson (1962) also described the correlation of water-level decline, subsidence, and earth fissuring in areas of significant ground-water withdrawal and presented subsidence profiles from 1905 to 1960 in the Picacho-Toltec area. Peterson (1962) related the locations of earth fissures to gravity anomalies and supported the hypothesis that earth fissures are tensile failures caused by differential compaction over buried pediments or fault scarps. Schumann and Poland (1970) correlated ground-water pumping with land subsidence and earth fissuring in south-central Arizona. They presented subsidence profiles and maps of earth fissures and gravity anomalies.

Acknowledgments

Many people contributed to the successful completion of the field work for this investigation. David C. Steinke, University of Arizona, designed electronic circuits used in the study. Caryn A. Carpenter and Eric R. Carpenter contributed surveying assistance. Test holes and piezometers were drilled and installed by personnel of the U.S. Bureau of Reclamation. Bruce L. Massey aided in installing tape-extensometer monuments and provided rigorous instruction in techniques of precise surveying. Francis S. Riley provided valuable comments and criticisms. Roger P. Denlinger assisted in dislocation modeling. Robert O. Burford furnished the mechanical components of the horizontal extensometer. James C. Savage designed the dislocation model MAIN113.

Approach

Continuously recorded measurements included horizontal extension and compression across the fissure, water-level fluctuations in a nearby piezometer, and barometric pressure, as well as ancillary measurements of instrument-vault temperature and power-supply voltage. Correlation of horizontal strain with water-level fluctuations was tested statistically using Pearson correlation coefficients (Sokal and Rohlf, 1969).

Repeated horizontal and vertical surveys of nearby stations along a 1,422-meter profile provided data on seasonal changes in the spatial

patterns of deformation. Detailed data on a system of fissures closer to the mountain front were obtained from a second profile. The pattern of deformation across the Picacho earth fissure was compared with a fault-dislocation model (Savage and Hastie, 1966, 1969) to test the usefulness of dislocation modeling.

The study site was selected to take advantage of data generated by the U.S. Geological Survey and the U.S. Bureau of Reclamation in a joint study of subsidence and fissure hazards along the route of the Central Arizona Project (CAP) aqueduct. The specific study site was selected to be near two piezometers that had been placed on opposite sides of the Picacho earth fissure to determine the effect of the fissure on water levels. Seismic-refraction profiles also were done near the site as part of the CAP subsidence study. These seismic profiles were used in the present study to determine basement geometry and to estimate material properties for preliminary finite-element modeling of deformation.

Hydrologic and geologic terms used in this report are defined by Bates and Jackson (1980), Poland and others (1972), and Lohman and others (1972). Holzer and others (1979) applied the term *Picacho fault* to the main fissure in this study because of the obvious vertical offset of the land surface. The more traditional term, earth fissure, used by Leonard (1929) for the tensile crack that he observed near Picacho, Arizona, in 1927 will be used in this report. This usage avoids confusion with structural features such as the Picacho Peak detachment fault (Brooks, 1986).

PHYSICAL SETTING

The Picacho basin is a broad alluvial basin bounded by mountains of mostly igneous and metamorphic rocks within the Basin and Range lowlands province in south-central Arizona (fig. 1). The basin trends slightly east of north and is 70 km long north to south and 35 km wide east to west. The mountains range in altitude above sea level from 1,374 m at Newman Peak to 495 m at Toltec Buttes. The alluvial slope is gentle to the northwest, from an altitude of about 533 m at the base of the Picacho Mountains to 425 m near Casa Grande. The principal drainage is by the ephemeral Santa Cruz River, which enters the basin from the southeast and distributes into the Santa Cruz Flats in the southern part of the basin.

The study area is in the Sonoran Desert. At the Eloy climatological station (fig. 1) for 1951-70, the January mean minimum temperature was 2.1 °C, the July mean maximum temperature was 40.6 °C, and the annual mean temperature was 21.2 °C. Mean annual rainfall at the Eloy station was 214 mm, with a maximum daily rainfall of 78 mm falling in January 1956 (Sellers and Hill, 1974; National Oceanic and Atmospheric Administration, 1973-85). About half the annual rainfall occurs during July through September from storms associated with humid air masses from the Gulf of Mexico. The other half of the annual rainfall occurs during October to March from cyclonic storms originating in the Pacific Ocean (Sellers and Hill, 1974). From 1980 to 1985, the amounts of annual rainfall measured at the Eloy station were 226 mm, 258 mm, 323 mm, 512 mm, 383 mm, and 343 mm, respectively. These years were wetter than normal; 1983 had about 2.4 times the normal rainfall. Potential annual evapotranspiration is about 1.1 m or more than five times the mean annual rainfall (Hardt and Cattany, 1965).

HYDROGEOLOGY

Picacho Basin

The water-bearing units in the Picacho basin are composed of alluvial deposits. These heterogeneous deposits are divided into a local gravel unit, lower sand and gravel unit, middle silt and clay unit, and upper sand and gravel unit. The local gravel unit, which ranges in thickness from 0 to 300 m and generally is a productive aquifer, is present only in the western part of the basin. The lower sand and gravel unit ranges from 0 to about 150 m thick. The middle silt and clay unit has the lowest permeability of the alluvial units, ranges from 0 to 600 m thick, and yields moderate quantities of water from sand and gravel lenses. The upper sand and gravel unit is the surface deposit in most of the area and ranges from less than 15 m to about 180 m thick (Hardt and Cattany, 1965).

Before 1930, depth to water was 30 m or more in only about 12 wells in the Eloy area. During the 1930's, development of ground water increased markedly. During 1940-45, depth to water increased from predevelopment levels of about 10 m to as much as 55 m (Smith, 1940). Turner and others (1947) estimated safe yield for the Eloy area at 3.1×10^7 m^3/yr; pumpage was estimated to be 3.38×10^8 m^3/yr or 11 times the safe yield. By 1985, total ground-water pumpage for the lower Santa Cruz basin was about 8×10^8 m^3/yr, and the depth to water was as much as 133 m below land surface in a trough of depression between Eloy and the Picacho Mountains (U.S. Bureau of Reclamation, 1976; U.S. Geological Survey, 1986).

Subsidence was detected in the Picacho basin as early as 1948 when a level line run in 1905 was rerun. Between 1905 and 1948, 30 mm of subsidence had occurred near Eloy. From 1948 to 1967, subsidence was as much as 2.3 m northeast of Eloy; in the Picacho basin 57,000 ha had subsided 150 mm or more and 15,500 ha had subsided 900 mm or more. From 1967 to 1973, subsidence of as much as 930 mm occurred near Picacho (Schumann and Poland, 1970; Winikka and Wold, 1976). By 1977, a total of 3.8 m of subsidence had been measured at a bench mark 5 km south of Eloy (Laney and others, 1978).

Fissure Study Site

At the study site near test hole TA-1 (figs. 2 and 3), the land surface slopes gently about 1 percent to the northwest. Between TA-1 and TA-3, the slope is also about 1 percent to the west. Slope of the potentiometric surface between the deep piezometers TA-1-1 and TA-3-1 (figs. 3 and 4) is about 0.2 percent to the west. Slope of the contact between the alluvium and the crystalline basement rock (seismic velocity, 4.7-6.0 km/sec) is about 45 percent or 25° to the west with no indication of development of a pediment or bedrock bench.

Alluvial deposits consist of three units that are poorly consolidated, poorly stratified, and commonly poorly sorted. Contacts between units are gradational over tens of meters. The upper unit is brown silty and clayey sand and gravel and extends from the land surface at an

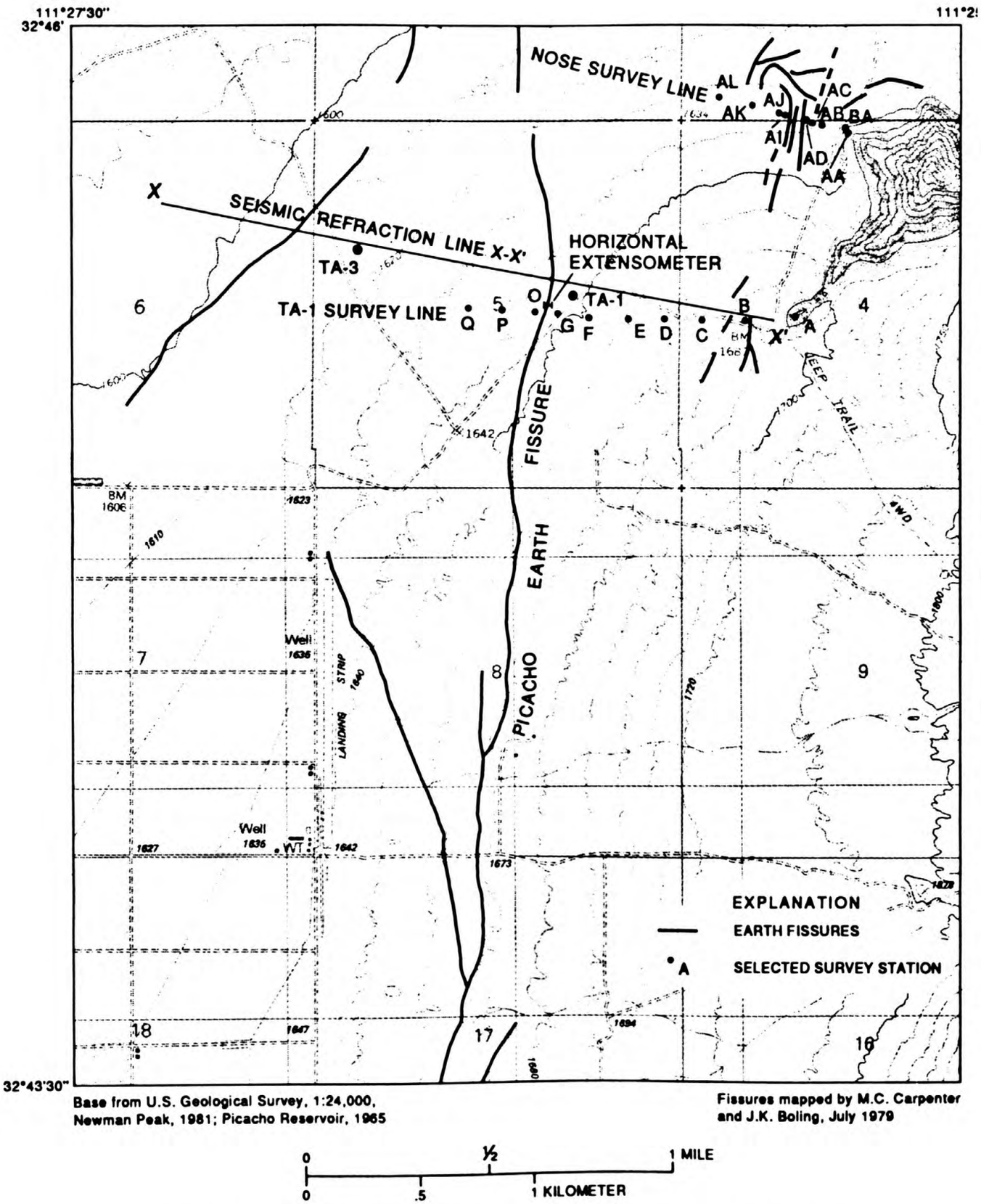

Figure 2.--Selected survey stations, test holes TA-1 and TA-3, seismic refraction line, and horizontal extensometer.

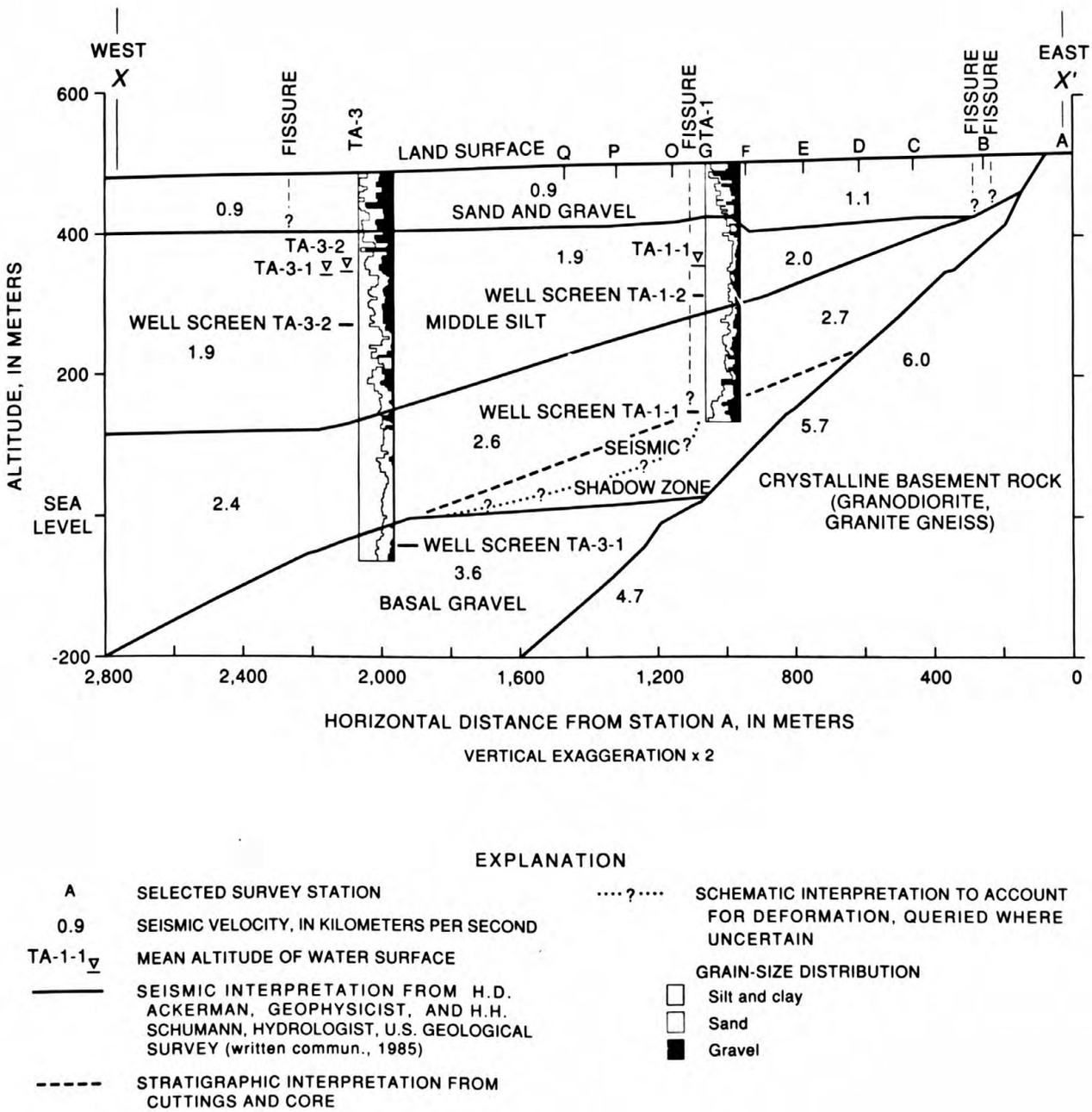

EXPLANATION

A	SELECTED SURVEY STATION
0.9	SEISMIC VELOCITY, IN KILOMETERS PER SECOND
TA-1-1 ▽	MEAN ALTITUDE OF WATER SURFACE
———	SEISMIC INTERPRETATION FROM H.D. ACKERMAN, GEOPHYSICIST, AND H.H. SCHUMANN, HYDROLOGIST, U.S. GEOLOGICAL SURVEY (written commun., 1985)
- - - - -	STRATIGRAPHIC INTERPRETATION FROM CUTTINGS AND CORE
····?····	SCHEMATIC INTERPRETATION TO ACCOUNT FOR DEFORMATION, QUERIED WHERE UNCERTAIN

GRAIN-SIZE DISTRIBUTION

- Silt and clay
- Sand
- Gravel

Figure 3.—Geologic section constructed from seismic refraction profile and grain-size distribution for test holes TA-1 and TA-3.

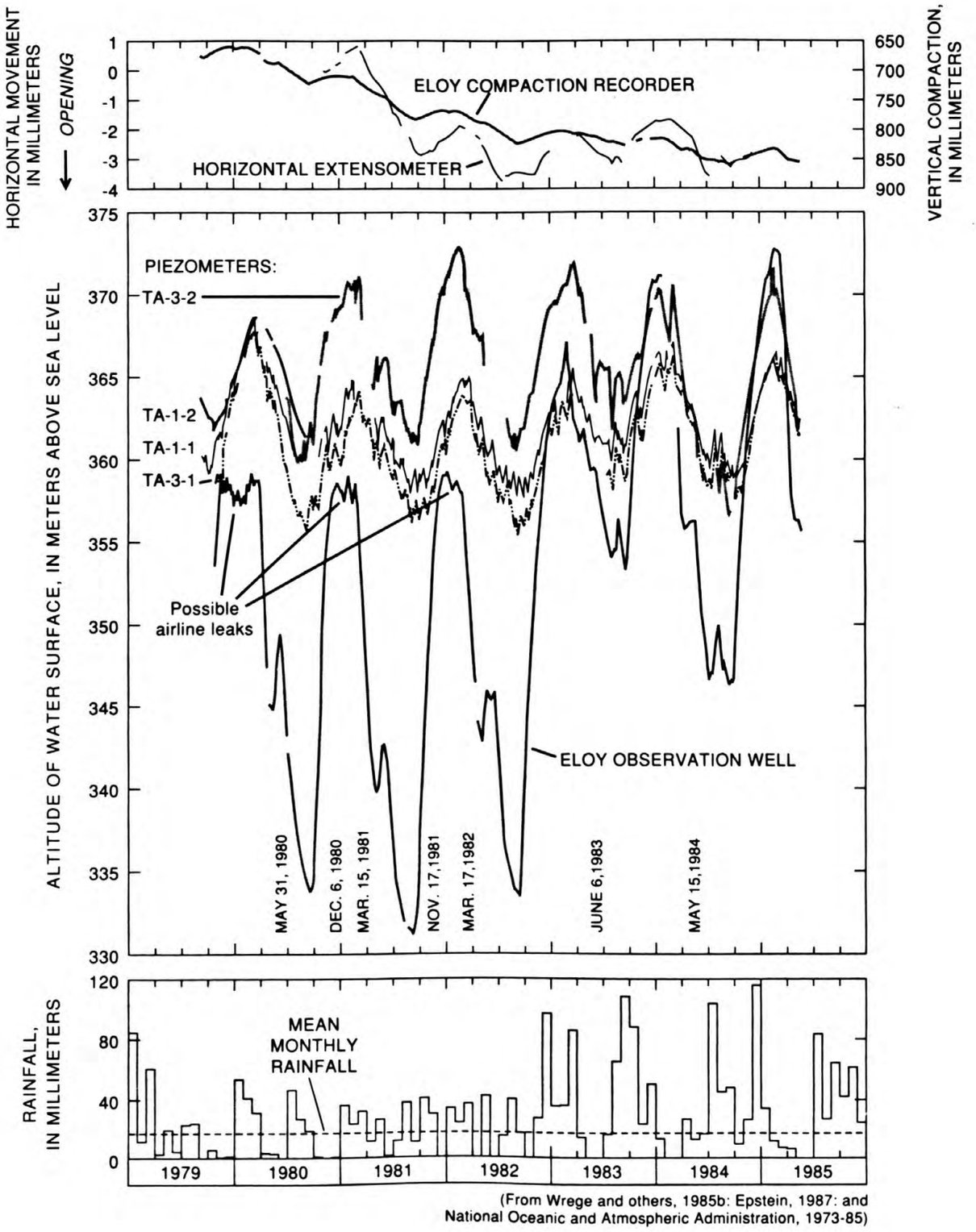

Figure 4.—Water levels in piezometers in test holes TA-1 and TA-3 and in the Eloy observation well, horizontal movement at the TA-1 horizontal extensometer, compaction at the Eloy compaction recorder, monthly rainfall at Eloy, and dates of surveys.

altitude of about 500 m above sea level to an altitude of about 400 m in each well. This unit has seismic velocities that range from 0.9 to 1.1 km/s (fig. 3). The middle unit consists of brown to dark-brown sandy, clayey silt, which is cemented to mudstone or siltstone in some intervals. This unit contains tuff, reworked tuff, and many sand stringers. The middle unit extends from an altitude of about 400 m to about 170 m in TA-1 and to about -20 m in TA-3. The middle unit has seismic velocities of 1.9 to 2.7 km/s. A slight increase in density gradient may characterize the vertical change in seismic velocity in the middle of this unit. The lower unit is a brown clayey, silty, sandy gravel and in TA-1 extends from an altitude of about 170 m to below the bottom of TA-1 and from an altitude of about -20 m to below the bottom of TA-3. Clasts in this unit are as large as boulders and include granite, granodiorite, schist, quartz, and feldspar. The clasts commonly are severely weathered. The lower unit has seismic velocities of 3.3 to 3.6 km/s. The crystalline basement rocks probably are granodiorite and granite gneiss and have seismic velocities of 4.7 to 6.0 km/s (R.L. Laney, hydrologist, U.S. Geological Survey, written commun., 1979; H.H. Schumann, hydrologist, U.S. Geological Survey, written commun., 1987).

A discrepancy exists between the contacts as determined from the seismic refraction profiling and the core description in TA-1. Although the seismic lines were shot in both directions, some ambiguity remained and is shown as a triangular seismic shadow zone in figure 3. Neither the geophysical logs of the holes nor the lithologic information from the holes was used for the interpretation of the seismic lines (H.D. Ackerman, geophysicist, U.S. Geological Survey, oral commun., 1984). A hypothetical low-density, low-velocity zone near TA-1 caused by a fissure that extends nearly to bedrock could be the reason that the refracting horizon at the top of the basal gravel appears to be deeper than the contact determined from core description and well cuttings. The contact between the middle silt and the basal gravel is presented as three alternatives (fig. 3). The lower contact is the seismic interpretation by H.D. Ackerman and H.H. Schumann (U.S. Geological Survey, written commun., 1985). The upper contact is a linear interpolation between the contacts determined in the wells. The middle contact is a speculative contact that qualitatively reflects the pattern of deformation measured along the TA-1 survey line.

Two piezometers were set in each of the two test holes--TA-1 and TA-3 (figs. 2 and 3). The holes were 200 mm in diameter and were drilled by normal rotary methods. Core was taken every 30 m. Deep and shallow piezometers, consisting of 30-millimeter black pipe, were nested in each hole and were designated with the suffixes -1 and -2, respectively. Steel well screens in piezometers TA-1-1, TA-1-2, TA-3-1, and TA-3-2 were set from 346 to 350 m, 186 to 190 m, 524 to 530 m, and 224 to 229 m, respectively. Piezometer TA-1-2 was vandalized in the fall of 1980 and provided only brief record.

The piezometer data show that as of 1985 none of the upper unit, most of the middle unit, and all of the lower unit were saturated. The middle unit has no well-defined confining unit but exhibits some aspects of confined behavior including rapid drawdown in response to pumping in a well more than 1 km away from the piezometer. The middle unit consists largely of fine-grained, low-permeability beds that could act as laterally discontinuous aquitards. Thin sand lenses may enhance vertical hydraulic interconnection within the middle unit and hydraulic connection to the basal gravel.

Water levels in the piezometers exhibited seasonal fluctuations of as much as 15 m with no apparent net decline from 1979 to 1985 (fig. 4). The annual high water level generally occurred in mid-March. The highest water level in TA-1-1 was 368.8 m on March 14, 1980. In TA-3-2, the highest water level was about 373 m on February 22, 1982. The annual low water level generally occurred in late August to early September. In TA-3-1, the lowest water level was 355.2 m on September 8, 1982. In TA-3-2, the lowest water level was 356.4 m on September 9, 1984 (Wrege and others, 1985b).

Water levels in the deep piezometers TA-1-1 and TA-3-1 are at nearly the same altitude and fluctuate in a similar way. The maximum difference in water level between these piezometers was only 3 m and occurred in July 1980 (fig. 5). In contrast, the maximum difference in water level between the shallow piezometer TA-3-2 and the deep piezometer TA-3-1 was as much as 10 m. The water level in piezometer TA-3-2 was higher than in TA-3-1 except during May through September 1984.

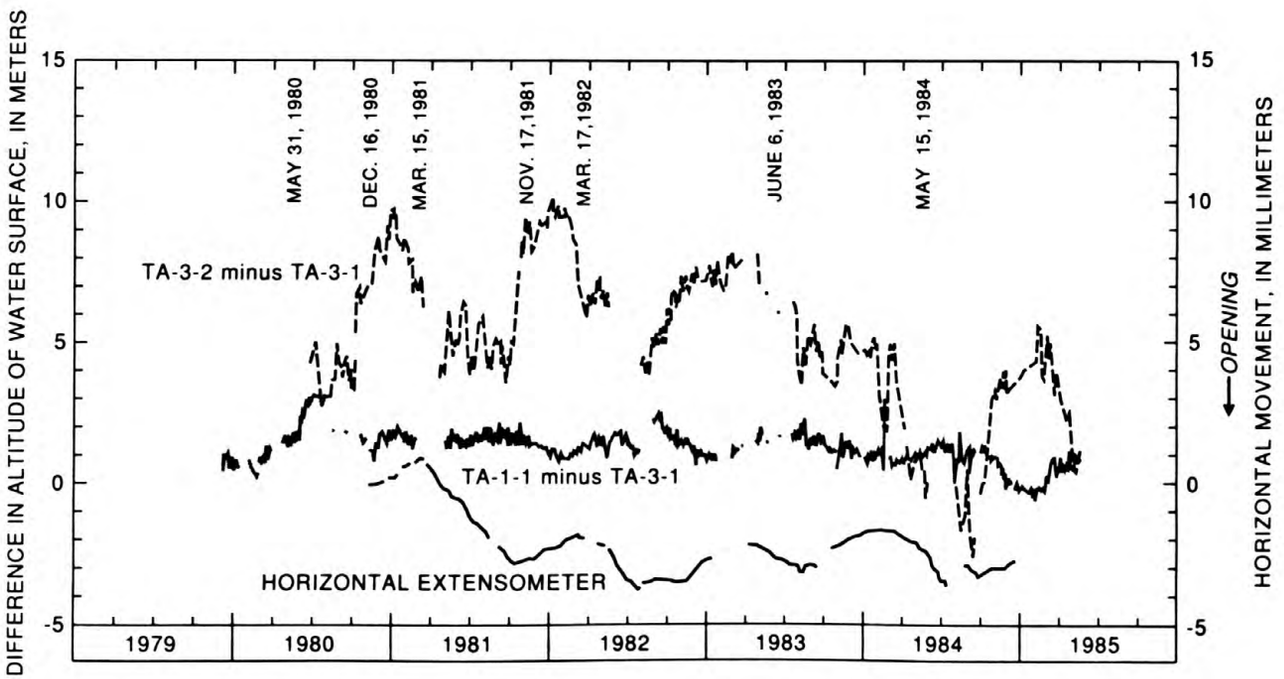

Figure 5.—Differences in altitudes of water level for selected pairs of piezometers in test holes TA-1 and TA-3, horizontal movement at the nearby horizontal extensometer, and dates of surveys.

In the observation well at the Eloy compaction recorder, water levels fluctuated seasonally about 30 m (fig. 4) (Epstein, 1987). Water levels in the Eloy observation well were considerably lower than those in the piezometers at the study site until about November 1982. From 1983 to 1985, minimum water levels at Eloy were not as low as in previous years and seasonal recoveries were higher than in TA-3-2 (fig. 4). The water-level rise at Eloy after November 1982 could reflect increased rainfall during the latter years of the study and the consequent reduction in pumping.

EARTH-FISSURE DEVELOPMENT

Earth fissures are associated with land subsidence caused by aquifer compaction in Arizona, California, and Nevada. Earth fissures in south-central Arizona commonly occur as long, curvilinear cracks in the land surface in alluvium near and subparallel to mountain fronts (Schumann and Poland, 1970). The ends of fissures may propagate as hairline cracks or as sequences of collapse holes that resemble rodent holes. The central parts of fissures generally are widened into fissure gullies by erosion and collapse of the opposing walls (Laney and others, 1978). Fissures vary in length from a few meters to as much as 15 km but generally range from a few tens of meters to a few hundreds of meters. Fissures can be widened by erosion to as much as 10 m. Visible depths of fissures can be as much as 10 m. One fissure northwest of Picacho Peak was taped to a depth of about 25 m (Johnson, 1980). Most fissures occur as long, linear features in the form of single, parallel, or anastomosing cracks. Fissures generally do not intersect at angles greater than about 30°, and polygonal patterns and en echelon cracks are rare. Vertical offset or dip-slip movement is visually apparent at only a few fissures, and no strike-slip movement has been observed. Measurements of horizontal movement have been made across only a few fissures, and continuous measurements have been made for short periods of time. Measured movement rarely has been greater than 30 mm (Boling, 1987) and generally has been a few millimeters.

Earth fissures have been reported to open during and after rainstorms (Boling, 1987). Because they commonly cross ephemeral stream channels at nearly right angles, fissures intercept storm runoff and redirect much or all the flow downward into the crack. This stream capture lowers local base level, causing rapid headward erosion. Fissures can intercept all drainage for several years before through-flowing drainage is reestablished. From a quantitative study of the amount of sediment transported downward into cracks from headcutting, bedload, and suspended-sediment load of contributing ephemeral streams and from collapse of the walls, Johnson (1980) inferred that fissures exhibit large volumes of void space in the subsurface. He speculated that this large void space could represent subsurface extent beyond the ends of surface expression, widening of the crack at depth, or penetration of the fissure to great depth within the alluvium.

Hypotheses of Earth-Fissure Formation

Several mechanisms have been proposed to account for earth fissures. One mechanism or a combination of mechanisms can produce fissures, and different mechanisms can operate in various geologic environments and under different induced stresses. Mechanisms that involve water-level declines and aquifer-system compaction include differential compaction, horizontal seepage stresses, and rotation of a rigid slab (fig. 6). Mechanisms that involve the unsaturated zone include hydrocompaction and increased moisture tension caused by evapotranspiration and water-table decline. Other proposed mechanisms include piping erosion, collapse of mines and caverns, soil rupture during an earthquake, new or

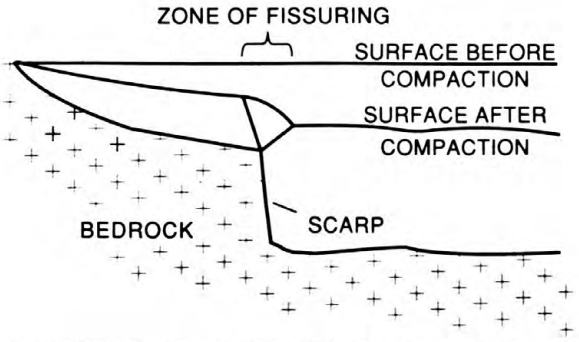

Earth fissuring caused by differential compaction of alluvium over a bedrock scarp

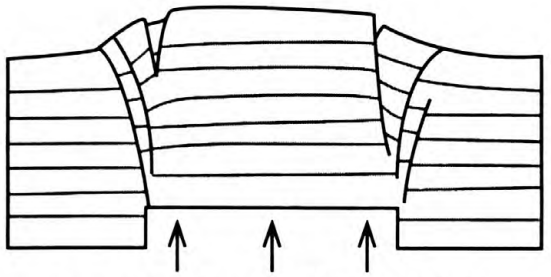

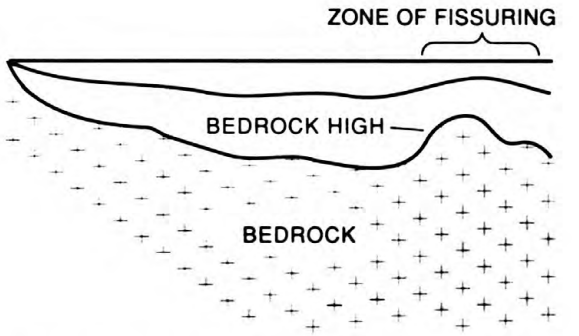

Earth fissuring caused by differential compaction of alluvium over a bedrock high

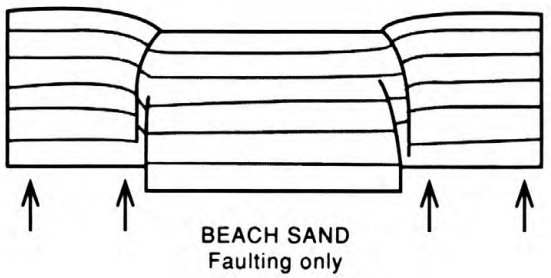

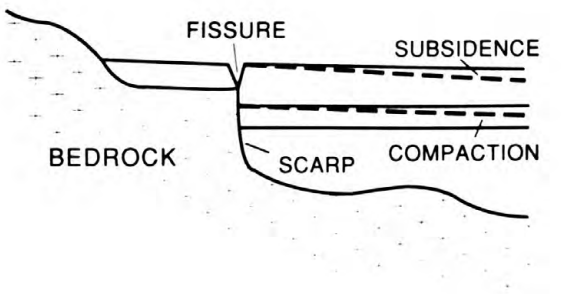

Earth fissuring caused by rotation of alluvial slab about a buried bedrock scarp as a result of compaction of underlying sediments (modified from Bouwer, 1977)

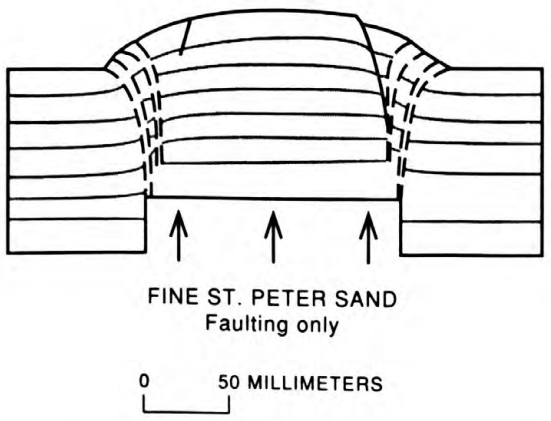

Results of sand-box experiments demonstrating fissuring and faulting phenomena consistent with shear and tensile failure of a body exhibiting differential offset at depth (generalized differential compaction) (modified from Sanford, 1959)

Figure 6.—Possible earth-fissure mechanisms.

renewed faulting, diapirism, and volume changes such as conversion of gypsum to anhydrite and oxidation of organic soils.

Because of the unusual cracks noted at the nearby El Tiro Mine, the earthquake hypothesis proposed by Leonard (1929) cannot be discounted for the fissure that he observed. In general, however, earth fissures occur in areas of low seismicity (Holzer, 1986). In particular, the Basin and Range province in Arizona is an area of low seismicity (Sumner, 1976). Rare earthquakes can cause or trigger fissuring in an area undergoing strain from ground-water decline or other causes.

Fletcher and others (1954) introduced the piping, or subsurface tunnel erosion, hypothesis. Erosional conduits or pipes typically develop in dispersive clayey soils where topographic relief permits seepage velocities high enough to transport fine-grained particles through primary or secondary porosity to a downgradient point of removal. Piping erosion commonly occurs near the edge of an arroyo or steep-sided wash when subsurface tubes develop as conduits for drainage into the arroyo. Heindl and Feth (1955) argued against piping as a sole cause of fissuring because drainage of fissures is internal. Piping takes place within a fissure along its length during development of fissure gullies (Laney and others, 1978), however, and can account for the presence of depressions at the ends of fissures.

Hydrocompaction was proposed by Pashley (1961) as a mechanism for earth fissuring near Casa Grande, Arizona. Hydrocompaction, or near-surface subsidence (Lofgren, 1960), occurs when high-porosity, moisture-deficient sediments compact as they are wetted for the first time since burial (Poland and others, 1972). Hydrocompaction has been noted as a cause of fissuring in alluvial-fan deposits in California (Bull, 1964, 1972; Lofgren, 1969; Riley, 1970b). In Arizona, hydrocompaction has been observed northeast of the town of Marana near the alignment of the Central Arizona Project aqueduct (H.H. Schumann, hydrologist, U.S. Geological Survey, written commun., 1988).

Lofgren (1971, 1972) proposed the hypothesis of horizontal seepage stresses directed toward the center of a deep cone of depression as a mechanism for earth fissuring. The seepage stress originates as a viscous drag of the flowing water on the aquifer skeleton and is either dissipated as heat or converted to work on the grains, translating them in the direction of flow. For this mechanism to cause earth fissuring, the accumulated centripetal translation of the aquifer must be distributed so that tensile strain in the overlying sediments exceeds the strain at failure of those materials.

Bouwer (1977) introduced the hypothesis of rotation of a rigid slab of alluvium around the edge of a buried fault (fig. 6). In Bouwer's model, the compacting alluvium is entirely below the buried fault edge and extends from the fault edge into the center of the basin. The model does not account for subsequent opening of earth fissures between existing fissures and the mountain front.

The mechanism of horizontal shrinkage in the unsaturated zone includes near-surface desiccation and uptake by phreatophytes as well as shrinkage in the deep unsaturated zone by capillary forces. Large-scale polygonal patterns of fissures occur in some playas and are attributed to

near-surface desiccation (Neal and others, 1968). Quasi-polygonal patterns of fissures near Bowie and Willcox, Arizona (Holzer, 1980) were attributed to water uptake by phreatophytes (Anderson, 1978). Holzer and Davis (1976) suggested that gravitational drainage in the deep unsaturated zone after dewatering of an unconfined aquifer could cause horizontal intergranular tensile stresses. Narasimhan (1979) demonstrated numerically that significant volumetric strain could occur from unsaturated drainage and argued that horizontal contraction could cause fissuring of soils.

An early and widely accepted hypothesis of earth-fissure formation is that of differential compaction over a bedrock structure (fig. 6) (Turner and others, 1947; Feth, 1951; Robinson and Peterson, 1962; Schumann and Poland, 1970; Jachens and Holzer, 1979). The bedrock structure could be a buried pediment, bedrock high, or steeply dipping fault. In addition to bedrock structures, sedimentary facies changes or pinchouts can cause lateral changes in compressibility of sediments or in thickness of compressible sediments. Differential compaction occurs when water levels decline and the resulting increase in effective stress is applied to compressible materials of varying thickness. A ground-water barrier, which could be a pre-existing fault or other structure, can cause a differential water-level decline in sediments on opposite sides of the barrier. Greater compaction will occur on the side of the ground-water barrier that has the greater water-level decline. The alluvium overlying the compacting interval flexes as a beam and exhibits tension, which is greatest at the land surface, over a convex upward structure. Fissuring occurs when the tensile strain exceeds the tensile strain at failure.

In this report, the term *generalized differential compaction* is used for the hypothesis of structurally or geometrically controlled elastic deformation that includes the Mohr criterion of failure. This criterion depends on the inherent shear strength of the material and the angle of internal friction of the material (Jaeger and Cook, 1979). Failure is by shear, under the Mohr criterion, when the least principal stress is compressive and by tensile fracture when the least principal stress is tensile. This generalization links vertical offset and horizontal tensile opening as two types of failure resulting from structurally controlled differential compaction.

Sanford (1959) provided an analytical and numerical treatment of the pattern of deformation, associated faults, and tensile fractures that would result from a vertical displacement at depth. His study provided a basis in elastic theory for the hypothesis of generalized differential compaction. Geometric properties such as shape of the displacement and length-width ratio of the deforming layer affect the pattern of deformation more than do the material properties such as Poisson's ratio. Both tensile fractures and faults occur in overlying sediments in response to the displacement at depth. Because the orientation of the principal stress axes varies with depth, the dip of a fracture varies with depth if the angle of internal friction is constant with depth. Scale models of the vertical displacements in clayey sand exhibited both tensile fractures and faults, whereas cohesionless sands exhibited only faults.

Several mechanisms could contribute to initial and subsequent fissure formation and movement in an area. Combinations of effects could hasten fissuring if each of them cause tensile strains to occur at the same time and in the same region. Superposition of complex patterns of

compressive and tensile strains in adjacent areas could reduce the magnitude of local tensile strains, thus delaying or preventing fissuring.

MEASUREMENT OF DEFORMATION AND WATER-LEVEL FLUCTUATIONS

Surveying Stations

Two survey lines, designated TA-1 and Nose (fig. 2, tables 1 and 2), were established in spring 1980 for measurement of horizontal and vertical deformation in subsiding alluvial sediments near the Picacho Mountains. TA-1 survey line consists of 17 stations extending from station A on an outcrop of granite gneiss, assumed to be stable, north 88° west, normal to and beyond the Picacho earth fissure, to station Q. Fissures cross the TA-1 survey line east of station B, between stations B and C, between stations J and K, and between stations K and L. Station K is in an apparent graben block within the fissure zone. Nose survey line consists of 13 stations extending from station AA on an outcrop of granite gneiss, assumed to be stable, north 74° west, approximately normal to and beyond three earth fissures, to station AL. Nose survey line does not cross the Picacho earth fissure but does cross shorter fissures between stations AD and AE, AF and AG, and AH and AI.

Station A is a 50-millimeter-diameter brass cap labeled "USGS A", which was center punched and cemented into a hole drilled into bedrock outcrop. The station is in a small saddle, near the west slope, on the end of the southwest-trending protrusion of bedrock in the NW¼NE¼SW¼, sec. 4, T. 8 S., R. 9 E., Newman Peak 7.5′ quadrangle (fig. 1). The west, south, and southeast slopes of the outcrop are covered with petroglyphs. The station is about 14.6 m higher than the alluvial surface.

Stations B-F and P and Q are iron rods 1.5 m long and 20 mm in diameter. The rods were driven vertically into the ground through the bottoms of holes dug 400 mm deep and 200 mm in diameter. The rods were greased where exposed in the holes, and the holes were filled with concrete to the land surface leaving the rod tips exposed 5 mm or less above the land surface. The rods were greased to allow vertical decoupling between the concrete and the rods to prevent the stations from jacking from expansion and contraction caused by changes in moisture content of the soil surrounding the concrete. The tips of the rods were center punched and punched with letters to designate the stations. Horizontal and vertical instability of these stations was estimated to be less than ±0.5 mm on the basis of the small relative horizontal movements across uncracked soil of dial-gage extensometers with similar rods and concrete and of small relative vertical movements among closely spaced stations in similar alluvium.

Stations G through O are 3-meter-long by 20-millimeter-diameter iron rods driven 1.05 m into the bottoms of 1.5-meter-deep by 300-millimeter-diameter holes that allow the rods to protrude 450 mm above the land surface. Iron pipes 1.5 m long by 100 mm diameter were concreted in the holes so that the pipes projected 410 mm above the land surface, which allowed the rods to project an additional 40 mm above the pipes. The insides of the pipes also were filled with concrete so that the iron rods were centered in the pipes. The iron rods were greased where they

Table 1.--Horizontal distances from station A and altitudes of stations along TA-1 survey line, 1980-84

[Values in meters. Altitude datum is sea level. Values with underlined digits are interpolated. Underlined digits are not significant]

Station	1980		1981		1982	1983	1984
	May 31	December 16	March 15	November 17	March 17	June 6	May 15
			Horizontal distances				
A	0.000	0.000	0.000	0.000	0.000	0.000	0.000
B	216.178	216.173	216.176	216.173	216.173	216.177	216.179
C	412.554	412.555	412.562	412.567	412.570	412.584	412.583
D	569.514	569.516	569.521	569.525	569.529	569.539	569.539
E	729.325	729.329	729.329	729.335	729.341	729.344	729.349
F	909.038	909.036	909.039	909.038	909.042	909.051	909.049
G	1,008.273	1,008.269	1,008.275	1,008.277	1,008.276	1,008.284	1,008.284
H	1,027.015	1,027.012	1,027.017	1,027.020	1,027.019	1,027.028	1,027.028
I	1,045.769	1,045.765	1,045.772	1,045.774	1,045.774	1,045.783	1,045.783
J	1,054.156	1,054.149	1,054.155	1,054.158	1,054.157	1,054.165	154.167
K	1,060.059	1,060.054	1,060.061	1,060.067	1,060.066	1,060.075	1,060.077
L	1,065.770	1,065.765	1,065.771	1,065.775	1,065.774	1,065.780	1,065.780
M	1,075.059	1,075.053	1,075.060	1,075.065	1,075.065	1,075.075	1,075.077
N	1,096.566	1,096.559	1,096.568	1,096.572	1,096.571	1,096.582	1,096.587
O	1,111.922	1,111.916	1,111.922	1,111.923	1,111.925	1,111.934	1,111.935
P	1,272.271	1,272.272	1,272.275	1,272.284	1,272.283	1,272.292	1,272.295
Q	1,422.361	1,422.357	1,422.365	1,422.374	1,422.368	1,422.379	1,422.376
			Altitude of stations				
A	527.4176	527.4176	527.4176	527.4176	527.4176	527.4176	527.4176
B	512.7901	512.7897	512.7896	512.7891	512.7889	512.7881	512.7875
C	509.8407	509.8304	509.8257	509.8129	509.8067	509.7835	509.656
D	507.1149	507.0992	507.0922	507.0727	507.0632	507.0280	507.009
E	504.8230	504.8036	504.7950	504.7709	504.7593	504.7159	504.6824
F	502.3826	502.3622	502.3531	502.3278	502.3155	502.2698	502.2346
G	501.9720	501.9517	501.9426	501.9179	501.9059	501.8597	501.8244
H	501.9312	501.9110	501.9018	501.8766	501.8649	501.8185	501.7834
I	501.8046	501.7849	501.7759	501.7506	501.7391	501.6927	501.6576
J	501.6292	501.6086	501.5997	501.5749	501.5635	501.5172	501.4821
K	501.6081	501.5866	501.5779	501.5522	501.5411	501.4950	501.4600
L	501.1246	501.0942	501.0838	501.0506	501.0386	500.9889	500.9536
M	501.0396	501.0105	501.0011	500.9680	500.9564	500.9075	500.8722
N	500.5917	500.5630	500.5559	500.5215	500.5110	500.4641	500.4294
O	500.7641	500.7346	500.7252	500.6923	500.6810	500.6319	500.5966
P	498.1885	498.1576	498.1486	498.1138	498.1037	498.0538	498.0186
Q	496.9990	496.9595	496.9508	496.9112	496.9025	496.8508	496.8157

Table 2.--Horizontal distances from station AA and altitudes of stations along Nose survey line, 1980-84

[Values in meters. Altitude datum is sea level]

Station	1980		1981		1982	1983	1984
	May 31	December 16	March 15	November 17	March 17	June 6	May 15
	Horizontal distances						
AA	0.000	0.000	0.000	0.000	0.000	0.000	0.000
BA	10.	10.	10.	10.	10.	10.	10.
AB	110.530	110.531	110.531	110.530	110.5301	10.536	110.528
AC	157.722	157.700	157.699	157.699	157.698	157.704	157.696
AD	176.649	176.627	176.627	176.626	176.625	176.633	176.626
AE	194.967	194.946	194.945	194.945	194.944	194.952	194.945
AF	211.584	211.563	211.562	211.562	211.561	211.570	211.564
AG	231.123	231.102	231.101	231.100	231.099	231.111	231.106
AH	245.076	245.055	245.054	245.054	245.053	245.064	245.060
AI	263.368	263.352	263.350	263.353	263.352	263.372	263.372
AJ	282.124	282.108	282.107	282.110	282.109	282.127	282.141
AK	431.058	431.064	431.065	431.067	431.069	431.089	431.084
AL	582.294	582.300	582.303	582.303	582.305	582.320	582.316
	Altitude of stations						
AA	505.9680	505.9680	505.9680	505.9680	505.9680	505.9680	505.9680
BA	--------	--------	--------	499.1516	499.1517	499.1519	499.1519
AB	498.6557	498.6568	498.6576	498.6556	498.6561	498.6574	498.6579
AC	499.1842	499.1854	499.1851	499.1842	499.1841	499.1846	499.1849
AD	499.1481	499.1483	499.1492	499.1467	499.1472	499.1482	499.1481
AE	498.9245	498.9251	498.9249	498.9232	498.9231	498.9237	498.9233
AF	498.8333	498.8332	498.8330	498.8306	498.8317	498.8316	498.8318
AG	498.7895	498.7884	498.7881	498.7846	498.7849	498.7835	498.7815
AH	498.6457	498.6440	498.6442	498.6406	498.6405	498.6390	498.6368
AI	498.3211	498.3142	498.3111	498.3020	498.3000	498.2873	498.2789
AJ	498.2553	498.2488	498.2462	498.2364	498.2344	498.2212	498.2129
AK	496.9218	496.9080	496.9053	496.8882	496.8845	496.8642	496.8491
AL	496.0811	496.0608	496.0550	496.0317	496.0246	495.9951	495.9735

contacted concrete. Ball bearings 25.39 mm in diameter, welded to 9.5-millimeter-diameter threaded rods, were screwed into threads previously drilled and tapped into the ends of the iron rods. The threaded rods were secured with lock nuts and thread-locking compound. This procedure produced stations that consisted of ball bearings about 450 mm above the land surface and that were stabilized by concrete and iron pipes. Horizontal and vertical instability of these stations was estimated to be less than ±0.5 mm on the basis of relative horizontal and vertical movements of closely spaced similar monuments in similar alluvium.

Station AA of the Nose survey line was a 50-millimeter-diameter brass cap labeled "USGS AA" set on a bedrock bench on a northwest-trending promontory in the NE¼NE¼NW¼, sec. 4, T. 8 S., R. 9 E, Newman Peak 7.5' quadrangle (fig. 2). The station was 6.8 m higher than the alluvial surface. Stations AB, AK, and AL were set like stations B-F of the TA-1 survey line. Stations AC through AJ were set like stations G through O. Station BA, set in November 1981, was a 25-millimeter-long steel carriage bolt that was 8 mm in diameter and was driven into a 7-millimeter-diameter hole drilled into bedrock at the contact between bedrock and the alluvial surface. Stations AA through AJ were destroyed by construction of the Central Arizona Project aqueduct in the summer of 1986.

Surveying Procedures

Slope distances from A to B, C, D, E, F, G, O, P, and Q and from AA to AB, AC, AJ, AK, and AL were measured using a Hewlett-Packard[1] HP3808A Electronic Distance Meter (EDM), Hewlett-Packard retroprisms, and tripods with plumb rods that display instrument or target height. Setup inaccuracies were estimated to be less than 1 mm on the basis of repeated tests at the calibration base line at the University of Arizona. The instrument was calibrated in October 1980 and July 1984. Deviation from calibration over that period was less than 5×10^{-5} percent. The instrument is specified for ±5 mm $\pm 2 \times 10^{-4}$ percent accuracy and is capable of $\pm 1 \times 10^{-4}$ percent accuracy if temperature and pressure corrections are made for differences between the refractive index of air for which the instrument is set and the refractive index of air along the line of sight at the time of measurement. In several tests for drift of instrument constant done at the University of Arizona calibration base line and at a National Geodetic Survey baseline near Salt Lake City, Utah, the instrument constant did not depart from 0 mm or drift at a resolution of 1 mm. For this reason, the ±5-mm part of the instrument specification was discounted. Estimated contributions to error for horizontal distances were 1 mm for combination of setup and change in instrument constant and 1 mm for station instability. These contributions and the $\pm 1 \times 10^{-4}$ percent accuracy give a root mean square error of 1.4 mm $\pm 1 \times 10^{-4}$ percent. The maximum error was 3 mm or ±1.5 mm along the two survey lines.

For the short measurements of 1.5 km or less along the two survey lines, end-point temperature and pressure measurements were made at the heights of the instrument and the retroprism. Temperature measurements were

---

[1]Use of trade names in this report is for identification purposes only and does not constitute endorsement by the U.S. Geological Survey.

made using shaded, calibrated thermometers or thermistors. Pressure measurements were made using Wallace and Tiernan aneroid barometers that were calibrated against a U.S. Weather Service mercury barometer. The standard deviation and mean were determined from ten replications of each distance measurement. Temperature and pressure corrections were applied to the mean value of the replications to give a measured slope distance. The measured slope distance was then trigonometrically reduced to horizontal distance using the target height, the instrument height, and the altitudes of the stations as determined from leveling surveys.

Slope distances between nearest pairs of stations from G-O and AC-AJ were periodically measured using a tape extensometer. The instrument incorporates two built-in dial gages and a surveying tape, which has registration pinholes punched at 50.8-millimeter intervals. One dial gage measures tape tension by the deflection of a proving ring. The second dial gage measures the distance from the punched hole in which the registration pin is locked to a reference point within the instrument. The instrument is mounted on a ball-bearing station and the surveying tape is stretched and connected to another ball-bearing station. Because of random errors of ±0.07 mm in the locations of the registration pinholes and nonstandard conditions of tape stretch and sag, the error of tape-extensometer distance measurements may be as high as ±1.0 mm for some measurements. Because tape tension is constant at 146 newtons (N) for all measurements, tape sag, as a function of length and tape tension, is constant for repeated measurements between pairs of stations. Thus, a constant error in the absolute distance between a pair of stations is eliminated as an error in the difference of distances between the pair for repeated measurements. The instrument measures changes in distance over intervals of as much as 30 m with a repeatability of ±0.13 mm or $\pm 4 \times 10^{-4}$ percent. The temperature of the tape during a measurement was monitored at a point near the center of the tape using a calibrated surface-measuring thermistor. Five replications, each with its own temperature correction, were made for each pair of stations. Data were keyed into a hand-held data logger that stored the data for transfer to a computer. The data logger also used previously stored data to calculate and display in the field the displacement and strain since the last set of measurements, using the previous distance and the current distance between stations. The tape extensometer was calibrated before and after each set of field measurements on a frame that had been measured with a caliper with an accuracy of 0.03 mm and a calibration traceable to the U.S. Bureau of Standards. Slope distances among tape-extensometer station pairs were trigonometrically reduced to horizontal distances using leveling data.

Tape-extensometer data were proportionally adjusted to agree with the EDM data. The EDM is more accurate over long distances; tape extensometry is more accurate over short distances. The only tape extensometer stations measured by the EDM were the end points of the tape extensometer lines (points G and O and points AC and AJ) (tables 1 and 2). The differences before adjustment between EDM distances and concatenated tape-extensometer distances from G to O and from AC to AJ amounted to no more than 2 mm in more than 103 m or 2×10^{-3} percent.

Leveling was performed along the two survey lines using a Zeiss Ni-1 level. Some Ni-1 levels have exhibited errors caused by magnetic effects (Holdahl and others, 1986). These errors are considered to be insignificant for the TA-1 and Nose survey lines because the lines are

oriented approximately east to west, or orthogonal to the earth's magnetic field, and no power lines were nearby at the times of the surveys. In addition, the same instrument was used for all surveys, and the change in altitudes of a station is of interest in this study, not the absolute altitude itself. The datum for establishing stations A and AA is the bench mark near station B at an altitude of 514.19 m. The leveling was double run and adhered to 1st Order, Class 1 standards (Federal Geodetic Control Committee, 1974) with the exception that only one rod was used. Because maximum sight length was 30 m, refraction errors were considered to be insignificant (Holdahl, 1981). Balance of sightings was assured by chaining and staking instrument locations for subsequent runs. The allowable closures for 1st Order, Class 1 standards are 3.6 mm for TA-1 survey line and 2.1 mm for Nose survey line. Corresponding nominal accuracies are ±1.8 mm and ±1.1 mm and apply to each line as a whole. Relative altitudes among closely spaced points should be more accurate than the nominal accuracy. For this reason, values of altitudes of stations in tables 1 and 2 are given to 0.1 mm.

All horizontal distances by EDM and tape extensometer were measured for both Nose and TA-1 survey lines for all seven observation times. All points on Nose survey line and stations F-Q on TA-1 survey line were leveled for all observation times. Stations A-E on the TA-1 survey line were leveled on May 31, 1980, and May 15, 1984, only. Altitudes of points B-Q (table 1) for December 16, 1980, through June 6, 1983, were interpolated by apportioning subsidence of stations B-F on the basis of proportional elapsed time between May 31, 1980, and May 15, 1984. Agreement between rates of subsidence for points AK and C, at about the same distance from the mountain front, is 3.2 percent and for points AL and D, also at about the same distance from the mountain front, is 5.7 percent; therefore, the interpolation scheme seems reasonable. Altitudes of points B-F for intermediate intervals between surveys, however, are not significant beyond 0.01 m. Relative altitudes from point F to point Q are consistent on the basis of the leveling performed from F to Q for all observation times.

Monitoring of Horizontal Movement and Water-Level Fluctuations

In the fall of 1980, a buried horizontal invar-wire extensometer (Schulz and Burford, 1977; Duffield and Burford, 1973) was installed spanning an interval of 29.61 m across the Picacho earth fissure along a line parallel to and 4 m north of the TA-1 survey line (fig. 2). The piers of the extensometer were placed opposite stations I and M, which are 29.29 m apart, so that strains measured using the horizontal extensometer could be compared with strains measured from station I to M.

The invar wire is strung through a 200-millimeter-diameter PVC pipe, buried at an average depth of 2 m. The extensometer piers and recording instrumentation are housed in two 1.2-meter-diameter fiberglass vaults, which extend from a depth of 0.2 m to 2.4 m below the land surface. The vaults are divided into upper and lower sections and sealed against moisture and air leakage around the piers, pipe, and covers. The upper section of each vault is filled with polystyrene "peanuts" in plastic bags for thermal insulation. Piers consisting of 2-meter-long by 100-millimeter-diameter iron pipe are set in concrete below the bottoms of the vaults so that the tops of the piers project about 450 mm above the vault floors. The

invar wire, which is attached to the west or anchor pier, 4 m north of station M, is suspended in catenary inside the pipe, and extends to the east or instrument pier, 4 m north of station I. There, the wire passes over a low-friction pulley sector mounted on the pier and supports a freely suspended 2-kilogram counterweight. The core of a linear-variable-differential-transformer (LVDT) displacement transducer is strung on the invar wire above the counterweight. Thus, changes in horizontal distance between the piers are converted to vertical movement of a core inside a transducer. A micrometer head with a resolution of 1 μm attached to the instrument pier can be adjusted to contact a reference surface fixed to the invar wire for calibration of the transducer as well as for maintaining continuity of measurement during resets of the invar-wire anchor point on the west pier.

A battery-powered data logger and audiocassette recorder were used to record the horizontal displacement data, water-level data in piezometer 1 at well TA-1, barometric pressure, power-supply voltage, and data from three thermistors measuring temperatures in the vaults and in the pipe. Resolution of the displacement transducer with the data logger was 1 μm. Resolution of the thermistors was 0.07 °C. The water-level sensor in piezometer 1 was a continuous-purge "bubbler" system incorporating a 0-170 kPa-gage pressure transducer with a resolution of 6 mm of water-level fluctuation and a 6-mm copper-tube air line. The barometric transducer was a 0-100 kPa-absolute pressure transducer with a resolution of 4 mm of water-level fluctuation.

Values of altitude of water level and horizontal movement are noon values extracted from an array of data that was sampled 10 times a day for more than 4 years and totaled more than 100,000 values (tables 3 and 4). Corrections to the horizontal-movement record include many resets of the invar-wire anchor and a temperature correction. The temperature correction used all three temperature records and was based on a thermal calibration done on September 10, 1981. Corrections to the water-level record include many resets of air-line length and periodic well taping. Test hole TA-1 subsided from an altitude of 502.13 m in May 1980 to 501.98 m in May 1984. This subsidence was applied as a correction to the water-level data by linear interpolation over the period of record.

Several gaps exist in the recorded data. Most of these gaps were due to failures of the data logger, probably because of effects of nearby lightning strikes on long signal leads to thermistors and pressure transducers. Lightning protection was used on all leads into the data logger and is believed to have saved the data logger from serious damage on many occasions. Nevertheless, the data logger had to be repaired several times by the manufacturer. Other gaps were caused by pressure-transducer failures, thermistor failures, and premature battery-voltage dropoff.

Measurement Errors

Several factors, which are grouped under the term measurement error, contributed to difficulties in interpreting displacements measured along the survey lines and strains measured by the horizontal extensometer. These factors include bench-mark instability, tripod-setup error, EDM

Table 3.--Altitude of water level in piezometer 1, test hole TA-1, 1980-84

[Values in meters. Altitude datum is sea level. Location is in SE¼SW¼NE¼, sec. 5, T. 8 S., R. 9 E., Salt and Gila River Baseline and Meridian]

	1980		1981											
Day	Nov.	Dec.	Jan.	Feb.	Mar.	Apr.	May	June	July	Aug.	Sept.	Oct.	Nov.	Dec.
1	------	361.36	361.09	363.06	364.62	361.51	361.25	362.02	------	358.78	------	357.89	357.97	360.06
2	------	360.85	361.50	363.39	364.74	361.44	361.72	361.97	------	359.02	------	358.30	358.56	360.10
3	------	360.75	361.18	363.53	364.85	361.29	362.16	362.10	------	359.62	357.54	358.16	358.47	360.16
4	------	361.26	361.05	363.58	364.88	361.16	362.28	362.16	------	359.31	357.50	358.25	358.50	360.22
5	------	361.52	361.02	363.63	365.00	361.15	361.84	362.02	------	359.33	357.79	358.68	358.50	360.38
6	------	361.69	361.55	363.69	365.02	361.17	361.56	361.59	------	359.03	357.54	358.56	358.41	360.40
7	------	361.87	361.73	363.62	365.04	361.07	361.34	361.39	------	358.96	357.92	358.55	358.28	360.44
8	------	362.00	361.49	363.12	365.03	361.01	361.32	361.24	359.79	359.05	358.09	358.52	358.21	360.48
9	------	362.12	361.36	363.22	365.00	360.98	361.25	361.22	359.65	359.18	358.25	358.50	358.17	360.53
10	------	362.26	361.30	363.62	364.76	360.95	361.26	------	359.47	359.38	357.93	358.55	358.18	360.59
11	------	362.42	361.58	363.81	364.38	360.85	361.21	------	359.34	359.33	357.91	358.50	358.40	360.77
12	------	------	361.84	363.87	364.14	360.73	360.24	------	359.63	359.08	358.21	358.49	358.99	360.90
13	------	------	362.27	363.88	364.00	360.75	361.08	------	360.27	------	358.27	358.44	359.21	360.98
14	361.51	------	362.50	364.03	363.85	360.73	360.88	------	360.39	------	358.30	358.51	359.32	361.05
15	361.58	------	362.69	364.20	------	360.67	360.66	------	359.98	------	358.41	358.08	359.43	361.06
16	361.57	------	362.84	364.26	------	360.62	360.52	------	359.55	------	358.39	358.14	359.49	361.16
17	361.57	------	362.95	------	------	360.56	360.37	------	359.41	------	358.44	358.28	358.94	361.23
18	361.75	------	363.05	------	------	360.48	360.35	------	359.41	------	358.60	358.84	358.97	361.24
19	361.90	------	363.18	------	------	360.34	360.95	------	359.36	------	358.69	359.13	358.94	361.29
20	361.42	------	363.30	------	------	360.29	361.20	------	359.33	------	358.83	358.82	359.03	361.30
21	360.78	------	363.36	------	------	360.36	361.45	------	359.32	------	358.83	359.08	359.06	361.41
22	360.64	------	363.44	------	------	360.48	361.58	------	359.37	------	358.96	358.72	359.10	361.36
23	360.41	361.03	363.55	363.81	362.53	361.21	361.73	------	359.25	------	358.90	358.49	359.15	361.37
24	------	361.49	363.66	364.01	362.35	361.84	361.69	------	359.21	------	358.88	358.45	359.26	361.37
25	------	361.91	363.77	364.12	362.22	361.85	361.96	------	359.08	------	358.39	358.27	359.39	361.54
26	------	362.09	363.81	364.27	362.06	361.77	362.15	------	359.10	------	358.08	358.22	359.40	361.65
27	------	361.66	363.76	364.43	361.88	361.78	362.07	------	359.04	------	357.80	358.27	359.68	361.77
28	361.22	361.43	363.88	364.52	361.76	361.54	361.89	------	358.95	------	357.63	358.36	359.49	361.83
29	361.32	361.28	363.42	------	361.68	361.38	361.90	------	358.89	------	357.51	358.05	359.73	361.77
30	361.41	361.21	363.18	------	361.66	361.19	361.77	------	359.05	------	357.45	357.87	359.89	361.59
31	------	361.15	363.10	------	361.55	------	361.72	------	358.87	------	------	357.79	------	361.06

Table 3.--Altitude of water level in piezometer 1, test hole TA-1, 1980-84--Continued

	1982											
Day	Jan.	Feb.	Mar.	Apr.	May	June	July	Aug.	Sept.	Oct.	Nov.	Dec.
1	360.76	363.31	364.30	------	361.76	359.94	358.93	------	------	------	359.31	360.55
2	360.77	363.36	364.36	------	361.74	359.95	358.88	------	------	------	359.36	360.65
3	361.15	363.45	364.39	------	361.67	359.80	358.85	------	------	------	359.33	360.73
4	361.27	363.43	364.36	------	361.57	359.96	358.82	------	------	------	358.89	360.86
5	361.62	363.07	364.30	------	361.58	360.10	358.83	------	------	------	358.68	360.96
6	361.29	363.34	364.26	------	361.91	360.15	358.73	------	------	------	358.55	360.97
7	361.18	363.37	364.27	------	362.15	360.23	359.11	------	------	------	358.47	360.55
8	361.61	363.54	364.31	------	362.31	360.21	359.54	------	------	------	358.47	360.37
9	361.85	363.49	363.98	------	362.29	360.26	359.49	------	------	------	358.89	360.65
10	362.05	363.52	363.82	------	362.27	360.26	359.11	------	------	------	359.20	360.91
11	362.18	363.53	363.75	------	362.31	360.26	358.92	------	------	------	359.36	361.02
12	362.26	363.60	363.68	------	361.95	360.28	358.81	------	------	------	359.45	361.16
13	362.17	363.64	363.65	------	361.65	360.30	358.79	------	------	------	359.12	361.28
14	362.35	363.68	363.89	------	361.43	360.41	358.75	------	------	358.28	358.96	361.32
15	362.48	363.67	364.04	------	360.60	358.97	358.14	------	------	358.14	359.00	361.37
16	362.53	363.68	364.11	------	360.72	358.73	358.05	------	------	358.05	359.48	361.45
17	362.33	363.78	364.04	------	360.81	358.57	357.99	------	------	357.99	359.72	361.55
18	362.20	363.90	363.80	------	360.67	358.48	357.92	------	------	357.92	359.86	361.62
19	362.10	363.96	363.88	------	360.60	360.21	358.39	------	------	357.87	359.96	361.69
20	362.02	363.96	363.97	------	360.48	360.27	358.33	------	------	357.95	360.05	361.76
21	362.00	364.02	363.98	------	360.41	360.26	358.35	------	------	357.97	360.14	361.75
22	362.30	364.09	363.99	361.66	360.34	359.80	358.33	------	------	357.99	360.28	361.80
23	362.49	364.12	364.02	361.55	360.22	359.51	358.58	------	------	358.12	360.35	361.93
24	362.68	364.15	------	361.51	360.10	359.33	358.77	------	------	358.55	360.40	361.95
25	362.81	364.18	------	361.44	360.01	359.18	358.44	------	------	358.84	360.37	361.97
26	362.91	364.20	------	361.38	360.15	359.09	358.28	------	------	359.03	360.42	362.02
27	362.97	364.25	------	361.33	360.11	358.97	358.73	------	------	359.08	359.97	362.06
28	363.08	364.27	------	361.34	360.09	358.86	359.09	------	------	358.67	359.86	362.11
29	363.15	------	------	361.79	360.15	358.84	359.28	------	------	358.98	360.29	362.19
30	363.15	------	------	361.95	360.06	358.96	359.22	------	------	359.22	360.52	362.27
31	363.24	------	------	360.00	------	------	------	------	------	359.27	------	361.83

Table 3.--Altitude of water level in piezometer 1, test hole TA-1, 1980-84--Continued

	1983											
Day	Jan.	Feb.	Mar.	Apr.	May	June	July	Aug.	Sept.	Oct.	Nov.	Dec.
1	361.99	------	------	------	362.52	361.26	360.80	------	------	------	363.40	363.99
2	362.16	------	------	------	362.43	360.90	360.74	------	------	------	363.08	364.12
3	362.21	------	------	------	362.27	360.79	360.69	------	------	------	362.81	364.15
4	361.77	------	------	------	362.40	360.75	360.66	------	------	------	362.63	364.26
5	361.56	------	------	363.77	362.44	360.71	360.66	------	------	------	362.45	364.30
6	362.00	------	------	363.67	362.15	360.69	360.63	------	------	------	362.34	364.36
7	362.22	------	------	363.62	362.00	360.64	360.60	------	------	------	362.25	364.45
8	362.34	------	------	363.55	361.94	360.55	360.57	------	------	------	362.18	364.55
9	362.45	------	------	363.18	361.88	360.58	360.54	------	------	------	362.13	364.63
10	------	------	------	363.02	361.83	360.79	360.51	------	------	------	362.22	364.65
11	------	------	------	363.00	361.74	360.88	360.50	------	------	------	362.72	364.71
12	------	------	------	363.15	361.68	360.91	360.53	------	------	------	362.97	364.80
13	------	------	------	363.15	361.72	360.88	360.59	------	------	------	363.11	364.84
14	------	------	------	363.13	361.88	360.87	360.61	------	------	------	362.68	364.92
15	------	------	------	363.12	361.90	360.88	360.63	------	------	------	362.46	364.99
16	------	------	------	363.08	361.97	360.95	360.65	------	------	------	362.35	365.01
17	------	------	------	363.08	361.92	361.02	360.63	------	------	------	362.28	365.10
18	------	------	------	363.09	362.04	361.04	360.61	------	------	------	362.28	365.13
19	------	------	------	363.05	362.15	361.04	360.60	------	------	363.19	362.21	365.20
20	------	------	------	363.05	362.39	361.08	360.58	------	------	363.18	362.21	365.30
21	------	------	------	363.03	362.15	361.09	360.60	------	------	363.21	362.32	365.32
22	------	------	------	362.99	361.99	361.02	360.55	------	------	363.33	362.88	365.36
23	------	------	------	363.08	361.91	360.97	360.41	------	------	363.41	362.67	365.41
24	------	------	------	363.15	361.58	360.94	------	------	------	363.53	362.59	365.48
25	------	------	------	363.50	361.35	360.95	------	------	------	363.60	363.16	365.55
26	------	------	------	363.19	361.20	360.91	------	------	------	363.68	363.40	365.60
27	------	------	------	363.06	361.18	360.86	------	------	------	363.74	363.23	365.67
28	------	------	------	363.01	361.37	360.85	------	------	------	363.78	363.54	365.69
29	------	------	------	362.74	361.09	360.95	------	------	------	363.83	363.73	365.68
30	------	------	------	362.58	361.02	360.86	------	------	------	363.90	363.85	365.74
31	------	------	------	------	361.22	------	------	------	------	363.95	------	365.81

Table 3.--Altitude of water level in piezometer 1, test hole TA-1, 1980-84--Continued

	1984											
Day	Jan.	Feb.	Mar.	Apr.	May	June	July	Aug.	Sept.	Oct.	Nov.	Dec.
1	365.87	364.74	366.18	364.05	362.79	360.96	359.97	------	359.15	359.06	358.96	359.15
2	365.93	364.66	365.73	363.97	362.74	360.91	360.06	------	359.17	358.99	358.94	359.20
3	365.95	364.60	366.09	363.91	362.70	360.98	360.21	------	359.22	359.01	358.91	359.20
4	366.01	364.57	366.21	363.85	362.73	360.87	359.91	------	359.24	359.11	358.97	359.13
5	366.08	364.62	366.34	363.82	362.72	360.67	359.80	------	359.15	358.97	359.02	359.11
6	366.11	364.71	366.46	363.81	362.64	360.39	359.75	------	359.08	358.94	358.98	359.18
7	366.18	364.70	366.08	364.27	362.56	360.23	359.98	------	359.06	358.98	358.97	359.18
8	366.21	364.69	365.68	364.62	362.52	360.10	359.71	------	359.15	359.02	358.95	359.22
9	366.25	364.77	365.48	364.77	362.53	359.98	359.89	------	359.14	359.04	358.92	359.23
10	366.27	365.36	365.22	364.27	362.51	359.98	359.63	------	359.18	359.04	358.97	359.23
11	366.36	365.60	365.06	364.06	362.47	360.23	359.53	------	359.22	359.05	358.93	359.24
12	366.36	365.77	364.99	363.91	362.45	360.40	359.21	------	359.25	359.06	358.90	359.27
13	366.42	365.92	364.82	363.73	362.40	360.54	359.04	------	359.21	359.06	358.97	359.30
14	366.43	366.08	364.67	363.57	362.38	360.51	------	------	359.22	359.07	359.04	------
15	366.43	366.03	364.62	363.46	362.81	360.40	------	------	359.22	359.11	358.99	------
16	366.50	365.59	364.56	363.45	362.53	360.34	------	------	359.13	359.09	358.96	------
17	366.42	365.41	364.54	363.37	362.40	360.26	------	------	359.08	359.15	358.92	------
18	366.36	365.37	364.53	363.25	362.32	360.12	------	------	359.11	359.11	358.99	------
19	366.41	365.84	364.49	363.13	362.27	359.92	------	------	359.07	359.04	359.04	------
20	366.39	365.45	364.45	363.01	362.23	359.72	------	------	359.04	359.02	359.08	------
21	365.91	365.36	364.41	363.05	362.19	359.77	------	359.48	359.05	359.01	359.11	------
22	365.68	365.83	364.48	363.07	362.11	359.63	------	359.49	358.95	358.99	359.04	------
23	365.61	365.48	364.46	363.16	361.74	360.08	------	359.42	358.92	358.99	359.03	------
24	365.90	365.35	364.46	363.13	361.55	359.77	------	359.35	358.93	358.97	359.08	------
25	365.39	365.40	364.47	363.11	361.41	359.68	------	359.30	358.93	358.96	359.11	------
26	365.37	365.83	364.40	363.05	361.24	359.61	------	359.26	358.94	358.96	359.07	------
27	365.27	366.04	364.29	362.97	361.19	359.55	------	359.23	359.05	358.95	359.06	------
28	364.95	366.13	364.16	362.94	361.31	359.49	------	359.20	359.15	358.95	359.09	------
29	364.87	366.27	364.20	362.83	361.30	359.38	------	359.17	359.13	358.94	359.08	------
30	365.08	------	364.24	362.81	361.27	359.78	------	359.15	359.09	358.96	359.11	------
31	364.84	------	364.09	------	361.30	------	------	359.21	------	358.94	------	------

Table 4.--Horizontal movement across Picacho earth fissure near test hole TA-1, 1980-84

[Values in millimeters are the noon daily measurements of the invar-wire extensometer, indicating change (positive = closing; negative = opening) from initial setting on starting date, November 14, 1980. Location is in SE¼SW¼NE¼, sec. 5, T. 8 S., R. 9 E., Salt and Gila River Baseline and Meridian]

	1980		1981											
Day	Nov.	Dec.	Jan.	Feb.	Mar.	Apr.	May	June	July	Aug.	Sept.	Oct.	Nov.	Dec.
1	-----	0.032	0.233	0.642	0.764	0.564	-0.176	-0.570	-1.149	-1.631	------	-2.777	-2.791	-2.670
2	-----	.037	.236	.656	.774	.543	-.180	-.585	-1.184	-1.647	------	-2.778	-2.782	-2.650
3	-----	.042	.241	.662	.788	.528	-.181	-.590	-1.208	-1.659	-2.162	-2.772	-2.764	-2.634
4	-----	.045	.244	.663	.800	.499	-.178	-.593	-1.219	-1.673	-2.168	-2.762	-2.756	-2.619
5	-----	.052	.247	.666	.816	.471	-.177	-.599	-1.223	-1.709	-2.191	-2.757	-2.748	-2.604
6	-----	.060	.254	.668	.819	.436	-.187	-.606	-1.232	-1.741	-2.215	-2.764	-2.741	-2.587
7	-----	.072	.261	.664	.827	.404	-.204	-.614	-1.262	-1.773	-2.240	-2.774	-2.734	-2.572
8	-----	.082	.259	.662	.837	.372	-.204	-.628	-1.296	-1.803	-2.263	-2.789	-2.728	-2.557
9	-----	.099	.264	.668	.840	.345	-.207	-.640	-1.329	-1.832	-2.285	-2.804	-2.723	-2.541
10	-----	.116	.266	.673	.878	.320	-.204	-.654	-1.365	-1.867	-2.294	-2.816	-2.717	-2.526
11	-----	.133	.264	.687	.880	.293	-.208	-.667	-1.395	-1.893	-2.299	-2.829	-2.710	-2.510
12	-----	-----	.282	.697	.875	.275	-.237	-.677	-1.415	-1.897	-2.305	-2.837	-2.700	-2.492
13	-----	-----	.312	.707	.873	.254	-.260	-.684	-1.415	------	-2.331	-2.847	-2.689	-2.471
14	0.000	-----	.336	.718	.862	.232	-.282	-.693	-1.409	------	-2.358	-2.847	-2.681	-2.451
15	.006	-----	-----	.730	-----	.207	-.314	-.707	-1.408	------	-2.383	-2.860	-2.672	-2.432
16	.008	-----	-----	.730	-----	.186	-.344	-.722	-1.424	------	-2.410	-2.852	-2.666	-2.422
17	.016	-----	-----	-----	-----	.165	-.373	-.735	-1.439	------	-2.439	-2.845	-2.671	-2.408
18	.026	-----	-----	-----	-----	.142	-.393	-.752	-1.443	------	-2.469	-2.835	-2.673	-2.390
19	.034	-----	-----	-----	-----	.119	-.415	-.766	-1.448	------	-2.495	-2.829	-2.682	-2.382
20	.037	-----	-----	-----	-----	.080	-.443	-.784	-1.455	------	-2.517	-2.820	-2.691	-2.373
21	.022	-----	-----	-----	-----	.070	-.473	-.800	-1.462	------	-2.539	-2.812	-2.700	-2.360
22	.015	-----	-----	-----	-----	.048	-.469	-.817	-1.471	------	-2.553	-2.807	-2.707	-2.357
23	.000	.194	-----	.731	.725	.019	-.469	-.836	-1.502	------	-2.575	-2.800	-2.715	-2.348
24	-----	.200	-----	.736	.703	-.004	-.484	-.872	-1.504	------	-2.599	-2.792	-2.721	-2.339
25	-----	.209	-----	.729	.680	-.027	-.488	-.936	-1.518	------	-2.624	-2.790	-2.724	-2.331
26	-----	.209	-----	.740	.656	-.053	-.488	-.960	-1.529	------	-2.647	-2.784	-2.725	-2.323
27	-----	.222	-----	.752	.645	-.072	-.503	-1.000	-1.546	------	-2.671	-2.777	-2.717	-2.315
28	.016	.225	-----	.758	.643	-.096	-.518	-1.045	-1.560	------	-2.698	-2.769	-2.719	-2.307
29	.022	.227	.612	-----	.638	-.124	-.530	-1.080	-1.581	------	-2.726	-2.780	-2.714	-2.303
30	.029	.229	.625	-----	.629	-.157	-.552	-1.115	-1.598	------	-2.755	-2.791	-2.691	-2.316
31	-----	.230	.634	-----	.595	-----	-.570	-----	-1.615	------	------	-2.799	------	-2.328

Table 4.--Horizontal movement across Picacho earth fissure near test hole TA-1, 1980-84--Continued

	1982											
Day	Jan.	Feb.	Mar.	Apr.	May	June	July	Aug.	Sept.	Oct.	Nov.	Dec.
1	-2.335	-2.080	-1.839	------	-2.198	-2.733	-3.386	------	-3.389	-3.426	-3.496	-3.175
2	-2.335	-2.068	-1.832	------	-2.203	-2.744	-3.396	-3.586	-3.389	-3.428	-3.498	-3.158
3	-2.328	-2.054	-1.831	------	-2.206	-2.765	-3.409	-3.555	-3.403	-3.432	-3.500	-3.134
4	-2.308	-2.049	-1.827	------	-2.213	-2.788	-3.423	-3.542	-3.420	-3.437	-3.498	-3.116
5	-2.303	-2.045	-1.830	------	-2.218	-2.812	-3.438	-3.548	-3.434	-3.442	-3.503	-3.105
6	-2.298	-2.038	-1.828	------	-2.222	-2.836	-3.453	-3.544	-3.447	-3.441	-3.507	-3.093
7	-2.292	-2.029	-1.827	------	-2.226	-2.856	-3.459	-3.540	-3.449	-3.441	-3.513	-3.082
8	-2.280	-2.025	-1.829	------	-2.228	-2.879	-3.463	-3.540	-3.448	-3.443	-3.519	-3.081
9	-2.270	-2.013	-1.853	------	-2.231	-2.906	-3.466	-3.541	-3.448	-3.441	-3.518	-3.065
10	-2.265	-2.007	-1.875	------	-2.234	-2.933	-3.473	-3.544	-3.448	-3.438	-3.512	-3.046
11	-2.254	-2.000	-1.900	------	-2.239	-2.962	-3.486	-3.546	-3.444	-3.441	-3.513	-3.010
12	-2.250	-1.988	-1.922	------	-2.251	-2.988	-3.499	-3.542	-3.439	-3.443	-3.499	-2.986
13	-2.243	-1.975	-1.928	------	-2.263	-3.014	-3.513	-3.536	-3.437	-3.447	-3.498	-2.965
14	-2.227	-1.966	-1.921	------	-2.280	-3.039	-3.529	-3.529	-3.434	-3.460	-3.498	-2.951
15	-2.223	-1.959	-1.918	------	------	-3.049	-3.545	-3.525	-3.430	-3.468	-3.494	-2.932
16	-2.217	-1.951	-1.912	------	------	-3.056	-3.562	-3.524	-3.426	-3.476	-3.495	-2.913
17	-2.210	-1.936	-1.911	------	------	-3.064	-3.579	-3.521	-3.424	-3.484	-3.490	-2.901
18	-2.210	-1.934	-1.927	------	------	-3.083	-3.594	-3.523	-3.415	-3.491	-3.470	-2.890
19	-2.217	-1.918	-1.930	------	-2.444	-3.090	-3.611	-3.527	-3.416	-3.495	-3.441	-2.875
20	-2.212	-1.906	-1.925	------	-2.470	-3.118	-3.645	-3.535	-3.418	-3.499	-3.414	-2.861
21	-2.207	-1.893	-1.929	------	-2.500	-3.148	-3.670	-3.542	-3.419	-3.502	-3.384	-2.855
22	-2.191	-1.886	-1.929	-2.123	-2.533	-3.173	-3.677	-3.545	-3.423	-3.502	-3.349	-2.844
23	-2.179	-1.881	-1.932	-2.130	-2.565	-3.198	-3.690	-3.549	-3.413	-3.505	-3.327	-2.823
24	-2.169	-1.877	------	-2.138	-2.599	-3.226	-3.707	-3.546	-3.412	-3.505	-3.304	-2.807
25	-2.159	-1.867	------	-2.144	-2.631	-3.254	-3.723	-3.494	-3.412	-3.508	-3.282	-2.793
26	-2.150	-1.855	------	-2.152	-2.646	-3.278	-3.740	-3.474	-3.411	-3.507	-3.267	-2.784
27	-2.142	-1.849	------	-2.159	-2.662	-3.308	-3.730	-3.456	-3.419	-3.506	-3.249	-2.775
28	-2.125	-1.843	------	-2.167	-2.674	-3.339	-3.720	-3.442	-3.419	-3.501	-3.231	-2.768
29	-2.117	------	------	-2.181	-2.688	-3.362	-3.694	-3.427	-3.417	-3.498	-3.216	-2.756
30	-2.105	------	------	-2.191	-2.708	-3.374	------	-3.412	-3.424	-3.497	-3.197	-2.749
31	-2.089	------	------	------	-2.721	------	------	-3.399	------	-3.498	------	-2.744

Table 4.--Horizontal movement across Picacho earth fissure near test hole TA-1, 1980-84--Continued

	1983											
Day	Jan.	Feb.	Mar.	Apr.	May	June	July	Aug.	Sept.	Oct.	Nov.	Dec.
1	-2.732	------	------	------	-2.216	-2.578	-2.797	-3.014	-2.920	------	-2.202	-1.982
2	-2.724	------	------	------	-2.234	-2.570	-2.803	-3.035	-2.926	------	-2.194	-1.973
3	-2.718	------	------	------	-2.242	-2.594	-2.815	-3.056	-2.934	------	-2.185	-1.964
4	-2.713	------	------	------	-2.248	-2.615	-2.825	-3.080	-2.946	------	-2.180	-1.955
5	-2.709	------	------	-2.179	-2.256	-2.635	-2.833	-3.106	-2.956	------	-2.173	-1.945
6	-2.706	------	------	-2.168	-2.275	-2.652	-2.843	-3.132	-2.967	------	-2.167	-1.933
7	-2.700	------	------	-2.167	-2.294	-2.668	-2.853	-3.157	-2.976	------	-2.160	-1.923
8	-2.693	------	------	-2.167	-2.314	-2.690	-2.858	-3.179	-2.989	------	-2.160	-1.911
9	-2.687	------	------	-2.183	-2.335	-2.722	-2.868	-3.188	-3.000	------	-2.155	-1.906
10	------	------	------	-2.195	-2.355	-2.727	-2.877	-3.183	-3.011	------	-2.148	-1.904
11	------	------	------	-2.207	-2.376	-2.724	-2.887	-3.174	-3.038	------	-2.140	-1.893
12	------	------	------	-2.203	-2.394	-2.726	-2.899	-3.166	-3.068	------	-2.134	-1.893
13	------	------	------	-2.201	-2.408	-2.724	-2.906	-3.161	-3.097	------	-2.127	-1.883
14	------	------	------	-2.195	-2.408	-2.725	-2.914	-3.159	-3.120	------	-2.123	-1.877
15	------	------	------	-2.193	-2.405	-2.728	-2.921	-3.143	-3.135	------	-2.115	-1.871
16	------	------	------	-2.191	-2.404	-2.732	-2.927	-3.112	------	------	-2.109	-1.867
17	------	------	------	-2.187	-2.405	-2.733	-2.934	-3.078	------	------	-2.102	-1.859
18	------	------	------	-2.187	-2.405	-2.733	-2.941	-3.040	------	------	-2.097	-1.856
19	------	------	------	-2.185	-2.408	-2.733	-2.949	-3.013	------	-2.391	-2.092	-1.847
20	------	------	------	-2.188	-2.407	-2.733	-2.957	-2.990	------	-2.378	-2.080	-1.844
21	------	------	------	-2.185	-2.406	-2.737	-2.965	-2.973	------	-2.359	-2.076	-1.840
22	------	------	------	-2.185	-2.406	-2.738	-2.970	-2.957	------	-2.342	-2.063	-1.835
23	------	------	------	-2.182	-2.407	-2.742	-2.967	-2.947	------	-2.324	-2.051	-1.829
24	------	------	------	-2.179	-2.426	-2.745	-2.960	-2.938	------	-2.310	-2.040	-1.824
25	------	------	------	-2.178	-2.450	-2.751	-2.950	-2.930	------	-2.294	-2.033	-1.818
26	------	------	------	-2.178	-2.480	-2.760	-2.941	-2.925	------	-2.275	-2.026	-1.806
27	------	------	------	-2.169	-2.501	-2.767	-2.934	-2.923	------	-2.261	-2.014	-1.800
28	------	------	------	-2.175	-2.507	-2.773	-2.934	-2.919	------	-2.249	-2.006	-1.799
29	------	------	------	-2.186	-2.529	-2.779	-2.953	-2.916	------	-2.235	-1.997	-1.789
30	------	------	------	-2.201	-2.550	-2.788	-2.975	-2.915	------	-2.223	-1.987	-1.781
31	------	------	------	------	-2.554	------	-2.994	-2.916	------	-2.212	------	-1.777

Table 4.--Horizontal movement across Picacho earth fissure near test hole TA-1, 1980-84--Continued

	1984											
Day	Jan.	Feb.	Mar.	Apr.	May	June	July	Aug.	Sept.	Oct.	Nov.	Dec.
1	-1.772	-1.719	-1.676	-1.894	-2.115	-2.623	-3.486	------	-2.952	-3.241	-3.041	-2.938
2	-1.767	-1.723	-1.676	-1.906	-2.123	-2.654	-3.491	------	-2.964	-3.237	-3.039	-2.929
3	-1.767	-1.722	-1.677	-1.916	-2.133	-2.672	-3.485	------	-2.979	-3.236	-3.038	-2.916
4	-1.763	-1.723	-1.678	-1.928	-2.141	-2.696	-3.478	------	-2.997	-3.219	-3.036	-2.912
5	-1.762	-1.723	-1.678	-1.942	-2.148	-2.732	-3.479	------	-3.009	-3.217	-3.034	-2.888
6	-1.753	-1.721	-1.672	-1.955	-2.160	-2.772	-3.485	------	-3.025	-3.218	-3.031	-2.884
7	-1.749	-1.718	-1.671	-1.964	-2.167	-2.818	-3.493	------	-3.045	-3.207	-3.027	-2.851
8	-1.743	-1.717	-1.672	-1.962	-2.175	-2.864	-3.503	------	-3.060	-3.189	-3.027	-2.851
9	-1.737	-1.712	-1.698	-1.969	-2.182	-2.910	-3.513	------	-3.075	-3.182	-3.026	-2.845
10	-1.735	-1.712	-1.688	-1.969	-2.191	-2.949	-3.529	------	-3.092	-3.164	-3.024	-2.829
11	-1.727	-1.708	-1.695	-1.975	-2.202	-2.970	-3.559	------	-3.097	-3.151	-3.023	-2.819
12	-1.718	-1.705	-1.703	-1.983	-2.214	-2.986	-3.593	------	-3.102	-3.143	-3.022	-2.805
13	-1.718	-1.699	-1.714	-1.988	-2.227	-3.010	-3.626	------	-3.115	-3.127	-3.023	-2.793
14	-1.720	-1.697	-1.723	-1.995	-2.240	-3.023	------	------	-3.130	-3.114	-3.022	------
15	-1.714	-1.695	-1.735	-2.003	-2.251	-3.037	------	------	-3.147	-3.105	-3.022	------
16	-1.709	-1.689	-1.745	-2.011	-2.267	-3.053	------	------	-3.151	-3.096	-3.022	------
17	-1.711	-1.694	-1.752	-2.017	-2.279	-3.073	------	------	-3.160	-3.090	-3.018	------
18	-1.708	-1.688	-1.762	-2.026	-2.296	-3.095	------	------	-3.172	-3.085	-3.017	------
19	-1.703	-1.687	-1.769	-2.037	-2.310	-3.126	------	------	-3.183	-3.052	-3.016	------
20	-1.701	-1.684	-1.778	-2.058	-2.322	-3.162	------	------	-3.203	-3.057	-3.014	------
21	-1.696	-1.679	-1.787	-2.064	-2.335	-3.187	------	-2.992	-3.227	-3.056	-3.014	------
22	-1.701	-1.680	-1.798	-2.068	-2.349	-3.222	------	-2.973	-3.254	-3.056	-3.011	------
23	-1.700	-1.681	-1.803	-2.072	-2.381	-3.250	------	-2.961	-3.271	-3.055	-3.009	------
24	-1.701	-1.677	-1.808	-2.078	-2.417	-3.285	------	-2.951	-3.279	-3.052	-3.004	------
25	-1.711	-1.679	-1.818	-2.083	-2.458	-3.314	------	-2.943	-3.287	-3.053	-2.994	------
26	-1.712	-1.679	-1.823	-2.088	-2.492	-3.344	------	-2.938	-3.295	-3.051	-2.979	------
27	-1.716	-1.677	-1.842	-2.090	-2.519	-3.378	------	-2.938	-3.283	-3.051	-2.964	------
28	-1.715	-1.674	-1.848	-2.092	-2.536	-3.412	------	-2.938	-3.273	-3.050	-2.944	------
29	-1.718	-1.676	-1.857	-2.095	-2.551	-3.441	------	-2.939	-3.261	-3.047	-2.945	------
30	-1.721	------	-1.874	-2.101	-2.568	-3.467	------	-2.942	-3.249	-3.043	-2.942	------
31	-1.720	------	-1.881	------	-2.585	------	------	-2.946	------	-3.042	------	------

instrument error, leveling-closure error, vertical component of a nearly horizontal resultant vector, and local movement of a station.

Several changes in procedure would reduce errors and establish error bands for some of these difficulties. Establishment of a survey array that consists of a series of quadrilaterals connected with common sides across critical areas would help in the determination of local movement of stations. Differences in movement for stations at about the same distance from the fissure would give an estimate of error for local movements. Sets of three closely spaced bench marks in representative sediments would provide a standard deviation and estimate of error for bench-mark stability for both horizontal distance measurements and leveling. For tape extensometry, diagonals of the quadrilaterals could not exceed 30 m. If lengths of both diagonals of a quadrilateral are measured as well as the lengths of all the sides and if the stations are leveled, the figure is overdetermined and measurement error can be estimated.

Instrument offset for the EDM for a particular set of measurements could be calculated using a three-point test at the measured line. The test consists of measuring three closely spaced colinear points A, B, and C, with the EDM set up on an end point, A, then remeasuring with the EDM set up on the middle point, B. The difference between the calculated distance, BC, from the first measurement and the measured distance, BC, from the second measurement is the instrument offset. The remainder of EDM instrument error would be determined at a calibration base line, as was done in the study. Tripod setup error for EDM measurements consists simply of a determination of the standard deviation of replications of tripod setup at a station.

Perhaps the greatest decrease in EDM error would be achieved by moving the instrument to a station near the fissure. This would result in shorter measurements across the area where the most accuracy is needed. The tie to bedrock would be made with a target station on bedrock. The instrument station near the fissure could be incorporated in a three-point test and in a comparison between the tape extensometer and EDM for each set of measurements.

A trigonometric check was made to determine whether the displacements measured with the horizontal extensometer could actually be vector components of differential subsidence across the fissure and was done for several reasons. First, horizontal strain across the area from station G through O, as measured by the EDM, was less than 20 microstrain. Second, the resolution of the horizontal extensometer was 0.03 microstrain or 1.0 μm, a small value compared with the net fault offset of about 20 mm. Third, the trigonometric effect, called the instrument-height, target-height correction, is known to be significant in repeated strain measurements using EDM when the lines depart from horizontal. Using the values 29.29 m for the station spacing between stations I and M, 3.533 mm for horizontal displacement, and 7.8 mm for vertical offset for March 17, 1981, to November 17, 1981, it was calculated that the piers of the horizontal extensometer would have to differ in altitude by 15 m for vertical offset to account for the strain measured by the horizontal extensometer. A similar calculation indicated that an initial difference in altitude of 10 mm would give an apparent extension of 3 μm for 7.8 mm of differential subsidence. The conclusion was that the horizontal extensometer measured actual horizontal strain but may have included as much as 10 μm of apparent horizontal movement caused by vertical slip across the fissure.

The horizontal extensometer had few problems. Eliminating the problem of vertical component of almost horizontal strain would entail incorporating the extensometer piers in the repeated surveys and making the trigonometric correction. The consistent nature of the record from the horizontal extensometer suggests that horizontal station instability of a pier is considerably less than 1 mm and may be smaller than the 50 μm/yr determined by Wyatt (1982) in weathered granodiorite.

CORRELATION OF HORIZONTAL STRAIN WITH WATER-LEVEL FLUCTUATIONS

The character of horizontal movement of the fissure was smooth, with no indication of sudden opening or closing at the level of resolution of the instrumentation, which was 1 μm and ten samples per day. The fissure exhibited seasonal opening from mid-March to August or September, followed by closing until mid-March (fig. 4). Maximum opening of the fissure during the study period was 3.740 mm and occurred from March 14, 1981, to October 15, 1981.

Water levels in the deep piezometers reached lows of 355 to 357 m during the summers of 1980, 1981, and 1982. In 1983, lows were 358 to 360 m; and, in 1984, lows were about 358 m. Maximum opening of the fissure during the study period occurred with the minimum water levels in 1982 (fig. 4). Although the water-level record at the study site does not extend to before 1979, earlier records at Eloy indicate that annual minimum water levels in 1980 and 1981 were the lowest since record began in 1965 (Epstein, 1987).

The early part of the graph showing water-level fluctuation and horizontal movement (fig. 7) to about November 1981 exhibits mostly irreversible or inelastic behavior. This inelastic behavior, which has a fairly flat slope and specific horizontal strain of 17 microstrain/m of water-level decline, may dominate when new low water levels are reached. Elastic or reversible behavior dominates during subsequent periods until new seasonal lows are reached. Steeper slope and lower specific horizontal strain of 5 microstrain/m of water-level decline are typical of the elastic behavior.

Small steep-sided or nearly vertical excursions are evident in the graphs showing water-level fluctuation and horizontal movement (figs. 7 and 8). These departures from the general trend of the relation were caused by short-term water-level fluctuations owing to brief cessation of nearby pumping during summer drawdown and brief pumping during winter recovery. The departures indicate that horizontal movement of the fissure is less responsive to short-term water-level fluctuations than to seasonal fluctuations.

Horizontal movement of the fissure was highly correlated with water-level fluctuations in the deep piezometers, TA-1-1 and TA-3-1 (figs. 4 and 8), and moderately well correlated for the shallow piezometer, TA-3-2. Pearson correlation coefficients (Sokal and Rohlf, 1969) were calculated for sections of the graphs in figure 8. Because of the largely irreversible character of fissure opening during 1981, the correlograms were separated into two sections. The separation was made at November 1, 1981, during a transition period from largely inelastic behavior during 1981 to

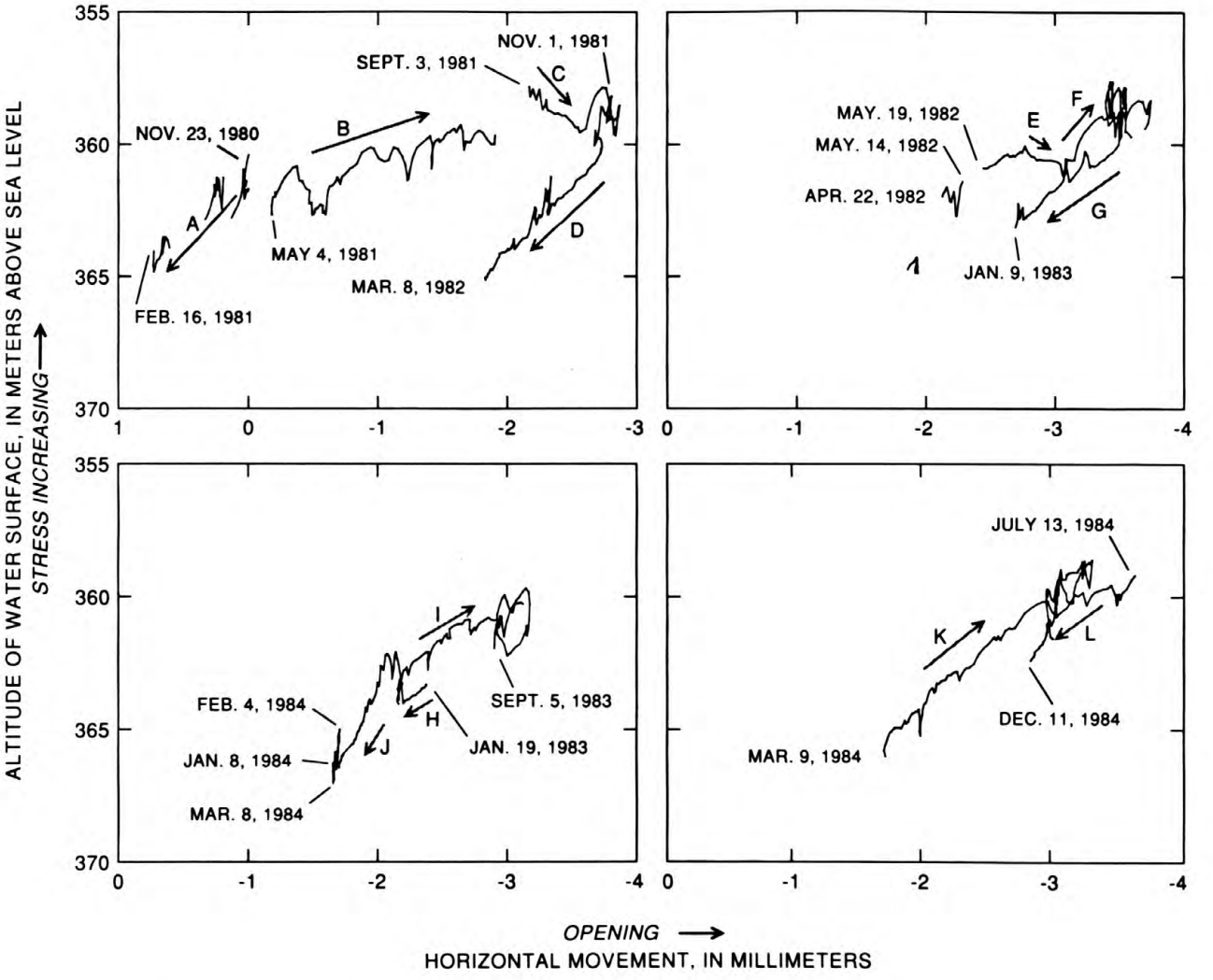

Figure 7.—Relation between horizontal movement across earth fissure and water-level fluctuations in deep piezometer TA-1-1. Gray arrows, letters A-L, and selected dates indicate time increasing along curve.

predominantly elastic behavior in subsequent years. Correlation coefficients between horizontal movement and TA-1-1 were 0.913 for the early period, November 14, 1980, to October 31, 1981, and 0.925 for the later period, November 1, 1981, to December 13, 1984. Corresponding values for TA-3-1 were 0.923 and 0.913, respectively. Correlation coefficients between water-level fluctuation in shallow piezometer TA-3-2 and horizontal strain were 0.891 for the early period and 0.678 for the later period.

Correlation coefficients between differences in water levels and horizontal strain were considerably lower than those between water-level fluctuations and horizontal strain (figs. 4 and 8). Coefficients for the difference between TA-3-2 and TA-3-1, which represent possible vertical seepage stresses are 0.569 for the early period and 0.045 for the later period. Coefficients for the difference between TA-1-1 and TA-3-1, which represent possible horizontal seepage stresses, were -0.164 for the early period and -0.415 for the later period.

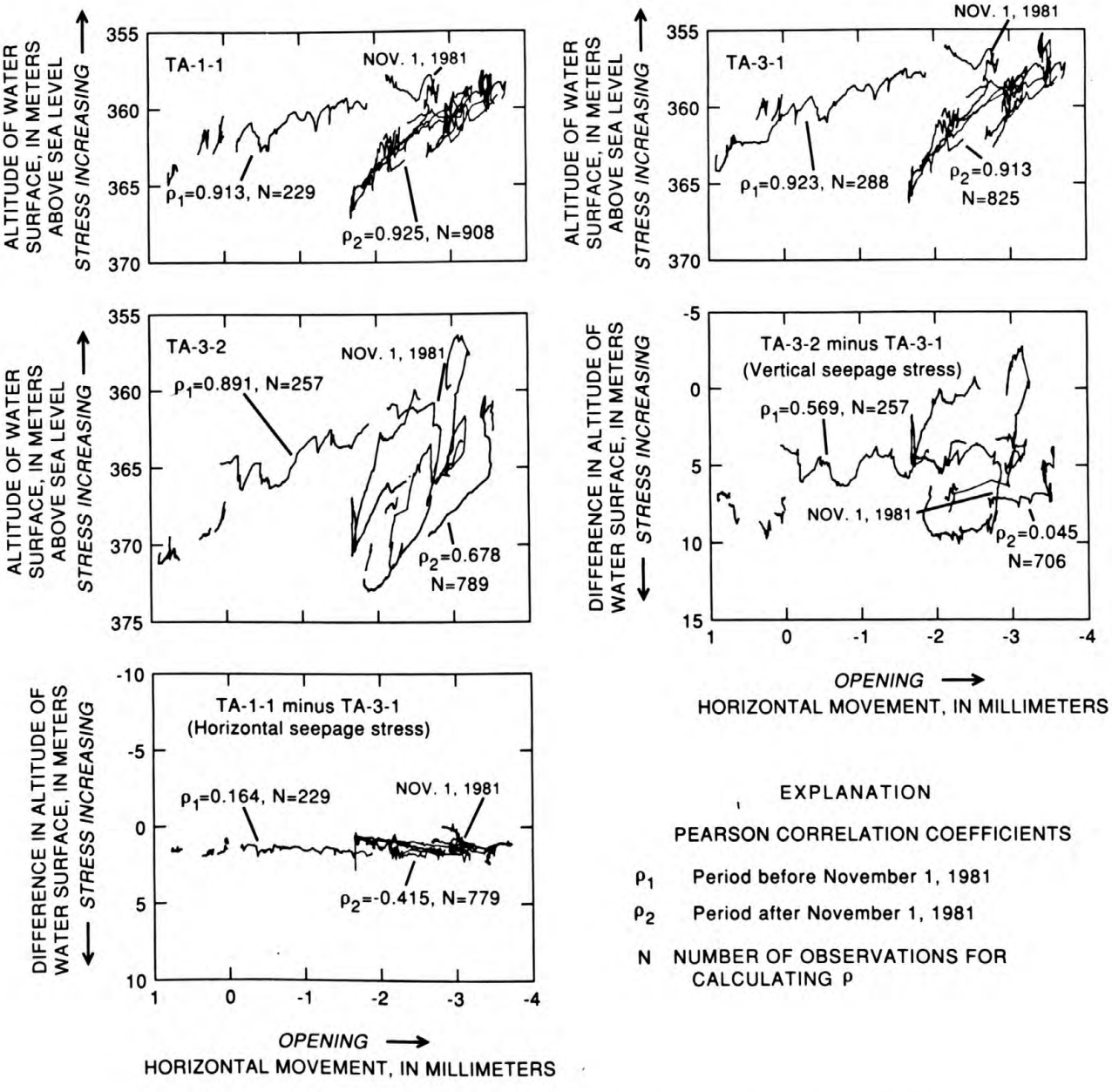

Figure 8.—Correlation of horizontal movement with water-level fluctuations in piezometers.

The water-level fluctuations in the deep piezometers are indicative of changes in effective stress that cause aquifer compaction. The high correlation between horizontal movement and deep water-level fluctuation is consistent with the hypothesis that differential compaction in the deep section of the aquifer is the forcing function for horizontal movement across the fissure.

Horizontal movement of the fissure also was highly correlated with compaction of the aquifer system at Eloy, although no direct causal

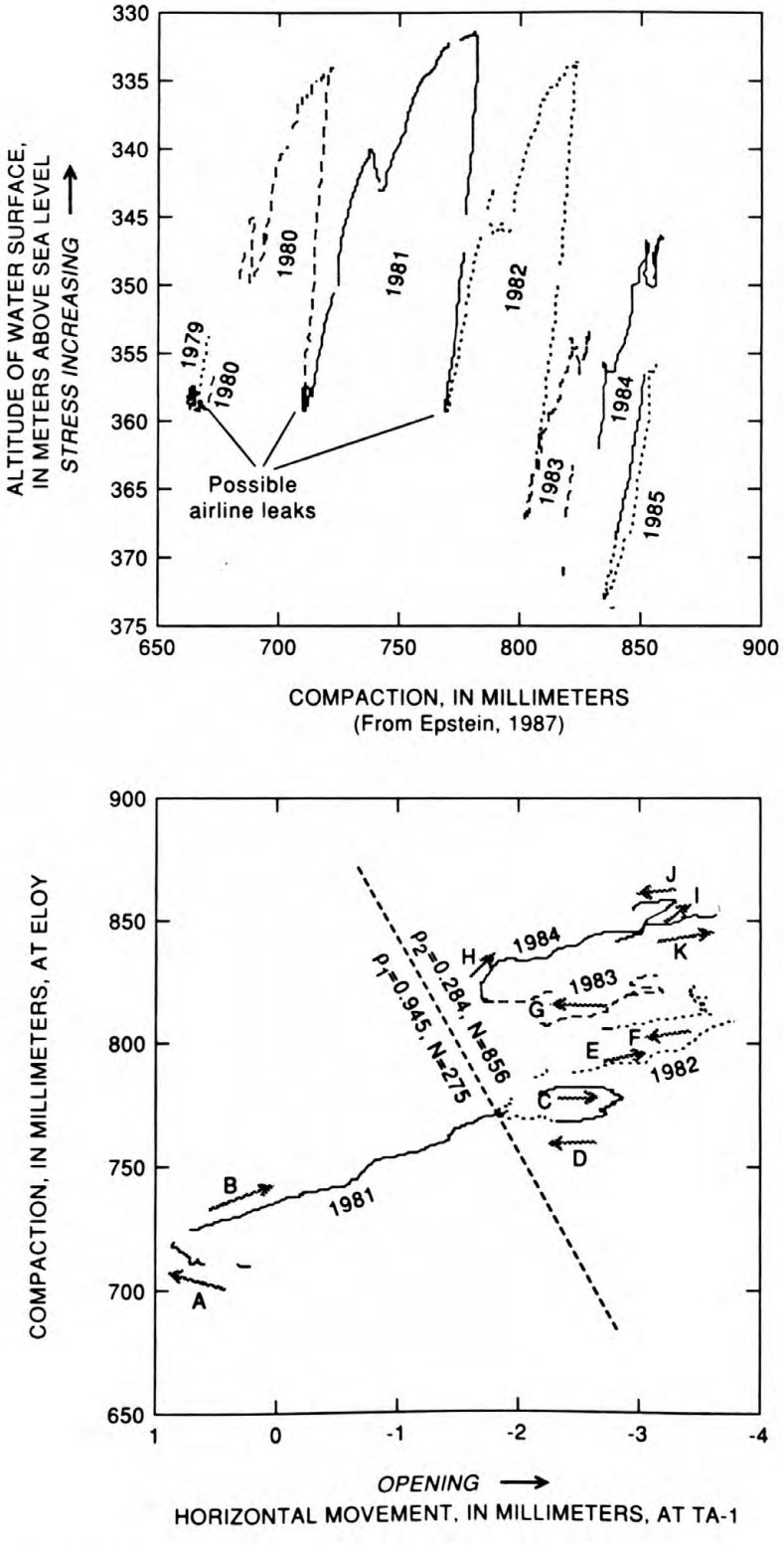

Figure 9.—Relation between water-level fluctuations and compaction at Eloy and correlation of horizontal movement at TA-1 with compaction at Eloy. Arrows, letters A-K, and years indicate time increasing along curve.

relation is inferred (fig. 9). The correlation coefficient between horizontal movement and compaction at Eloy was -0.945 for November 14, 1980, to October 31, 1981. The correlation coefficient was -0.284 for November 1, 1981, to December 13, 1984. The graph of compaction and horizontal movement is linear during most periods of water-level decline, increasing compaction, and fissure opening. Successive hysteresis loops in the Eloy stress-compaction graph (fig. 9) are shifted to the right, indicating a component of irreversible compaction. This shift probably reflects delayed response of low-permeability units to sustained drawdown, superimposed on the elastic response to the cyclic loading caused by seasonal water-level fluctuations. This effect could account for the upward shift in segments of the horizontal-strain and compaction correlogram and the low correlation coefficient of -0.284 for November 1981 to December 1984.

Horizontal movement is marginally correlated with water-level fluctuations in shallow piezometer TA-3-2 (fig. 8). The correlation coefficient between horizontal movement and TA-3-2 was 0.891 for November 14, 1980, to October 31, 1981, and 0.678 for November 1, 1981, to December 13, 1984. The pore-pressure changes indicated by the water-level fluctuations in TA-3-2 probably are indicative of changes in effective stresses in the upper part of the middle silt unit. The resulting compaction could be laterally uniform and thus might not contribute to the differential compaction that is the probable cause of horizontal strain across the fissure.

The correlation is low between horizontal movement at the fissure and differences in altitude of water surfaces (figs. 5 and 8). The difference in altitude of water surfaces between two piezometers is equal to the seepage stress accumulated between the two points if a flow path exists between the points. The seepage energy is dissipated as heat along the flow path or is converted to work on the grains by viscous drag of the flowing water on the grains. The correlation coefficient of horizontal movement is as low as 0.045 for the particular vertical seepage stress at TA-3 that is represented by the difference in water levels between TA-3-2 and TA-3-1. The correlation coefficient for horizontal seepage stress between TA-1-1 and TA-3-1 is -0.164. Low correlation coefficients indicate a lack of causal relation between the fissure movement and the two seepage stresses.

A direct correlation does not appear to exist between horizontal movement and rainfall (fig. 4). Episodes of fissure opening at other fissures near the Picacho Mountains have been correlated with rainfall-runoff events (Boling, 1987); therefore, it is notable that the Picacho earth fissure did not exhibit any sudden openings during rainstorms during the study period. In a general way, rainfall was inversely correlated with fissure movement. During 1983-85, which were years of greater-than-average rainfall, a combination of increased recharge and reduced pumping probably caused the recovery of water levels. This recovery could have caused the reduction in the rate of fissure opening.

Placement of piezometers in intervals in which pore-pressure changes reflect ongoing compaction is crucial to the correct understanding of the stress-strain relation involved in the deformation. When TA-1-2 was vandalized, data on shallow pore-pressure changes on the upthrown side of

the fissure that would have contributed to the understanding of deformation at TA-1 were lost. The additional piezometer would have enabled comparison of shallow water levels to determine whether the fissure is a hydrologic barrier in the silt unit. Also, the data would have enabled an analysis of shallow horizontal seepage stresses between TA-1-2 and TA-3-2 and vertical seepage stresses between TA-1-2 and TA-1-1 on the upthrown side of the fissure.

In the correlograms showing water-level fluctuation and horizontal movement, the presence of nearly vertical excursions and hysteresis loops (figs. 7 and 8), on the time scales of short pumping cycles and annual water-level fluctuations, respectively, as well as different slopes for the different sections of the curves can be explained by consolidation theory of an aquifer system that comprises interbedded fine- and coarse-grained sediments. The essential assumption is that flexuring caused by differential compaction drives the horizontal strains in the overlying sediments. Extrapolation from stress-strain analyses of vertical borehole-extensometer data (Riley, 1970a; Helm, 1975, 1976; Epstein, 1987) can account for the phase lag and varying slopes exhibited in the correlograms. Alternatively, a quasi-black-box rheological model might be applied if the aquifer is considered to be a homogeneous material. Such a model might be a modified Kelvin substance with two coefficients relating stress or water-level fluctuation and strain magnitudes and one coefficient relating strain rate to stress (Jaeger and Cook, 1979).

Placement of additional piezometers in the deeper part of the silt unit probably would have provided additional insight into the deformation process. A head gradient may exist from the lower part of the silt unit to the basal gravel. Pore-pressure changes measured in the lower part of the silt probably would be better correlated with horizontal strain at the land surface than are pore-pressure changes measured in the basal gravel.

SURVEYED HORIZONTAL AND VERTICAL DISPLACEMENTS

The origins of station trajectories along the Nose and TA-1 survey lines are their topographic locations (fig. 10). The scales of horizontal and vertical movement are rake scales. The vertical and horizontal displacements are both exaggerated 1,000 times, preserving an undistorted vector representation of the trajectories. A single trajectory represents the path that the station followed in the vertical plane of the survey line, with the origin of a vector placed at the end point of the preceding vector. Because of the magnification of the displacements in relation to the scale of the profile, it appears that closely spaced stations have collided but, in fact, they have moved only slightly in relation to each other. The dates of the surveys are indicated on each graph as well as on the time series plots of water-level fluctuations and horizontal movement (figs. 4 and 5). Combined trajectories were selected instead of separate time series plots of all the horizontal and vertical displacements of stations because of the small number of surveys and the large number of stations and to present graphically the two-dimensional aspect of vector displacements.

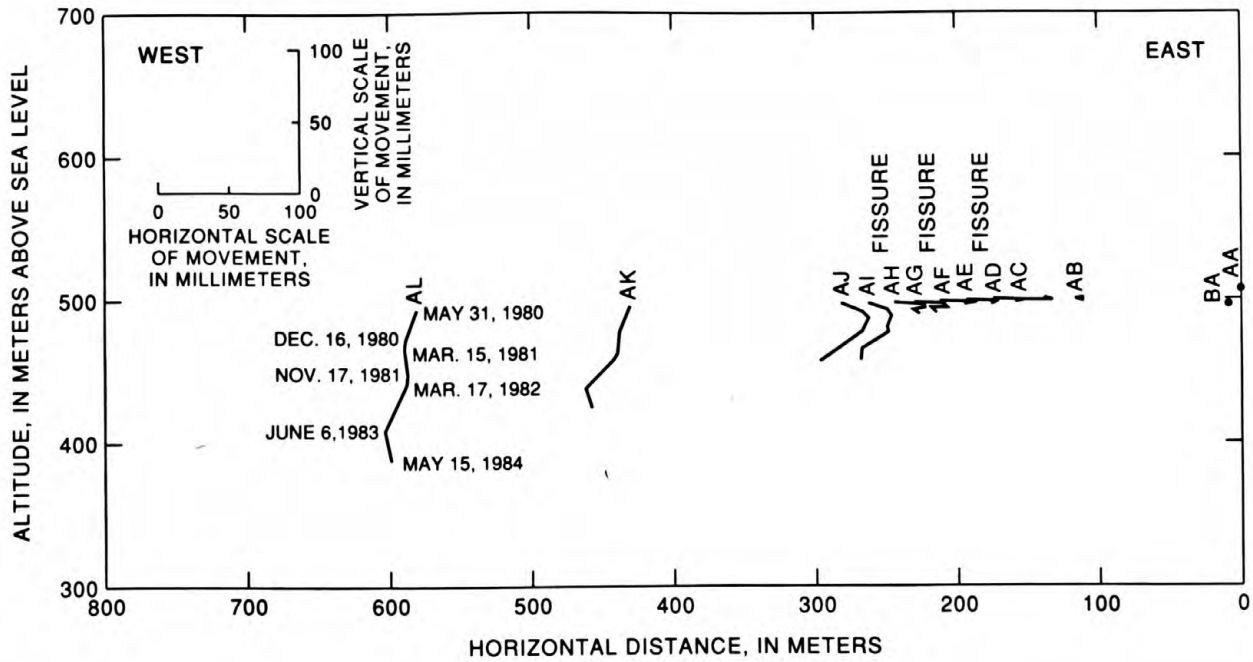

Figure 10.—Station trajectories along Nose survey line, 1980-84, with station AA as a reference frame.

Movements Along Nose Survey Line

Seven surveys were done using station AA, which is set in bedrock, as the frame of reference for the Nose survey line (fig. 10). The horizontal measurement error is ±1 mm. Vertical measurement error is a maximum of ±1.1 mm over the whole survey line and probably is less than ±0.5 mm among closely spaced stations. Stations along the Nose line were located so that pairs of stations were in blocks of unfissured alluvium between the fissures. Comparison of fissure movement with strain in the unfissured blocks then is possible.

Movement of stations AB through AF near the mountain front generally was horizontal during the study period. Stations AG and AF were transitional and had slight vertical movement. Stations AI and AJ exhibited slightly more vertical than horizontal movement. At stations AK and AL, vertical movements exceeded horizontal movements by factors of about 3 and 5, respectively.

Stations AC through AF spanned two fissures and two unfissured blocks and exhibited similar behavior for all time intervals between surveys. Net vertical movement and average vertical movement were less than 2 mm for any interval between surveys. Uniformity of movement from AC to AF indicates little movement on the fissure between AD and AE. From May 31, 1980, to December 16, 1980, stations AC through AF moved an average of 21 mm eastward toward the mountain front. This movement, which is bounded by the 1-millimeter basinward movement of AB, resulted in horizontal compression between AB and AC of 490 microstrain for that interval between surveys. Altitudes of stations AB and AC rose a marginally significant

1.2 mm in that period, which is consistent with horizontal compression in that area. Stations AC through AF moved little from December 16, 1980, to March 17, 1982. From March 17, 1982, to June 6, 1983, those stations moved an average of 9 mm westward into the basin without appreciable vertical movement. From March 17, 1982, to June 6, 1983, the areas between stations AC and AD and between AF and AG exhibited horizontal extensions of 100 and 150 microstrain, respectively, in response to fissure opening of 9 mm between stations AH and AI. During the same period, the areas between stations AI and AJ exhibited compression of 110 microstrain. From June 6, 1983, to May 15, 1984, those stations reversed and moved an average of 7 mm toward the mountain front. Average net movement of those stations from May 31, 1980, to May 15, 1984, was 23 mm toward the mountain front. Average net horizontal compression was 120 microstrain for that area.

Between June 6, 1983, and May 15, 1984, station AI showed predominantly vertical movement while AJ continued to move basinward as well as downward. The intervening area, therefore, exhibited horizontal extension of 750 microstrain. The expected value of 200 to 600 microstrain of extension at failure as estimated by Jachens and Holzer (1982) was exceeded and may indicate a higher local value of strain at failure or strain-rate dependence of strain at failure. A concealed, incipient fissure, which could be verified using the techniques of seismic surface-wave attenuation (Wrege and others, 1985a), could be present between AI and AJ.

The fissure between AH and AI exhibited net opening of 20 mm from May 31, 1980, to May 15, 1984. That fissure opened 5 mm from May to December 1980 and 3 mm from March to November 1981. The fissure closed 1 mm from December 1980 to March 1981 and had 0 mm of horizontal movement from November 1981 to March 1982. The fissure opened 9 mm from March 1982 to June 1983 and 4 mm from June 1983 to May 1984.

The fissure between stations AH and AI exhibited three styles of opening accompanied by vertical offset across the fissure. Fissure opening from May to December 1980 occurred while movement of stations AC through AJ was toward the mountain front. Fissure opening from March 1981 to November 1981 accompanied predominantly vertical movements in that area. Fissure opening from March 1982 to June 1983 occurred while movement of nearby stations was toward the basin.

Fissures between stations AD and AE and between AF and AG exhibited movement that commonly was 1 mm or less during the study period. An exception is the opening of the fissure between AF and AG of 3 mm from March 17, 1982, to June 6, 1983, which correlated with the opening of 9 mm of the fissure between AH and AI. Movements during 1980 and 1981 across the fissure between AD and AE were in the same sense as movements across the fissure between AH and AI but were below the estimated measurement error.

No attempt was made to model the fissure system crossed by the Nose survey line with a dislocation model for several reasons. First, several closely spaced fissures are nearby that could contribute to movement of stations. Second, stations were sparse beyond AJ, and only two stations were in each unfissured block between fissures. Third, because of the proximity of the fissures to the bedrock contact, the assumption of homogeneity in an elastic half space could be seriously violated.

Movements Along TA-1 Survey Line

Seven surveys of the TA-1 survey line were done, and the frame of reference is station A that is set in bedrock (figs. 11-13). Vertical displacements along this survey line were characterized by increasing subsidence from station B through E, extremely uniform subsidence from station F through K, fault offset between stations K and L, decreasing subsidence from station L through N, and increasing subsidence from station O through Q (figs. 11-13). Horizontal displacements along this survey line were characterized by movement toward the basin decreasing from station C through E, remaining generally constant from station F through M, and varying from station N through Q.

From May 31, 1980, to May 15, 1984, station B moved only 1 mm toward the basin, horizontal strain between stations B and C was tensile and had a value of 140 microstrain, and station C moved 29 mm into the basin. Horizontal strain was compressive and had a value of 72 microstrain between stations E and F. Stations F through J moved an average of 12 mm into the basin, station K moved 18 mm into the basin, and station L moved only 10 mm into the basin. Stations M through Q moved 18, 21, 13, 24, and 14 mm, respectively, into the basin. The area from stations G through O exhibited 20 microstrain of extension; and the area from station I through M had 140 microstrain of extension. Between stations L and M, just west of the fissure, the accumulated extension amounted to 840 microstrain, which is a value higher than expected for strain at failure (Jachens and Holzer, 1979, 1982). The high strain is similar to the strain between stations AI and AJ on the Nose survey line and could indicate the presence of an incipient fissure, a higher local value for strain at failure, or strain-rate dependence of strain at failure.

Subsidence from May 31, 1980, to May 15, 1984, ranged from 2.6 mm at station B to 140.6 mm at station E. From station F through K, subsidence varied from 147.0 to 148.1 mm. Net vertical offset between stations K and L was 22.9 mm. Subsidence decreased from 171 mm at station L to 162.3 mm at station N and increased to 183.3 mm at station Q.

Deformation observed along the TA-1 survey line was simpler than deformation observed along the Nose survey line. The mountainward movement of Nose line stations AB through AJ from May 31, 1980, to December 16, 1980, was accompanied by similar movement of stations F through Q. Otherwise, movement near the Picacho earth fissure along the TA-1 survey line was predominantly vertical and did not exhibit the complexity of the area near the fissure between stations AH and AI on the Nose survey line (figs. 10-13).

DISLOCATION MODELING OF PICACHO EARTH FISSURE

A dislocation as used in this report is a rectangular tear within an isotropic, homogeneous semi-infinite elastic body or half space. The three types of dislocations are screw, edge, and tensile (Okada, 1985), which are analogous to a strike-slip fault; a dip-slip fault; and a tensile crack, dike, or sill injection, respectively.

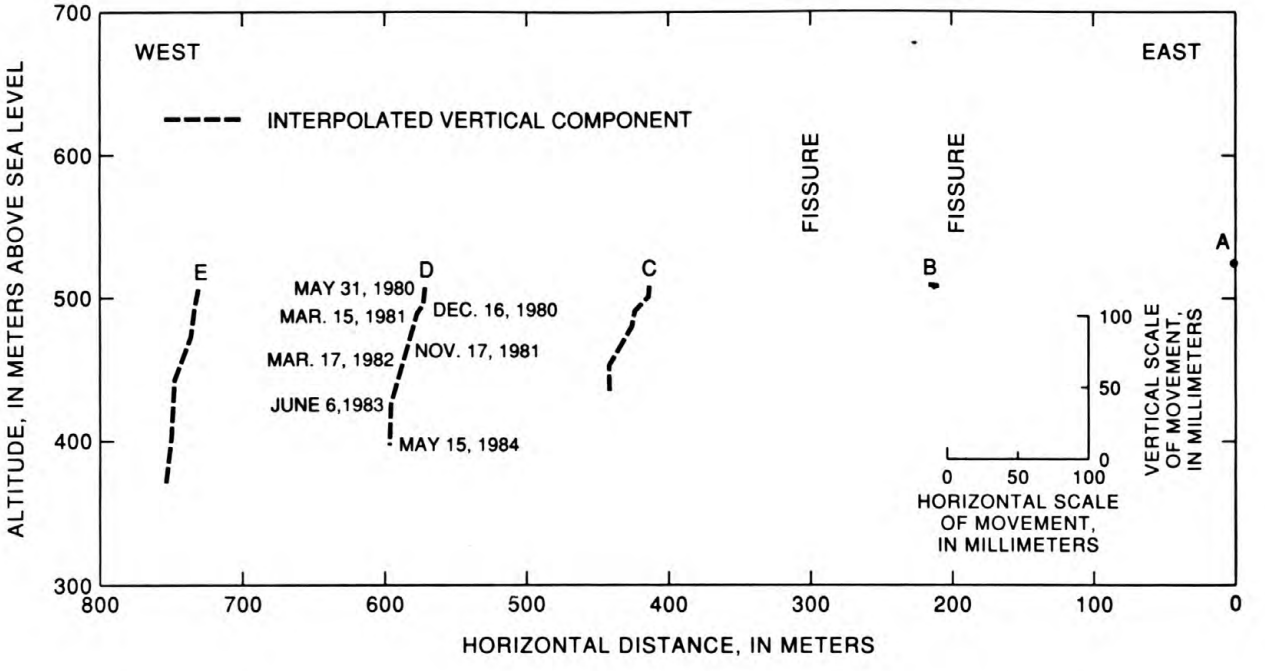

Figure 11.—Station trajectories along TA-1 survey line, stations B-E, 1980-84, with station A as a reference frame.

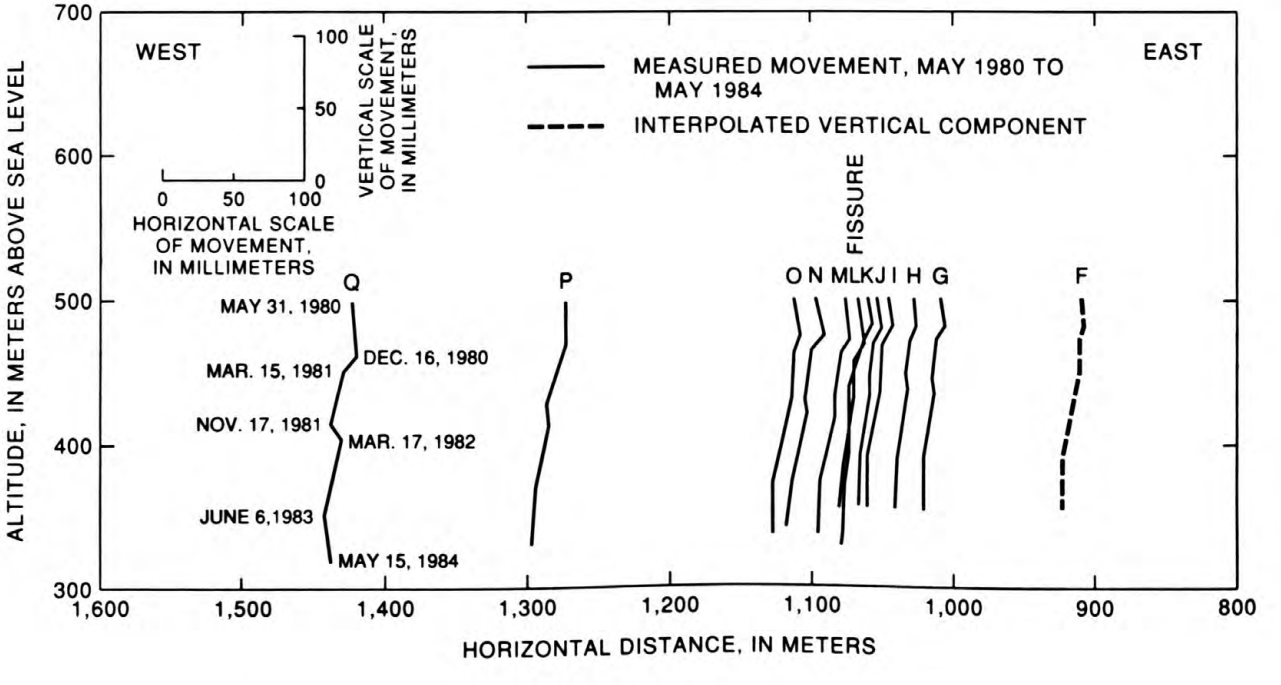

Figure 12.—Station trajectories along TA-1 survey line, stations F-Q, 1980-84, with station A as a reference frame.

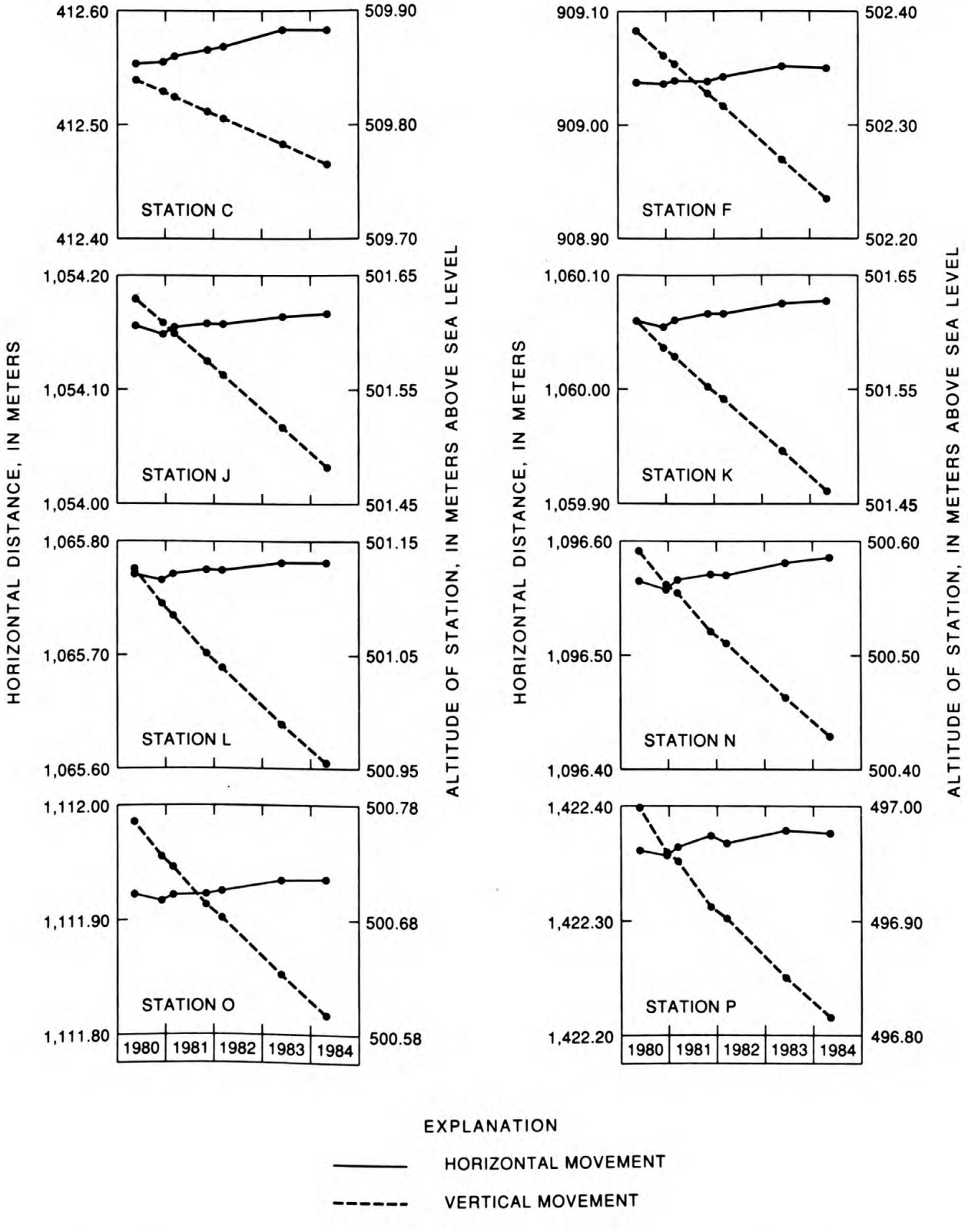

Figure 13.—Time series of horizontal and vertical displacements of selected stations along TA-1 survey line.

Okada (1985) presented the displacement field $u_i(x_1, x_2, x_3)$ caused by a Volterra dislocation $\Delta u_j(\xi_1, \xi_2, \xi_3)$ across the surface Σ in a homogeneous, isotropic medium as

$$u_i = \frac{1}{F}\iint_{\Sigma} \Delta u_j \left[\lambda \delta_{jk} \frac{\partial u_i^n}{\partial \xi_n} + \mu\left(\frac{\partial u_i^j}{\partial \xi_k} + \frac{\partial u_i^k}{\partial \xi_j}\right)\right] \nu_k \, d\Sigma,$$

where

δ_{jk} = the Kronecker delta,

λ = Lame's parameter,

μ = shear modulus,

u_i^j = the ith component of displacement at coordinates (x_1, x_2, x_3) caused by the jth direction point force with magnitude F at coordinates (ξ_1, ξ_2, ξ_3),

ν_k = the direction cosine normal to the surface $d\Sigma$,

and the summation convention holds.

In a Cartesian coordinate system (fig. 14) in which elastic medium occupies the volume with $z \leq 0$ and the x-axis is parallel to the strike of the fault, the elementary dislocations U_1, U_2, U_3 are strike-slip, dip-slip, and tensile components of dislocation, respectively. The length of the fault is L, depth is D, width is W, and dip is θ. For dip angles $0° < \theta < 90°$, tensile fault opening, right lateral strike-slip faulting, and dip-slip thrust faulting are positive. If $\lambda = \mu$, then Poisson's ratio is 0.25. For vertical dip-slip faults and horizontal faults of all types, deformation is independent of Poisson's ratio. Singularities exist at the perimeter of the rectangular fault but have effects only in close proximity to the fault edges (Chinnery and Petrak, 1968).

Complete equations for surface displacements, normal and shear strains in the horizontal plane, and tilts or shear strains in a vertical plane are given by Okada (1985). Singularities at observation points above the perimeter of the fault in some earlier derivations are absent in Okada's equations. Field applications of dislocation theory to dip-slip fault movements include Savage and Hastie (1966, 1969) and Holdahl (1986). A tensile fault model has been applied to explain correlation of strains and water-level fluctuations in fractured rock (Evans and Wyatt, 1984).

A suite of theoretical plots was generated using the program MAIN113, which calculates displacements and strains caused by dislocations (Savage and Hastie, 1966). The plots are of displacements of the stations along the survey line for dip-slip faults of various dips and widths (fig. 15). The plots were used for visual comparison with measured displacements at the survey stations. The frame of reference for the displacements shown in figure 15 is a point on the upthrown side of the fault and was selected for this particular study to be compatible with the technique used to remove regional subsidence from measured displacements near the Picacho earth fissure. For other applications, a choice of reference frame at the land surface away from the fault would better illustrate the characteristic uplift near the edge on the upthrown side

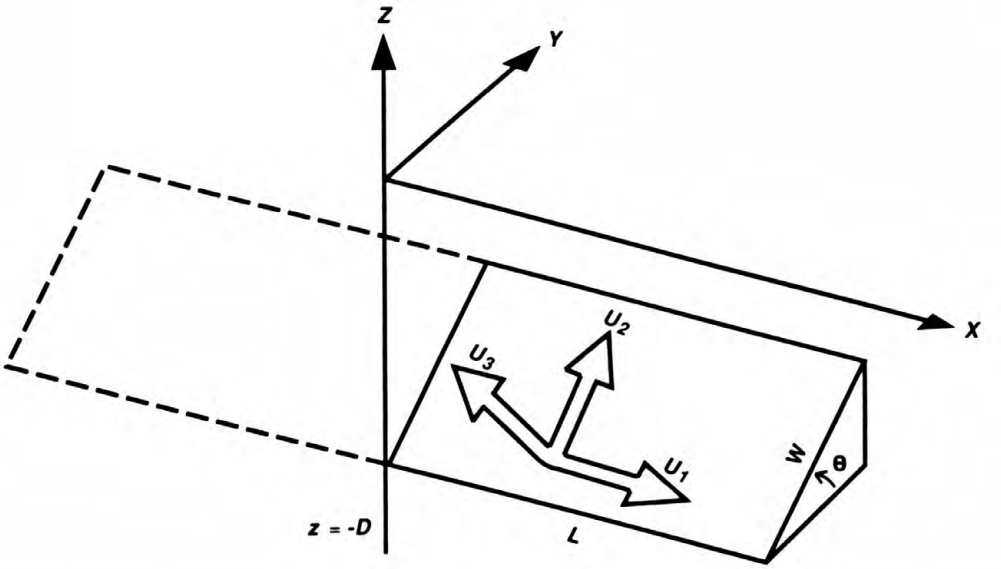

EXPLANATION

D = DEPTH (OKADA CONVENTION)	***X*** = COORDINATE ALONG LENGTH ***L*** IN PLANE OF LAND SURFACE
L = LENGTH	***Y*** = COORDINATE ORTHOGONAL TO ***X*** IN PLANE OF LAND SURFACE
W = WIDTH	***Z*** = VERTICAL COORDINATE
θ = DIP ANGLE	
U_1, U_2, U_3 = STRIKE SLIP, DIP SLIP, AND TENSILE COMPONENTS OF DISLOCATION	

Figure 14.—Dislocation model parameters (from Okada, 1985).

of the fault for theoretical plots and would avoid near-edge effects for real data.

The theoretical plots show the effect of varying the width of the fault from 50 to 500 m and varying the dip of the fault from reverse 70° to normal 70°. The horizontal span of distinctive deformation is about four times the width of the fault. As the modeled fault deepens, the near downthrown side loses its cusp-shaped character and flattens. Similarly, the relative displacements on the upthrown side broaden and flatten. However, the relative displacements on the upthrown side are small and may not exceed measurement error or may be masked by local deformation. In these plots, which do not distort deformation with vertical exaggeration, the use of the vector combination of horizontal and vertical components of displacement allows better estimates of fault dip than the use of vertical displacements only.

A dip-slip dislocation model was selected to characterize the pattern of displacement measured near the Picacho earth fissure for two reasons. First, the vertical offset across the fissure was five times greater than the tensile opening during the 4-year period of observation. Second, Sanford's (1959) sandbox model and theoretical results indicate that surface dip-slip faults and tensile cracks occur in response to vertical offset concentrated over a short horizontal distance at depth.

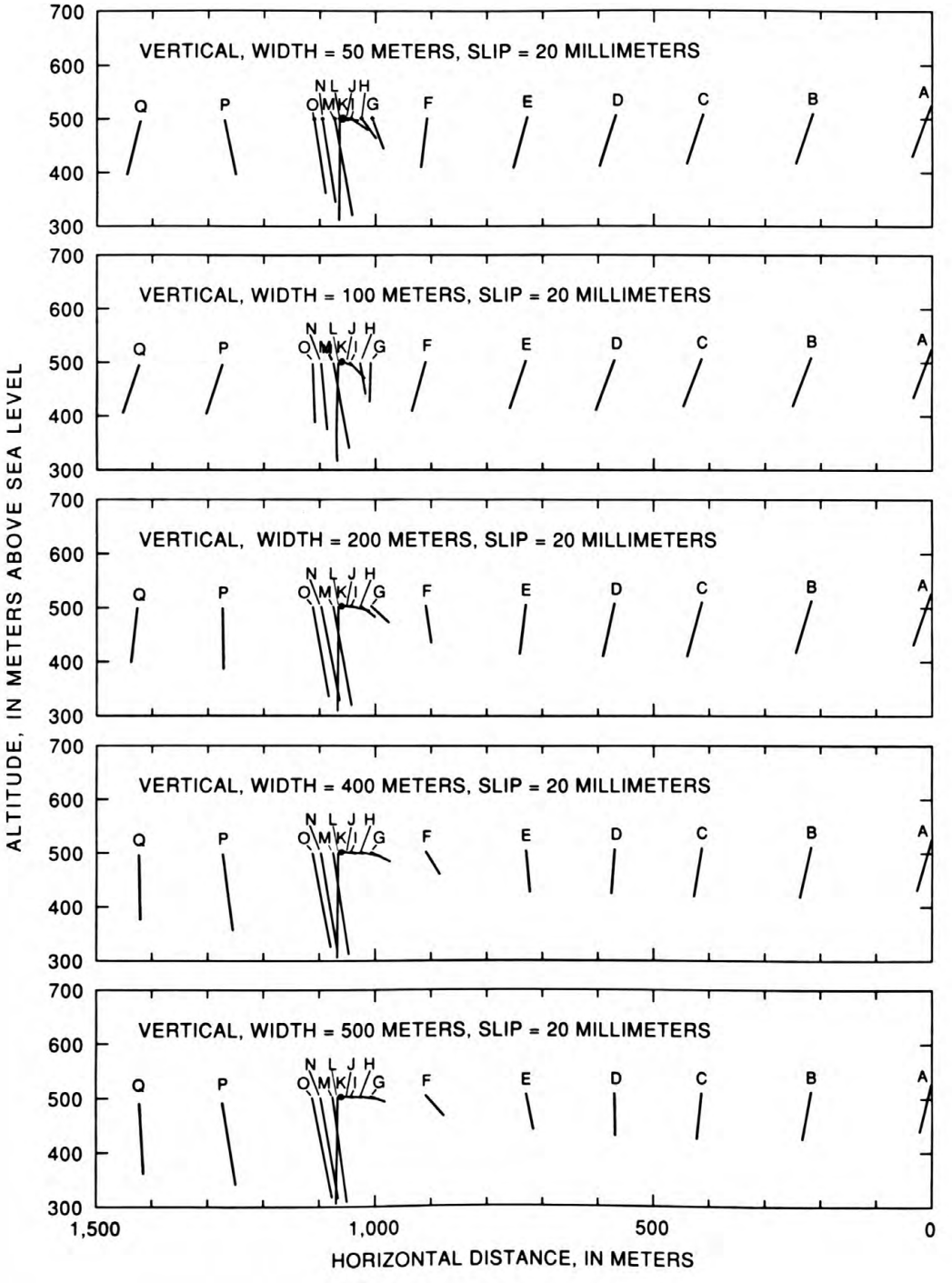

Figure 15.—Effects of fault width and dip on the

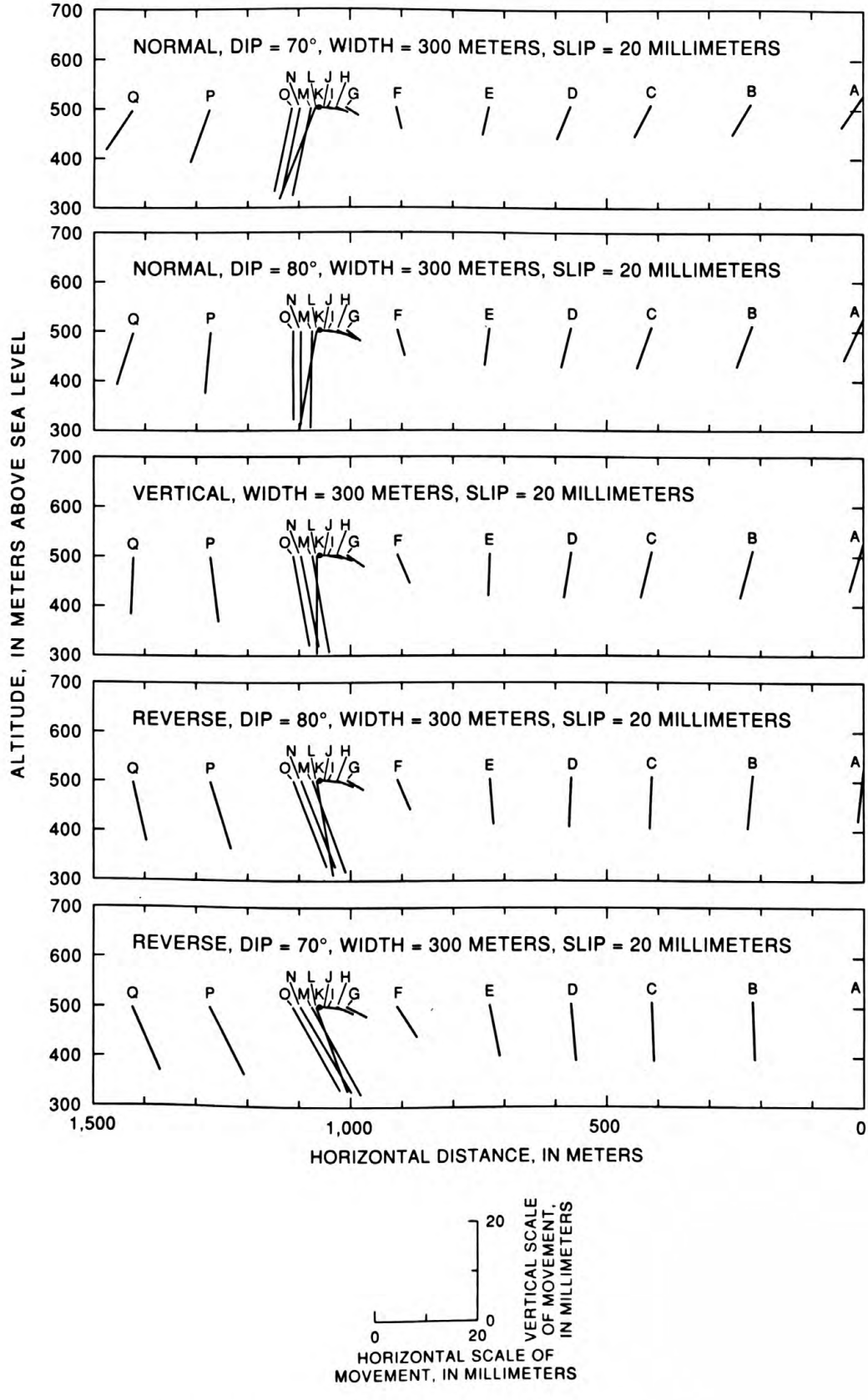

pattern of vector displacements near a dip-slip fault.

An effort was made to remove the effect of differential subsidence from the measured movement using a finite-element, stress-strain model (Zienkiewicz, 1977) in order to produce a residual pattern of deformation for dislocation modeling. The model mesh was based on the geometry of the seismic refraction line (fig. 3). Ratios of Young's moduli were determined using seismic P-wave velocities and an assumed Poisson's ratio of 0.25 (Birch, 1966). The applied stress was the water-level fluctuation of TA-1-1 and TA-3-1. The resulting pattern of horizontal strain was one of compression across the area from station F through O. Modeled subsidence approached a limiting value from station F through O, which was the expected result for a concave-upward basement contact. The model gave a pattern of horizontal tension and subsidence increasing markedly toward the basin across the area centered at TA-3, which was the expected result for a convex-upward basement contact. Varying Poisson's ratio from 0.25 to 0.48 did not significantly alter the modeled results. The modeled pattern of surface deformation using the basement contact as determined by the seismic-refraction profile (fig. 3) differed markedly from the observed displacements along TA-1 survey line. In addition, the contact between basal gravel and silt differed between the lithologic description of TA-1 and the seismic refraction line. Therefore, the basement contact near TA-1 was considered to be too poorly known to apply the stress-strain model.

As an alternative to the use of the finite-element model for removal of differential subsidence from the pattern of deformation, station K was selected as a reference frame (fig. 16). This change in frame of reference had the advantage of removing a central or average value of subsidence from the pattern of deformation, leaving a residue that could be fitted to a dislocation model. For example, total subsidence for station K was 148 mm compared with 148 mm for station F and 183 mm for station Q for the study period. Choice of reference frame did not affect dislocation-model results because the reference-frame adjustment was applied after the model run. The choice of reference frame does affect the pattern of deformation that is modeled, however, because each reference frame produces a different residual pattern of deformation. All stations from F to K were tried as reference frames before station K was selected as the representative station. Differences in patterns of deformation using station K or other stations on the upthrown side of the fault as reference frames did not exceed the measurement error for the modeled time periods.

For selected intervals between surveys, patterns of movement relative to station K were fit visually to a suite of plots of modeled movement for faults with various dips and widths (fig. 15). A two-dimensional fault model was used because of the great length of the Picacho earth fissure (15 km), the distance to other fissures, and the similarity in pattern of deformation between the Nose survey line and the TA-1 survey line. The length of the modeled fault was 19.8 km, and the depth to the top of the fault was 0.1 m. Although field evidence indicates that the fissure breaks the surface, an algorithm in MAIN113 requires a depth to the top of the fault of greater than 0. The depth of 0.1 m was large enough for the algorithm to give valid results but small compared with the distance to the nearest station.

A visual-fitting procedure was used because the statistical fitting provided by the program MAIN113 was highly influenced by points P and Q. That program allows statistical weighting of stations by means of the standard deviation of the error of the station. A visual procedure was

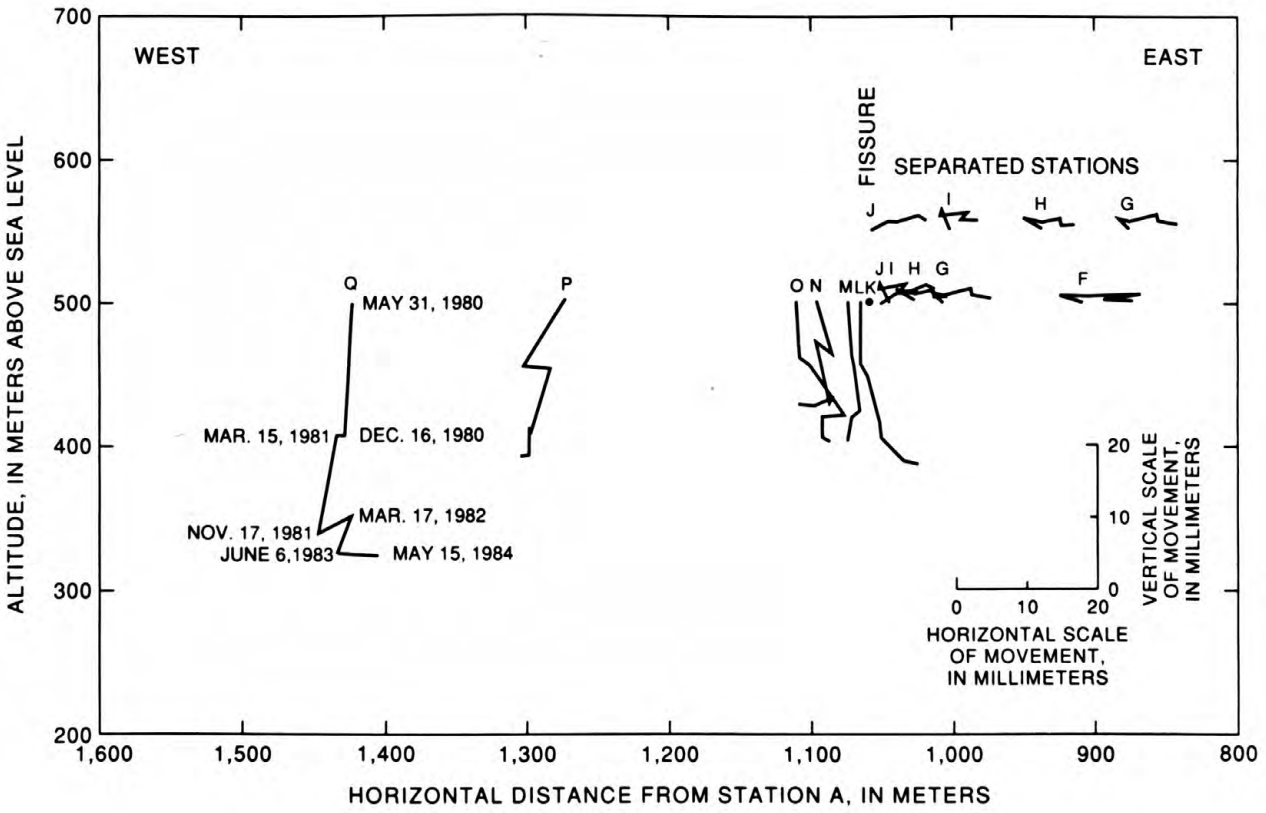

Figure 16.—Station trajectories along TA-1 survey line, stations F-Q, 1980-84, with station K as a reference frame. Because of overlap, the trajectories of stations G, H, I, and J are also shown separately.

used, however, because the finite-element model could not be used to separate objectively total movement of stations P and Q into components caused by fault movement and components caused by differential subsidence.

No single fault model gave a good fit for the net movement from May 1980 to May 1984. The best fit was a vertical fault with a width of 300 m, depth of 0.1 m, and slip of 20 mm (figs. 14, 15, and 17). On the upthrown side, movement measured relative to station K was essentially horizontal whereas modeled movement exhibited the characteristic pattern of convex upward movement. On the downthrown side near the fault, several stations exhibited movement similar to that modeled. Stations P and Q subsided two to three times as much as modeled movement. Because of the seasonal effects on the pattern of displacements that do not appear to be fault movement (fig. 16), probably no single fault model should be expected to fit the total measured displacement.

Measured displacements from May 1980 to December 1980 provided a good fit to a vertical fault that had a width of 300 m, depth of 0.1 m, and a slip of 9-mm (fig. 18). Stations on the upthrown side of the fault did not fit the modeled movement. Four stations on the downthrown side near the fissure had measurement-error ellipses that contain or nearly contain the modeled displacements. Model fit for stations P and Q was poor for this time period. The dip of the fault was well defined by the pattern of

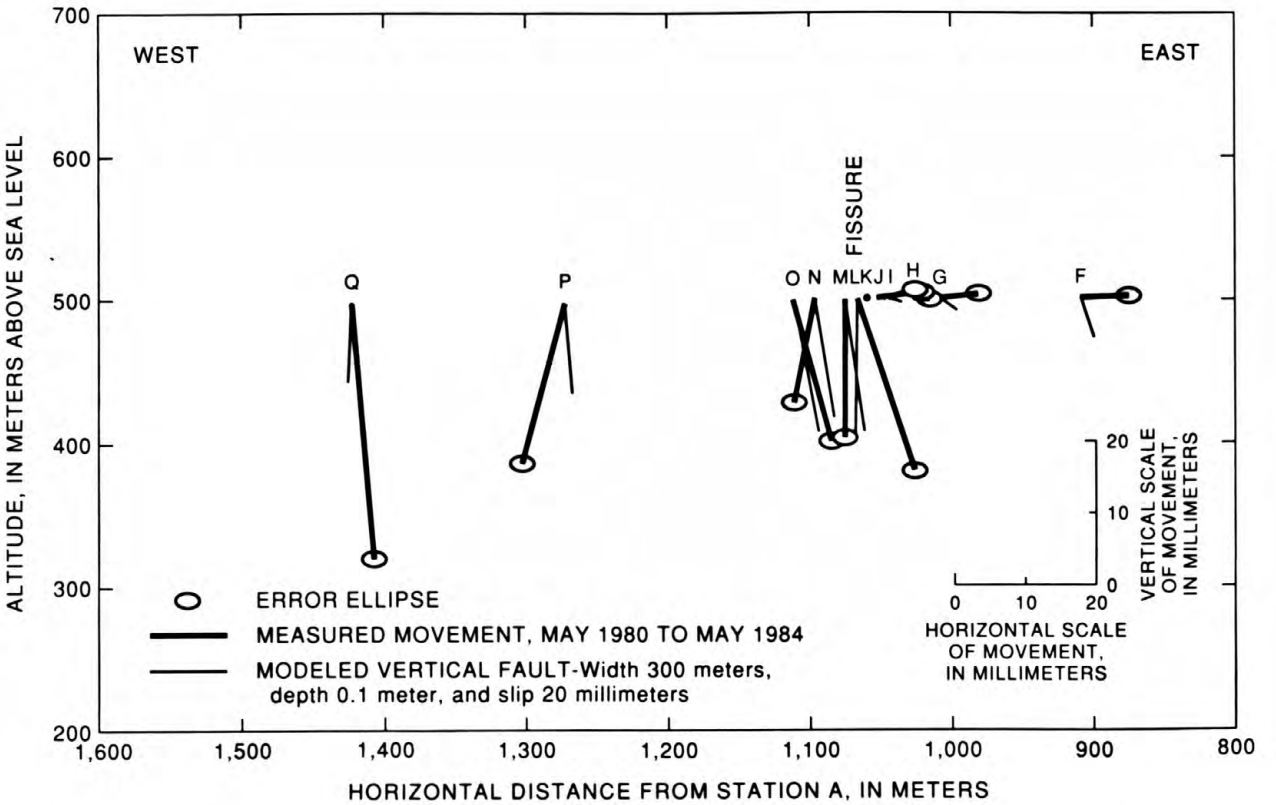

Figure 17.—Movement from May 31, 1980, to May 15, 1984, stations F-Q, with station K as a reference frame, compared with a vertical fault with width 300 meters, depth 0.1 meter, and slip 20 millimeters.

displacements on the downthrown side near the fissure. In the absence of stations between O and P and beyond Q, the width cannot be more precisely determined than between 200 and 400 m. The measured displacements for this time period correspond with a period when water levels in piezometers TA-1-1 and TA-3-1 declined to annual lows (fig. 4). At the same time, the lowest water levels of record (since 1965) were observed in the Eloy extensometer well (Epstein, 1987).

Displacements for December 16, 1980, to March 15, 1981, are shown in figure 19. Few stations exhibited any movement greater than their error ellipses. No attempt was made to model movement for this time period during which water levels recovered to seasonal highs (fig. 4). Movement seemed to be locally random without any indication of systematic fault rebound or fissure closing.

The best fit for movement from March 15, 1981, to November 17, 1981, was the same model as for May to December 1980 (fig. 20). The fit for this time period, however, was not as good as for the earlier one. As before, there was no fit on the upthrown side. On the downthrown side near the fault, the fit was good enough to define the dip of the fault but provided no definition of the width of the fault. This measured movement corresponded closely with a water-level decline from an annual high to an

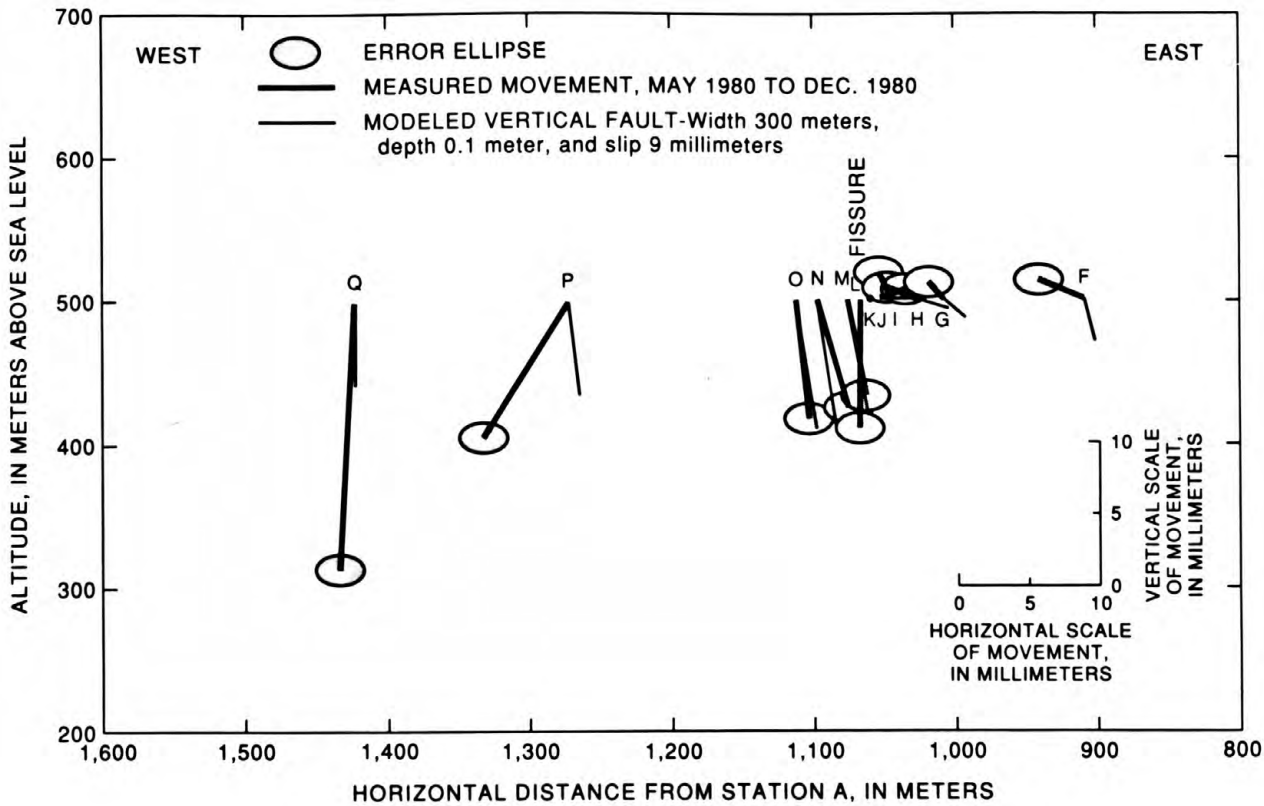

Figure 18.—Movement from May 31, 1980, to December 16, 1980, stations F-Q, with station K as a reference frame, compared with a vertical fault with width 300 meters, depth 0.1 meter, and slip 9 millimeters.

annual low (fig. 4). Water levels did not decline below previous lows during this time period.

From November 17, 1981, to March 17, 1982 (fig. 21), movements seemed to be locally random, as during the previous period of water-level recovery. Most movements were small, within the error ellipses, and did not appear to be fault reversal. The time period corresponded with a period of water-level recovery from an annual low to an annual high (fig. 4).

From March 17, 1982, to June 6, 1983, the fault exhibited vertical offset of about 4 mm (fig. 22). The pattern of deformation did not appear to fit a particular dislocation and was not modeled. Movement during this time period corresponded with water-level fluctuation from an annual high water level to a midpoint in water-level decline during a year in which annual low water levels were higher than in previous years (fig. 4).

Movement from June 6, 1983, to May 15, 1984, was essentially horizontal (fig. 23). Movement was toward the mountain front on the upthrown side of the fault and varied from toward the mountain front to toward the basin on the downthrown side of the fault. Because of the inconsistency of movement on the near downthrown side, no attempt was made to model this movement. At the beginning and end of this time period, water levels were approximately equal (fig. 4) before and after a period when

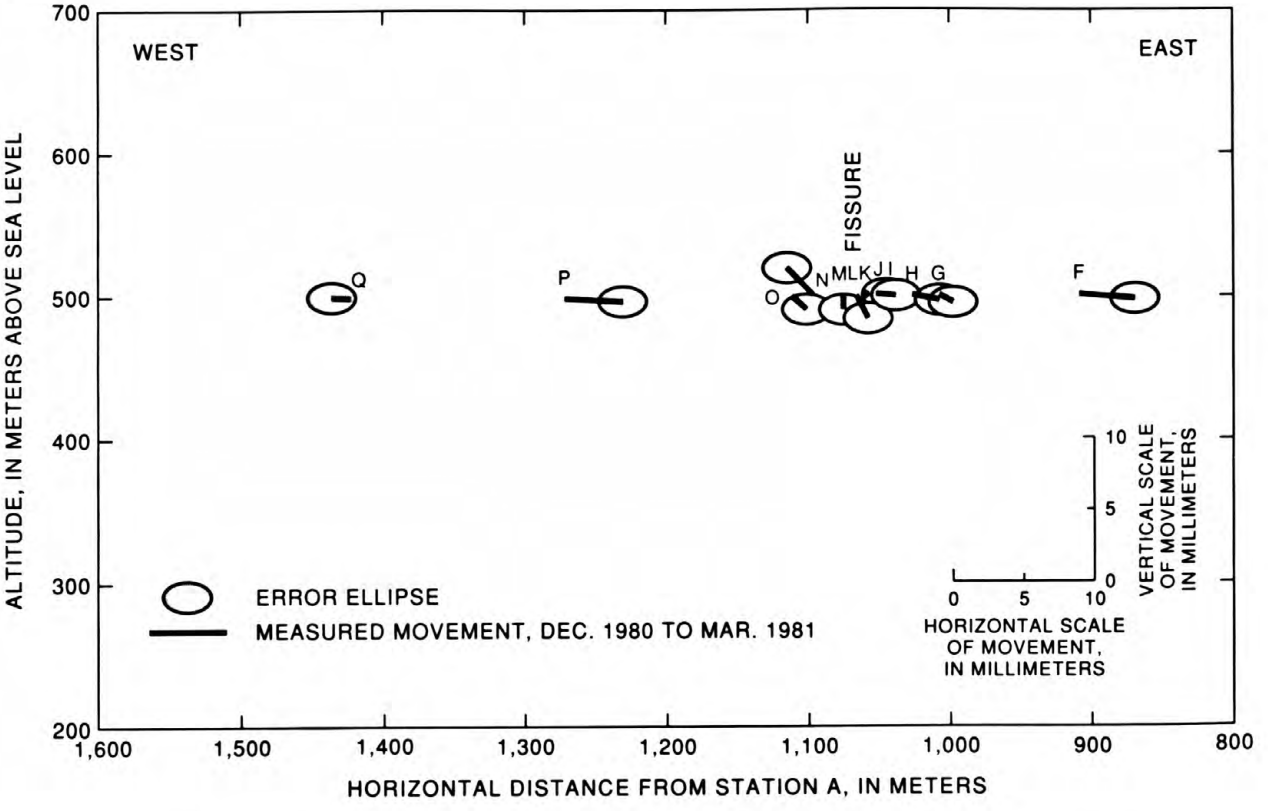

Figure 19.—Movement from December 16, 1980, to March 15, 1981, stations F-Q, with station K as a reference frame.

water-level recoveries in the deep piezometers were higher than normal for the study period.

The usefulness of dislocation modeling to estimate dip and width of faulting of the Picacho earth fissure depends on several factors. First, because differential compaction is inferred to cause the fault movement (Sanford, 1959), removal of differential subsidence to look for the pattern of displacements caused by the dislocation would require complex stress-strain modeling and could introduce spatial error. Whether it is done empirically or by modeling, removal of the pattern of deformation caused by differential subsidence over a sloping, irregular bedrock surface depends on the extent to which the geometry of the contact, the material properties of the alluvium, and the distribution of changes in effective stress are known. Second, the sloping bedrock contact (fig. 3) violates the assumption of a homogeneous, isotropic half space. Dislocation modeling of an obliquely layered medium (Sato and Yamashita, 1975) suggests that vertical components of displacements on the upthrown side of the fault would be shifted upward because Young's modulus of the alluvium is lower than that of the basement rocks. Third, fault movement might be along several interrelated faults whose dips change with depth (fig. 6, and Sanford, 1959). The superposition of patterns of deformation from a complex pattern of faults may defy interpretation or may appear to be a simpler fault than actually exists. Fourth, having only one station between O and Q and none west of Q limited the ability to estimate the width of the fault.

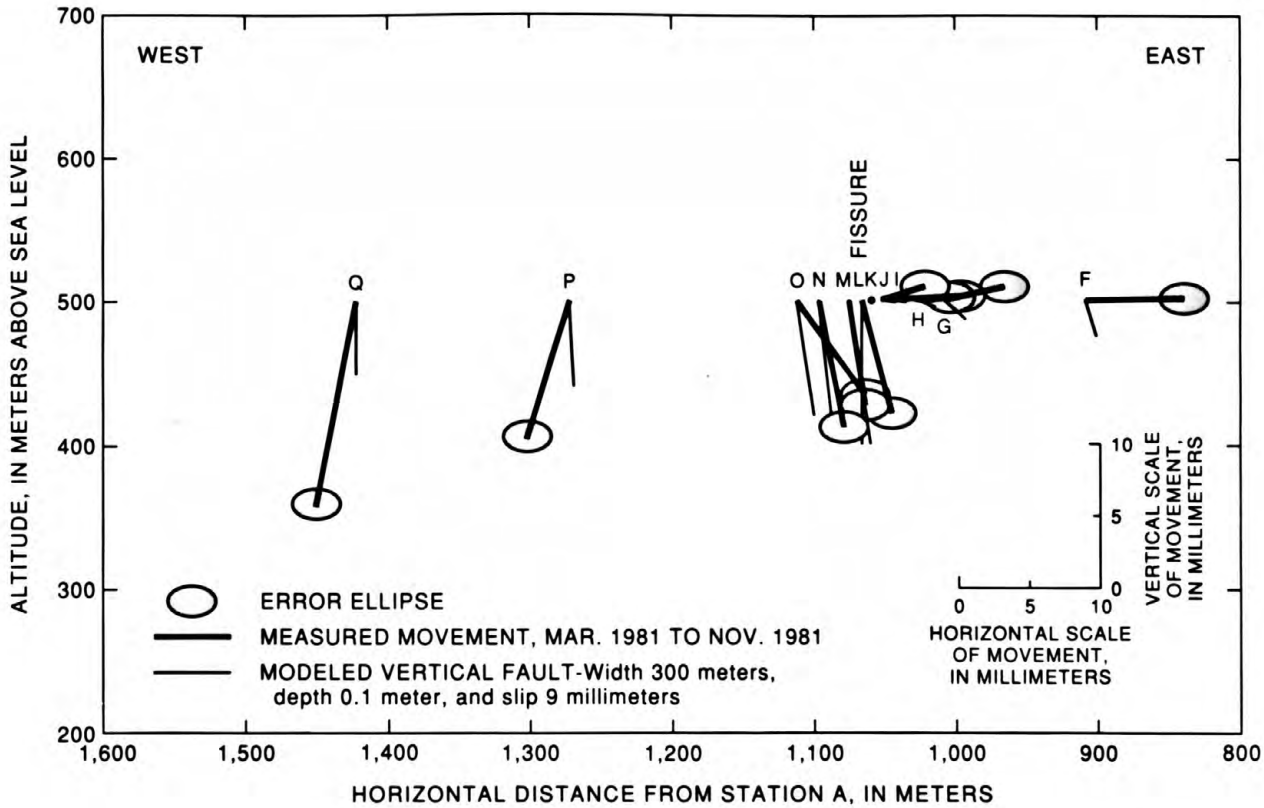

Figure 20.—Movement from March 15, 1981, to November 17, 1981, stations F-Q, with station K as a reference frame, compared with a vertical fault with width 300 meters, depth 0.1 meter, and slip 9 millimeters.

In spite of these difficulties, dislocation modeling gave a good fit for fault movements for the periods May 1980 to December 1980 and March 1981 to November 1981. The lack of fit on the upthrown side may be caused by the effects of differential subsidence and the violation of homogeneous half space. Lack of fit for stations P and Q is probably caused by the effects of differential subsidence.

The fault model selected (figs. 18 and 20) with a depth of 0.1 m, a width of 300 m (fig. 14), and a dip of 90° is consistent with other arguments indicating that deformation extends from the land surface to a depth of about 300 m at the fissure. First, photographic evidence from 1936 (U.S. Soil Conservation Service, 1936) and 1927 indicates that the fissure extended to the surface as a feature that predates major water-level declines in the area. The fissure could be the surface expression of a tectonic fault that has been tectonically inactive since the gradation of the present alluvial surface. Another possibility is that the original fissure developed in response to prehistoric water-level declines. Second, assuming that the basal gravel generally has low compressibility, the width of the fault is about equal to the thickness of compressible material (fig. 3). Third, water-level fluctuations in the basal gravel, which probably reflect changes in effective stress in the deeper part of the silt unit, are correlated with fault movement and horizontal strain. Fourth, a possible bedrock irregularity directly below the fissure could be an

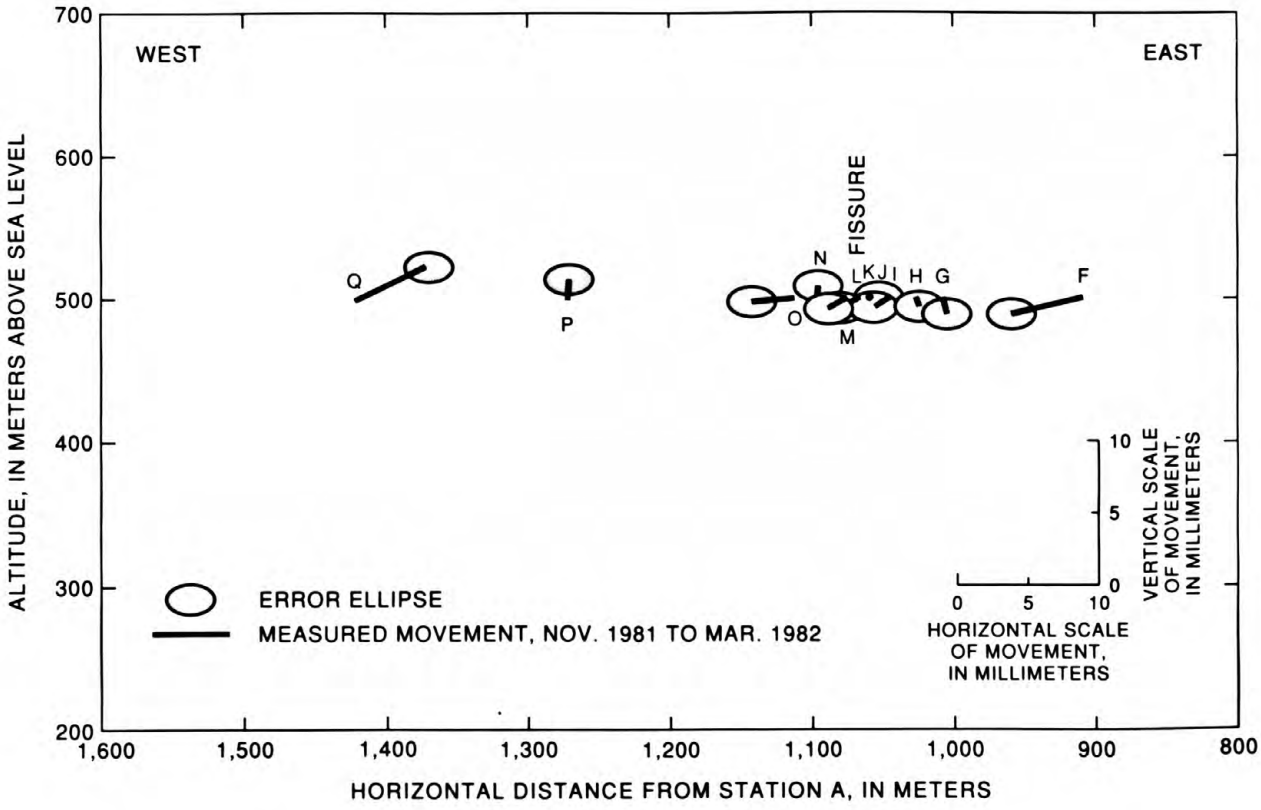

Figure 21.—Movement from November 17, 1981, to March 17, 1982, stations F-Q, with station K as a reference frame.

indication of a tectonic fault that exhibits offset in the lower part of the alluvium and is consistent with a dip of about 90°.

COMPARISON OF CONTINUOUS MEASUREMENTS WITH SURVEY RESULTS

The continuous measurements of horizontal strain across a span of 30 m and the discrete surveying measurements over a much larger span supplement each other. Ideally, the combined sets of horizontal strain data would allow a comparison between the field measurements and the displacements from the selected dislocation model to determine whether the horizontal strains are completely accounted for by the model or whether modeling a superimposed tensile crack is warranted. The measurement error of ±1.5 mm in the combined tape extensometer and EDM measurements and the uncertainties in fit with the model preclude that analysis. A comparison between horizontal strains measured by combined surveying techniques and by the horizontal extensometer was possible, however, and suggests nonuniformity of strain near the fissure.

The fissure openings recorded from spring to summer during 1981 and 1982 (fig. 4) corresponded with fault offset (figs. 18 and 20). From

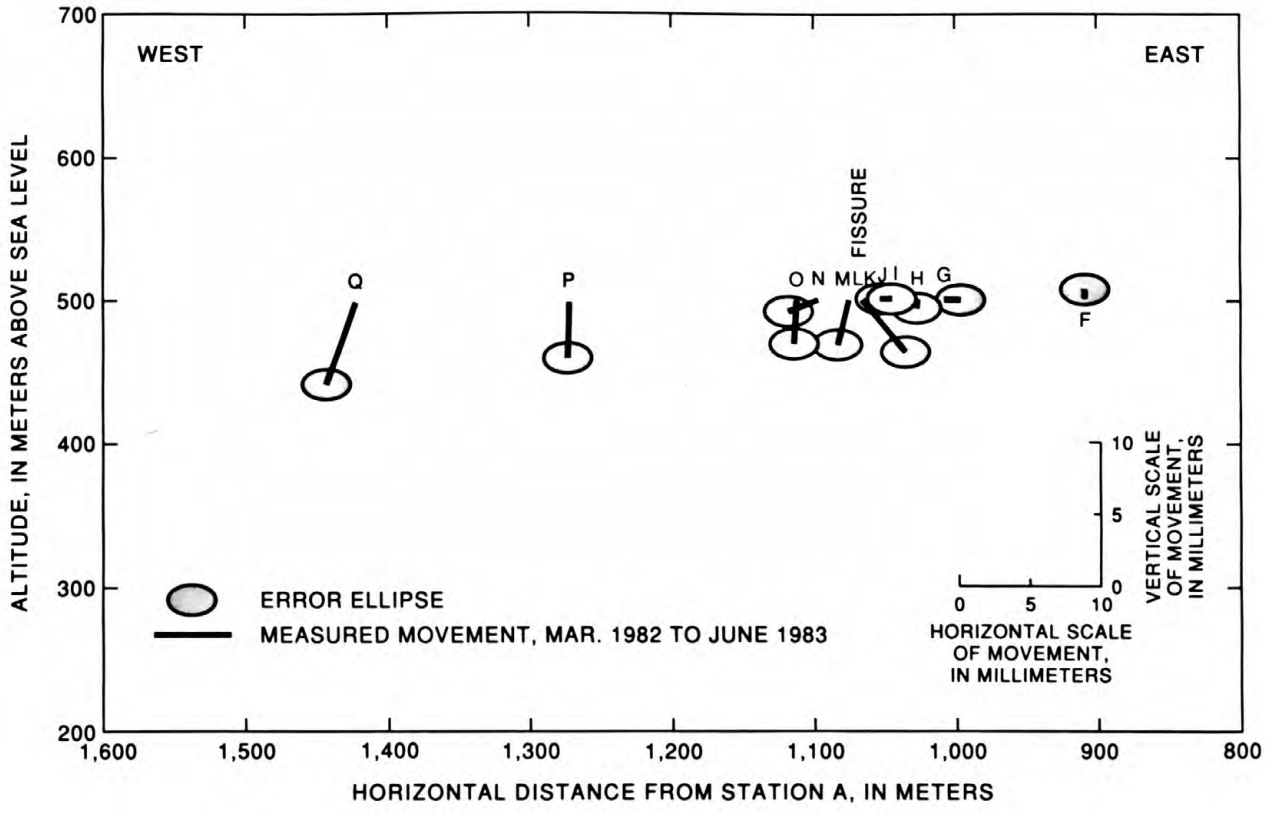

Figure 22.—Movement from March 17, 1982, to June 6, 1983, stations F-Q, with station K as a reference frame.

March 15, 1981, to November 17, 1981, displacement of station M, relative to station I, was 3 ±1.5 mm extension, and the extension of the horizontal extensometer was 3.533 mm. From March 17, 1982, to June 6, 1983, the values were 1 ±1.5 mm and 0.741 mm, respectively.

During periods of fissure closing such as December 16, 1980, to March 15, 1981, and November 17, 1981, to March 17, 1982, the extensometer measurements also agreed well with relative displacement between stations I and M. Relative movements between I and M were 0 ±1.5 mm for both time periods, and the respective compression values for the extensometer were 0.704 mm and 0.760 mm. From June 6, 1983, to May 15, 1984, stations I and M exhibited an opening of 2 ±1.5 mm, and the extensometer closed 0.401 mm.

Little can be inferred about the concentration of horizontal strain near the Picacho earth fissure for time intervals between surveys because almost all relative movements between nearest pairs of stations G through O were within the measurement error. The exceptions were stations L to M for March 17, 1982, to June 6, 1983, and stations N to O for June 6, 1983, to May 15, 1984. These stations exhibited 4 ±1.5 mm relative opening and 4 ±1.5 mm closing, respectively. Notable strains within the measurement error were stations I to J, from May 15 to December 16, 1980, with 350 microstrain of compression and stations J to K, for the same time period, with 330 microstrain of extension. These strains probably reflect a

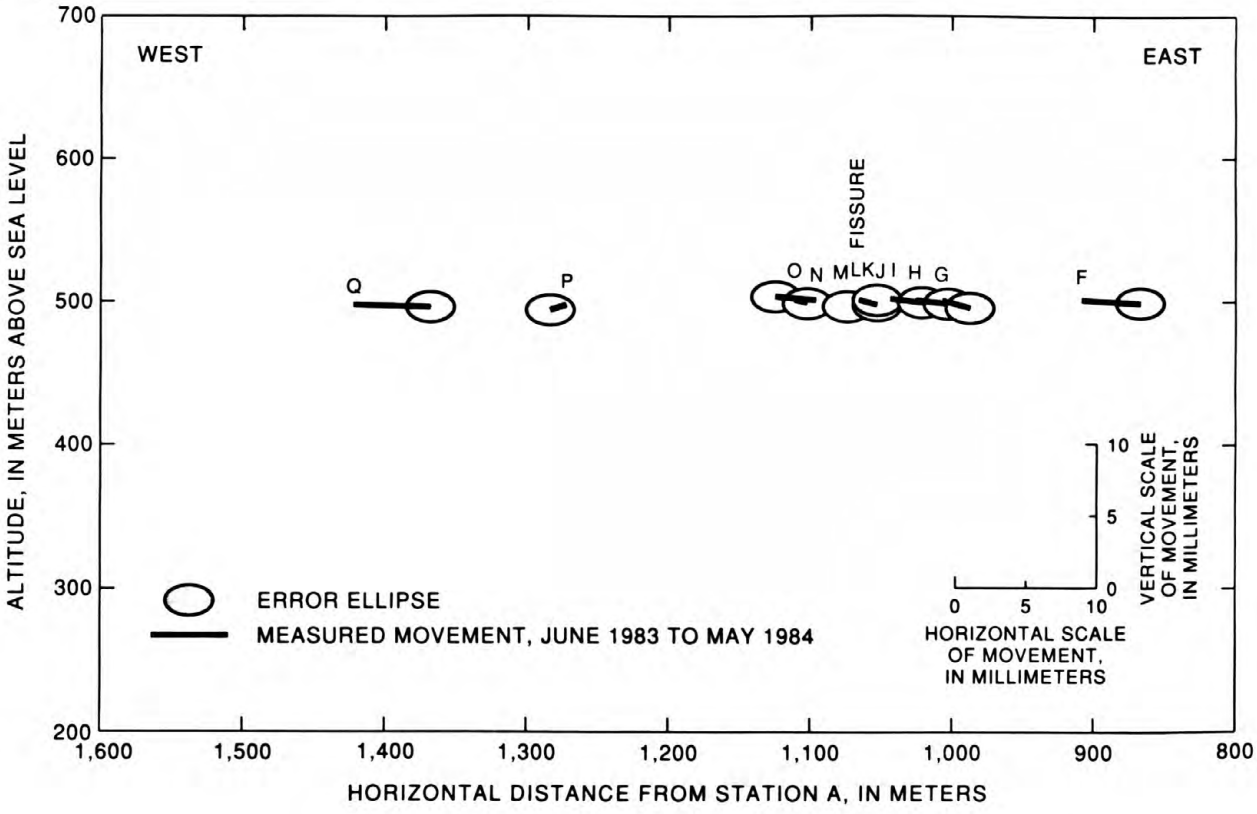

Figure 23.—Movement from June 6, 1983, to May 15, 1984, stations F-Q, with station K as a reference frame.

local movement of station J toward the mountain front. A similar probable local movement of station K was reflected in 500 microstrain of extension between J and K and 340 microstrain of compression between K and L from March 15 to November 17, 1981.

Some net horizontal displacements for stations near the fissure from May 31, 1980, to May 15, 1984, exceeded the measurement error and suggested that strain is concentrated near the fissure. Values in microstrain between pairs of stations were as follows: 110 extension between G and H, 40 extension between H and I, 350 compression between I and J, 1,160 extension between J and K, 1,370 compression between K and L, 840 extension between L and M, 140 extension between M and N, and 520 compression between N and O. For comparison, strain across the larger span from G to O was 20 microstrain extension and across the intermediate span from I to M was 140 microstrain extension. The largest strains, which change sign between adjacent pairs of stations, probably reflect local movements of stations J, K, and L because of their proximity to the edges of the fissure.

COMPARISON OF RESULTS WITH PREVIOUS WORK

Two of the results of this study are consistent with the results of Holzer and others (1979) near the study site of Holzer (1978) and

Pankratz and others (1978). First, movement of the fissure is concluded to be caused by changes in effective stress as represented by water-level fluctuations in TA-1-1 and TA-3-1. Second, seasonal effects of deformation caused by water-level fluctuations, as suggested by Holzer and others (1979) on scant evidence, were well substantiated in this study (figs. 4, 7, 12, and 16). Horizontal strain across the fissure was highly correlated with water-level fluctuations. Fault movement occurred during periods of water-level decline; however, instead of fault reversal during periods of water-level recovery, only slowing of subsidence and apparent local movements or adjustments occurred.

The modeled fault differs between the two studies. Holzer and others (1979) obtained a normal fault with slip of about 260 mm, width of 190 m, and dip of 70° to the west. The modeled fault for this study has slip of 9 mm, width of 300 m, and dip of 90°. Several factors could have caused the differences in modeled faults. First, the study areas are 4.5 km apart, and the fault could differ in dip and width along its length. As indicated by Sanford (1959), several dips and complexities of faulting might result from deformation associated with a bedrock step. Second, Holzer and others (1979) and Boling (1987) found evidence of a hydrologic barrier to ground-water flow in the alluvium at their study site. The hydraulic gradient between TA-1-1 and TA-3-1 is very low, indicating a lack of any hydrologic barrier at the TA-1 site. Differences in material properties and in saturated thickness between the two sites could produce different angles of internal friction. These could, in turn, contribute to a difference in dip. Third, Holzer and others (1979) modeled movement spanning 14 years from 1963 to 1977. The total movement of about 260 mm during that period could represent a significant increase in signal-to-noise ratio so that the dip of 70° is correct, or it could represent a combination of movements along several faults of varying dips interspersed with deformations that are not fault movements (figs. 16-23). Fourth, Holzer and others (1979) modeled only vertical displacements. Holzer and Thatcher (1979) used horizontal displacements between a pair of stations on opposite sides of the fissure to substantiate their finding of a dip of 70° to the west. Measurements of horizontal displacements between a single pair of monuments on opposite sides of a fault or fissure cannot eliminate the possibility of superposition of a tensile crack and dip-slip fault. In this study, it appears that measurements of horizontal displacements of several stations on each side of the fissure contribute substantially to the ability to determine fault dip (figs. 15, 18, and 20) and to whether a simple dip-slip fault model is sufficient or superposition of a tensile crack is warranted. Holzer and others (1979) argued that the fissure initially resulted from water-level declines caused by pumping. Photographic evidence for existence of the Picacho earth fissure in 1927 and 1936 (U.S. Soil Conservation Service, 1936) is invoked to argue that the fissure predates major pumping and water-level declines.

Holzer and others (1979) estimated that the average rate of slip on the Picacho earth fissure at their site was about 20 mm/yr from 1968 to 1978. The average rate of slip at the TA-1 site was about 5 mm/yr from 1980 to 1984. The seasonal rate of slip at TA-1 was at least as great as 16 mm/yr from May 1980 to December 1980. The lower average value of slip at TA-1 may reflect differences along the trace of the fissure or a slowing of slip in recent years.

SUMMARY AND CONCLUSIONS

Vertical and horizontal displacements were monitored along two survey lines near the Picacho Mountains in south-central Arizona to determine correlation between water-level fluctuations and earth-fissure movement and to use dislocation modeling to characterize fissure development. Near the mountain front, movements were generally small, and horizontal displacements dominated over vertical displacements. With increasing distance into the basin, subsidence increased markedly and horizontal displacements decreased. No land-surface recovery, relative to stations on bedrock, was observed along the TA-1 survey line. However, rates of subsidence were reduced in winter, and some stations along TA-1 survey line on the downthrown side of the fissure showed winter recovery relative to station K on the near upthrown side. Station C on the TA-1 survey line exhibited the largest net horizontal movement of 29 mm toward the basin.

Along the Nose survey line, stations between AB and AI exhibited movement toward the mountain front, which could have been caused by elastic rebound from the release of tensile stress as the fissure deepened between stations AH and AI. This fissure exhibited 20 mm of net opening and 33 mm of net vertical offset. The area between stations AB and AC exhibited horizontal compression of 490 microstrain from May 31 to December 16, 1980, in response to opening of the fissure between stations AH and AI of 5 mm. The zone between stations AI and AJ exhibited horizontal extension of 750 microstrain from June 6, 1983, to May 15, 1984, a value thought to be large enough to induce fissuring.

Along the TA-1 survey line, from May 31, 1980, to May 15, 1984, subsidence was uniform at 148 ±1.8 mm from station F through K, while vertical offset of about 20 mm accumulated across the fissure between stations K and L. Horizontal extension between stations L and M was 840 microstrain, the largest value measured during the study. The large value of strain could indicate the presence of an incipient or newly forming subsurface fissure between those stations or, perhaps, a dependence of strain at failure on strain rate. The maximum measured subsidence at station Q was 183 ±1.8 mm.

Four modes of deformation occurred at the fissures during the study period. Between stations AH and AI, opening and vertical offset occurred with predominantly horizontal movement toward the mountain front from May to December 1980, with predominantly vertical movement in the area from March to November 1981, and along with horizontal movement toward the basin from March 1982 to June 1983. Deformation across the Picacho earth fissure was predominantly vertical offset from May to December 1980 and March to November 1981.

Continuous measurements of horizontal movement across the Picacho earth fissure are the first long-term, continuous measurements of earth-fissure movement. Horizontal movement across the fissure was smooth without sudden opening or closing. The fissure generally opened from mid-March to August or September, followed by closing until mid-March. Horizontal movement of the fissure was highly correlated with water-level fluctuations in deep piezometers TA-1-1 and TA-3-1.

High correlation between horizontal movement of the fissure and water-level fluctuations in the deep piezometers and lower correlation with shallow piezometer TA-3-2 supports the hypothesis of differential compaction for fissure movement. High correlation between horizontal movement and compaction at Eloy before November 1, 1981, also supports this hypothesis. Generalized differential compaction adds dip-slip faulting to horizontal tensile strain as a failure mechanism for fissure development. Vertical offsets measured across the Picacho earth fissure and between stations AH and AI support the hypothesis of generalized differential compaction for fissure movement.

Observation of fissure opening by movement toward the mountain front suggests that the hypotheses of rotation of a rigid plate and seepage stresses are not the primary mechanisms of fissure formation at the study site. The rigid-plate hypothesis does not account for the predominant mode of failure of the Picacho earth fissure being dip-slip movement and for the opening of a fissure between an existing fissure and the mountain front. The seepage-stress hypothesis is also unsupported at the study site because of the low correlation between head gradients and horizontal movement.

Dislocation modeling of a vertical fault within the alluvium provided a close fit to patterns of deformation observed at the Picacho earth fissure for periods from spring to winter. Periods from winter to spring did not show reversal of fault movement but did show local readjustment that was mostly horizontal. The modeled fault movement adds support to the hypothesis of generalized differential compaction as a mechanism for fissure formation and movement.

REFERENCES CITED

Anderson, S.R., 1978, Earth fissures in the Stewart area of the Willcox basin, Cochise County, Arizona: Tucson, University of Arizona, unpublished master's thesis, 72 p.

Bates, R.L., and Jackson, J.A., 1980, Glossary of Geology, 2d ed.: Falls Church, Virginia, American Geological Institute, 751 p.

Birch, F., 1966, Compressibility—Elastic constants, *in* Clark, S.P., ed., Handbook of Physical Constants—Revised Edition: Geological Society of America Memoir 97, 587 p.

Boling, J.K., 1987, Earth-fissure movements in south-central Arizona, U.S.A.: Tucson, University of Arizona, unpublished master's thesis, 99 p.

Bouwer, H., 1977, Land subsidence and cracking due to ground-water depletion: Ground Water, v. 15, no. 5, p. 358-364.

Brooks, W.E., 1986, Distribution of anomalously high K_2O volcanic rocks in Arizona—Metasomatism at the Picacho Peak detachment fault: Geology, v. 14, p. 339-342.

Bull, W.B., 1964, Alluvial fans and near-surface subsidence in western Fresno County, California: U.S. Geological Survey Professional Paper 437-A, 71 p.

_____1972, Prehistoric near-surface subsidence cracks in western Fresno County, California: U.S. Geological Survey Professional Paper 437-C, 85 p.

Chinnery, M.A., and Petrak, J.A., 1968, The dislocation fault model with a variable discontinuity: Tectonophysics, v. 5, no. 6, p. 513-529.

Duffield, W.A., and Burford, R.O., 1973, An accurate invar wire extensometer: U.S. Geological Survey, Journal of Research, v. 1, no. 5, p. 569-577.

Epstein, V.J., 1987, Hydrologic and geologic factors affecting land subsidence near Eloy, Arizona: U.S. Geological Survey Water-Resources Investigations Report 87-4143, 28 p.

Evans, K., and Wyatt, F., 1984, Water table effects on the measurement of earth strain: Tectonophysics, v. 108, p. 323-337.

Federal Geodetic Control Committee, 1974, Classification, standards of accuracy, and general specifications of geodetic control surveys: Rockville, Maryland, National Oceanic and Atmospheric Administration, 12 p.

Feth, J.H., 1951, Structural reconnaissance of the Red Rock quadrangle, Arizona: U.S. Geological Survey open-file report, unnumbered, 30 p.

Fleischer, R.L., 1981, Dislocation model for radon response to distant earthquakes: Geophysical Research Letters, v. 8, no. 5, p. 477-480.

Fletcher, J.E., Harris, K., Peterson, H.B., and Chandler, V.N., 1954, Piping: American Geophysical Union Transactions, v. 35, no. 2, p. 258-262.

Hardt, W.F., and Cattany, R.E., 1965, Description and analysis of the geohydrologic system in western Pinal County, Arizona: U.S. Geological Survey open-file report, unnumbered, 92 p.

Harvey, J.P., 1981, Groundwater extraction and radon anomalies in the Picacho area, south-central Arizona: Tucson, University of Arizona, unpublished master's thesis, 120 p.

Heindl, L.A., and Feth, J.H., 1955, Discussion of symposium on land erosion, "Piping," by J.E. Fletcher, K. Harris, H.B. Peterson, and V.N. Chandler: American Geophysical Union, Transactions, v. 36, no. 2, p. 122-125.

Helm, D.C., 1975, One-dimensional simulation of aquifer system compaction near Pixley, California—1. Constant parameters: Water Resources Research, v. 11, no. 3, p. 465-478.

_____1976, One-dimensional simulation of aquifer system compaction near Pixley, California—2. Stress-dependent parameters: Water Resources Research, v. 12, no. 3, p. 375-391.

Holdahl, S.R., 1981, A model of temperature stratification for correction of leveling refraction: National Oceanic and Atmospheric Administration Technical Memorandum NOS NGS-31, 27 p.

_____1986, Readjustment of leveling networks to account for vertical coseismic motions: Tectonophysics, v. 130, p. 195-212.

Holdahl, S.R., Strange, W.E., and Harris, R.J., 1986, Empirical calibration of Zeiss Ni-1 level instruments to account for magnetic errors: National Oceanic and Atmospheric Administration Technical Memorandum NOS NGS-45, 23 p.

Holzer, T.L., 1978, Results and interpretations of exploratory drilling near the Picacho fault, south-central Arizona: U.S. Geological Survey Open-File Report 78-1016, 41 p.

_____1980, Reconaissance maps of earth fissures and land subsidence, Bowie and Willcox areas, Arizona: U.S. Geological Survey Miscellaneous Field Studies Map MF-1156, 2 sheets.

_____1986, Ground failure caused by groundwater withdrawal from consolidated sediments—United States, *in* Johnson, A.I., Carbognin, L., and Ubertini, L., eds., Land Subsidence, Proceedings of the Third International Symposium on Land Subsidence, Venice, Italy, 1984: International Association of Scientific Hydrology Publication 151, p. 817-828.

Holzer, T.L., and Davis, S.N., 1976, Earth fissures associated with water table declines [abs.]: Geological Society of America, Abstracts with Programs, v. 8, no. 6, p. 923-924.

Holzer, T.L., and Thatcher, W., 1979, Modeling deformation due to subsidence faulting, *in* Saxena, S.K., ed., Evaluation and Prediction of Subsidence, Proceedings of the Engineering Foundation Conference, Pensacola Beach, Florida, 1978: American Society of Civil Engineers, 594 p.

Holzer, T.L., Davis, S.N., and Lofgren, B.E., 1979, Faulting caused by groundwater extraction in south-central Arizona: Journal of Geophysical Research, v. 84, no. B2, p. 603-612.

Jachens, R.C., and Holzer, T.L., 1979, Geophysical investigations of ground failure related to ground-water withdrawal—Picacho basin, Arizona: Ground Water, v. 17, no. 6, p. 574-585.

_____1982, Differential compaction mechanism for earth fissures near Casa Grande, Arizona: Geological Society of America Bulletin, v. 93, no. 10, p. 998-1012.

Jaeger, J.C., and Cook, N.G.W., 1979, Fundamentals of rock mechanics, 3d ed.: New York, Halsted Press, 593 p.

Johnson, N.M., 1980, The relation between ephemeral stream regime and earth fissuring in south-central Arizona: Tucson, University of Arizona, unpublished master's thesis, 158 p.

Laney, R.L., Raymond, R.H., and Winikka, C.C., 1978, Maps showing water-level declines, land subsidence, and earth fissures in south-central Arizona: U.S. Geological Survey Water-Resources Investigations Report 78-83, 2 sheets.

Leonard, R.J., 1929, An earth fissure in southern Arizona: Journal of Geology, v. 37, no. 8, p. 765-774.

Lofgren, B.E., 1960, Near-surface subsidence in western San Joaquin Valley, California: Journal of Geophysical Research, v. 65, no. 3, p. 1053-1062.

_____1969, Land subsidence due to the application of water: Geological Society of America, Reviews in Engineering Geology II, p. 271-303.

_____1971, Significant role of seepage stresses in compressible aquifer systems [abs.]: American Geophysical Union Transactions, v. 52, no. 11, p. 832.

_____1972, Sensitive response of basin deposits to regional stress changes [abs.]: Geological Society of America, Abstracts with Programs, v. 5, no. 7, p. 715-716.

Lohman, S.W., and others, 1972, Definitions of selected ground-water terms—Revisions and conceptual refinements: U.S. Geological Survey Water-Supply Paper 1988, 21 p.

Narasimhan, T.N., 1979, The significance of the storage parameter in saturated-unsaturated groundwater flow: American Geophysical Union, Water Resources Research, v. 15, no. 3, p. 569-576.

National Oceanic and Atmospheric Administration, 1973-85, Climatological data, Arizona, January 1973 through December 1984: U.S. Department of Commerce, v. 77, no. 1, to v. 89, no. 12.

Neal, J.T., Langer, A.M., and Kerr, P.F., 1968, Giant desiccation polygons of Great Basin Playas: Geological Society of America Bulletin, v. 79, p. 69-90.

Okada, Y., 1985, Surface deformation due to shear and tensile faults in a half-space: Seismological Society of America Bulletin, v. 75, no. 4, p. 1135-1154.

Pankratz, L.W., Ackerman, H.D., and Jachens, R.C., 1978, Results and interpretation of geophysical studies near the Picacho fault, south-central Arizona: U.S. Geological Survey Open-File Report 78-1106, 20 p.

Pashley, E.F., Jr., 1961, Subsidence cracks in alluvium near Casa Grande, Arizona: Arizona Geological Society Digest, v. 4, p. 95-101.

Peterson, D.E., 1962, Earth fissuring in the Picacho area, Pinal County, Arizona: Tucson, Arizona, University of Arizona, unpublished master's thesis, 35 p.

Poland, J.F., Lofgren, B.E., and Riley, F.S., 1972, Glossary of selected terms useful in studies of the mechanics of aquifer systems and land subsidence due to fluid withdrawal: U.S. Geological Survey Water-Supply Paper 2025, 9 p.

Riley, F.S., 1970a, Analysis of borehole extensometer data from central California, *in* Tison, L.J., ed., Land Subsidence, Tokyo Symposium, v. 1: International Association of Scientific Hydrology Publication 88, p. 423-431.

_____1970b, Land-surface tilting near Wheeler Ridge, southern San Joaquin Valley, California: U.S. Geological Survey Professional Paper 497-G, 29 p.

Robinson, G.M., and Peterson, D.E., 1962, Notes on earth fissures in southern Arizona: U.S. Geological Survey Circular 466, 7 p.

Sanford, A.R., 1959, Analytical and experimental study of simple geological structures: Geological Society of America Bulletin, v. 70, p. 19-52.

Sato, R., and Yamashita, T., 1975, Static deformations in an obliquely layered medium part II. dip-slip fault: Journal of Physics of the Earth, v. 23, p. 113-125.

Savage, J.C., and Hastie, L.M., 1966, Surface deformation associated with dip-slip faulting: Journal of Geophysical Research, v. 71, no. 20, p. 4897-4904.

Savage, J.C., and Hastie, L.M., 1969, A dislocation model for the Fairview Peak, Nevada, earthquake: Seismological Society of America Bulletin, v. 59, no. 5, p. 1937-1948.

Schulz, S., and Burford, R.O., 1977, Installation of an invar wire creepmeter, Elkhorn Valley, California: U.S. Geological Survey Open-File Report 78-203, 42 p.

Schumann, H.H., and Poland, J.F., 1970, Land subsidence, earth fissures, and groundwater withdrawal in south-central Arizona, U.S.A., *in* Tison, L.J., ed., Land Subsidence, Tokyo Symposium, v. 1: International Association of Scientific Hydrology Publication 88, p. 295-302.

Sellers, W.D., and Hill, R.D., eds., 1974, Arizona climate 1931-1972, Tucson, Arizona, University of Arizona Press, 2d ed., 616 p.

Smith, G.E.P., 1940, The groundwater supply of the Eloy District in Pinal County, Arizona: University of Arizona College of Agriculture, Agricultural Experimental Station, Technical Bulletin no. 87, 42 p.

Sokal, R.L., and Rohlf, F.J., 1969, Biometry: The principles and practices of statistics in biological research: San Francisco, W.H. Freeman and Company, 776 p.

Sumner, J.S., 1976, Earthquakes in Arizona: Arizona Bureau of Mines, Field Notes, v. 6, no. 1, p. 1-5.

Turner, S.F., and others, 1947, Further investigations of the ground-water resources of the Santa Cruz Basin, Arizona: U.S. Geological Survey open-file report, unnumbered, 49 p.

U.S. Bureau of Reclamation, 1976, Central Arizona Project—geology and groundwater resources report, Maricopa and Pinal Counties, Arizona: U.S. Bureau of Reclamation, 2 volumes, v. 1, 188 p., v. 2, 110 p.

U.S. Geological Survey, 1986, Annual summary of ground-water conditions in Arizona, spring 1984 to spring 1985: U.S. Geological Survey Open-File Report 86-422W, 1 sheet.

U.S. Soil Conservation Service, 1936, Aerial photographs—Picacho Reservoir, AZ 362, quadrangle 11; and Red Rock, AZ 385, quadrangle 17; Area 6, Series L, Pima and Papago Indian Reservations, Arizona: Washington, D.C., U.S. Department of Agriculture, Cartographic Division, unpublished data.

Winikka, C.C., and Wold, P.D., 1976, Land subsidence in central Arizona, *in* Johnson, A.I., and Yamamoto, S., eds., International Symposium on Land Subsidence, 2d, Anaheim, California, 1976, Proceedings: International Association of Hydrological Sciences Publication 121, p. 95-103.

Wrege, B.M., Hasbrouck, W.P., and Schumann, H.H., 1985a, Seismic surface-wave attenuation across earth fissures in the alluvium, south-central Arizona: Dublin, Ohio, National Water Well Association Conference on Surface and Borehole Geophysical Methods *in* Ground Water Investigations, February 12-14, 1985, Fort Worth, Texas, p. 121-131.

Wrege, B.M., Schumann, H.H., and Wallace, B.L., 1985b, Geohydrologic data along the Tucson aqueduct of the Central Arizona Project in Pinal and Pima Counties, Arizona: U.S. Geological Survey Open-File Report 85-565, 77 p.

Wyatt, F., 1982, Displacements of surface monuments—horizontal motion: Journal of Geophysical Research, v. 87, no. B2, p. 979-989.

Zienkiewicz, O.C., 1977, The finite element method: London, McGraw-Hill, 787 p.